Final Report on the Evaluation of the Regional Atmospheric Modeling System in the Eastern Range Dispersion Assessment System

Prepared By:
Applied Meteorology Unit

Prepared for:
Kennedy Space Center
Under Contract NAS10-96018

NASA
National Aeronautics and
Space Administration

Office of Management

Scientific and Technical
Information Program

2001

Executive Summary

This report presents the final results from an Applied Meteorology Unit (AMU) evaluation of the upgraded version of the Regional Atmospheric Modeling System (RAMS) Numerical Weather Prediction (NWP) model as run in the Eastern Range Dispersion Assessment System (ERDAS). ERDAS is designed to provide emergency response guidance to the 45th Space Wing/Eastern Range Safety (45 SW/SE) in support of operations at the Eastern Range in the event of an accidental hazardous material release or an aborted vehicle launch.

ERDAS uses the RAMS NWP model to generate prognostic wind and temperature fields for input into ERDAS diffusion algorithms. In addition, RAMS predicts a number of other meteorological quantities on four nested grids with horizontal resolutions of 60, 15, 5, and 1.25 km, respectively. Since the 1.25-km grid is centered over the Kennedy Space Center (KSC) and Cape Canaveral Air Force Station (CCAFS), real-time RAMS forecasts provide an opportunity for improved weather forecasting in support of space operations through high-resolution NWP over the complex land-water interfaces of KSC/CCAFS. The 45 SW/SE and the 45th Weather Squadron (45 WS) tasked the AMU to evaluate the capabilities and accuracy of RAMS for all seasons and under various weather regimes during 1999 and 2000.

The AMU subdivided the RAMS evaluation into three seasons, including the 1999 Florida warm season (May–August), the 1999-2000 cool season (November–March), and the 2000 warm season (May–September). Much of this final report focuses on the 1999-2000 cool and 2000 warm seasons since the ERDAS RAMS interim report summarized the results of the 1999 warm season.

The RAMS evaluation includes an objective and subjective component. The objective component involves point forecast error statistics at all available observational locations on grid 4 (1.25 km resolution), and selected observations on grids 1–3. The point error statistics that were examined include the Root Mean Square (RMS) error (total error), bias (systematic error component), and error standard deviation (random error component). The objective evaluation in this report consists of five segments for examining these point error statistics:

- Verification of the operational RAMS for the 1999-2000 cool and 2000 warm seasons,

- Surface wind regime classification for the 2000 warm season,

- Thunderstorm day regime classification for the 2000 warm season,

- Comparison of point error statistics between the operational configuration and a RAMS configuration with a coarser horizontal resolution, and

- Comparison of RAMS errors to the Eta model errors at the Shuttle Landing Facility (station symbol TTS).

The subjective component of the RAMS evaluation focused on the verification of fronts, precipitation across the Florida peninsula, and low-level temperature inversions at the Cape Canaveral rawinsonde during the 1999-2000 cool season. The warm-season subjective evaluation focused on the verification of sea breezes during 1999 and 2000, precipitation on grid 4 during 2000, and thunderstorm initiation on grid 4 during 2000.

The most notable point-forecast errors associated with the operational RAMS forecasts are as follows:

- RAMS had a surface-based, daytime low-level cold temperature bias that occurs during all seasons, reaching a maximum of 4.5°C in the cool season and 3.5°C in the warm season. This cold bias is consistent with the results found in the ERDAS RAMS interim evaluation report.

- The vertical temperature profile throughout the atmosphere was typically too stable during both seasons (e.g. too cold near the surface and too warm aloft by 0.5–1.0°C); however, in the lowest 0.5 km during the early morning hours, the RAMS temperature profile is too unstable (too warm at the surface by 0.5–1.0°C and too cold at 0.5 km by nearly 3°C).

- A surface-based nocturnal moist bias was found during the cool season whereas a daytime dry bias occurred in the 2000 warm season.

- At the KSC/CCAFS wind towers, wind direction RMS errors grew rapidly from 20° at initialization to 40° within the first 2 hours of model integration.

- The largest wind direction RMS errors of 60–70° occurred at the surface during the late night and early morning hours associated with light and variable winds common during those times.

- RAMS also experienced a slight low-level easterly wind bias and a southerly wind bias (maximum magnitude about 1–2 m s^{-1}) at all levels above the surface during both seasons.

The sea-breeze evaluation was examined for the operational RAMS configuration using data from the 1999 and 2000 warm-seasons. In addition, the operational RAMS sea-breeze forecasts were compared to a coarser resolution, 3-grid configuration of RAMS and to the operational National Centers for Environmental Prediction (NCEP) Eta model. The results of these verifications are given below:

- RAMS did an excellent job in forecasting the onset and movement of the east coast sea breeze (ECSB). The 1200 UTC forecast cycle exhibited the highest probability of detection (0.98) and best overall skill.

- Despite the low-level cold temperature bias, RAMS demonstrated this high skill in predicting the occurrence of the ECSB because the cold temperature bias was prevalent over both land and water. As a result, the thermal contrast between land and water that drives the sea-breeze circulation was represented well by the model.

- The RMS error in timing of the sea-breeze onset was between 1.5–2.1 h at all towers and the bias was negligible.

- In the 4-grid/3-grid sea-breeze comparison during 2000, the higher-resolution 4-grid configuration outperformed the 3-grid forecasts in nearly all skill categories.

- RAMS was more skillful than the Eta model for the 0000 UTC cycle only.

- In the 1200 UTC forecast cycle, the RAMS probability of detection was significantly higher than the Eta model, but so was the false alarm rate and bias. The resulting improvement in skill scores of the RAMS over the Eta model were not statistically significant because RAMS tended to over-forecast the sea-breeze occurrence at TTS.

- These results indicate that, despite the comparable or slightly better objective error statistics in the Eta model, the phenomenological verification of the ECSB improves over the Eta model when running the RAMS model with fine horizontal grid spacing such as in the current configuration.

For the precipitation and thunderstorm initiation verifications, the AMU divided grid 4 into six zones, 3 coastal and 3 inland. Precipitation and thunderstorm activity were verified each day during peak convective hours (1500–2300 UTC, or 1100–1900 EDT). For the thunderstorm initiation verification, the AMU defined a RAMS thunderstorm based on a predicted minimum vertical velocity in the charge zone of a forecast storm, combined with forecast precipitation at the ground. The results of the precipitation verification indicate that:

- RAMS predicted precipitation with the highest skill over the inland zones whereas the model had the poorest skill over the coastal zones, especially the southeastern zone of grid 4.

- The 1200 UTC cycle was generally more skillful than the 0000 UTC forecasts. Based on the 1200 UTC cycle, the most accurate precipitation forecasts occurred between 1600–2000 UTC and the least accurate forecasts occurred after 2000 UTC. The reduction of skill after 2000 UTC could be caused by the model's inability to forecast adequately the evolution and interaction of thunderstorm outflow boundaries.

The results of the thunderstorm initiation verification suggest the following:

- The 1200 UTC RAMS forecast cycle predicted daily thunderstorm occurrence much better than the 0000 UTC cycle.

- Thunderstorms were under-predicted in all grid-4 zones of the 0000 UTC cycle, and in the southeastern zone of the 1200 UTC cycle.

- Among the correctly predicted thunderstorm days, RAMS initiated the first thunderstorm correctly in one or more grid-4 zones about 50% of the time. Meanwhile, RAMS predicted the first daily thunderstorm to within 3 hours of actual initiation about 75% of the time.

The AMU performed a variety of sensitivity tests to isolate the cause(s) of the RAMS objective error statistics, in particular the surface-based cold temperature bias. The only experiment that improved the cold bias (by about 3°C) involved running RAMS with an alternative radiation scheme that ignores the effects of clouds on incoming short-wave radiation. As a result of this experiment, the AMU found that RAMS generated widespread fog at the surface at all times over the ocean, and during the nocturnal hours over land. The fog could be the cause of the low-level cold bias since the fog reduces solar heating during the morning hours when the cold bias rapidly developed. The AMU has not identified the cause of this low-level fog in RAMS.

Table of Contents

List of Figures

List of Abbreviations and Acronyms

Term	Description
45 SW/SE	45th Space Wing/Eastern Range Safety
45 WS	45th Weather Squadron
ABFM	Airborne Field Mill
AMU	Applied Meteorology Unit
CC	Chen and Cotton
CCAFS	Cape Canaveral Air Force Station
CGLSS	Cloud to Ground Lightning Surveillance System
CSI	Critical Success Index
CSR	Computer Sciences Raytheon
DAB	Daytona Beach, FL 3-letter station identifier
DRWP	Doppler Radar Wind Profiler
ECSB	East Coast Sea Breeze
ERDAS	Eastern Range Dispersion Assessment System
FAR	False Alarm Rate
GARP	Global Atmospheric Research Program
GATE	GARP Atlantic Tropical Experiment
GEMPAK	General Meteorological Package
GOES	Geostationary Operational Environmental Satellite
GUI	Graphical User Interface
HP	Hewlett Packard
HSS	Heidke Skill Score
HYPACT	Hybrid Particle and Concentration Transport
ISAN	Isentropic Analysis
JAX	Jacksonville, FL 3-letter station identifier
KSC	Kennedy Space Center
MARSS	Meteorological And Range Safety Support
MCO	Orlando, FL 3-letter station identifier
METAR	Aviation Routine Weather Report
MIA	Miami, FL 3-letter station identifier
MIDDS	Meteorological Interactive Data Display System
MLB	Melbourne, FL 3-letter station identifier
MP	Mahrer and Pielke
MPI	Message-Passing Interface
MRC	Mission Research Corporation
NCEP	National Centers for Environmental Prediction
NWP	Numerical Weather Prediction
NWS	National Weather Service
PBI	West Palm Beach, FL 3-letter station identifier
POD	Probability of Detection

1. Introduction

The Eastern Range Dispersion Assessment System (ERDAS) was developed by Mission Research Corporation (MRC)/ASTER Division (formerly ASTeR, Inc.) for the United States Air Force (USAF). ERDAS is designed to provide emergency response guidance for operations at the Kennedy Space Center (KSC) and Cape Canaveral Air Force Station (CCAFS) in the event of a hazardous material release or an aborted vehicle launch. ERDAS was delivered to the Eastern Range at CCAFS in March 1994. Under Applied Meteorology Unit (AMU) option-hours funding from the USAF Space and Missile Systems Center (SMC), ENSCO was tasked to evaluate the prototype ERDAS during the period March 1994 to December 1995. The evaluation report concluded that ERDAS provided significant improvement over current toxic dispersion modeling capabilities but contained a number of deficiencies. These deficiencies were corrected in the next generation of ERDAS that is part of the newly upgraded Meteorological and Range Safety Support (MARSS) replacement system.

1.1 Task Background

The MARSS replacement system contains an upgraded version of the Regional Atmospheric Modeling System (RAMS) that is designed to run on workstations with multiple processors. Developed at Colorado State University, RAMS is a dynamical numerical weather prediction model with optional parameterization schemes for representing physical processes in the atmosphere. The model may be run in two or three dimensions and in hydrostatic or non-hydrostatic modes. RAMS includes a terrain-following vertical coordinate, a variety of lateral and upper boundary conditions, and capabilities for mixed-phase microphysics. Details on the history, overview, and applications of RAMS can be found in Pielke et al. (1992) whereas a description of ERDAS can be found in Lyons and Tremback (1994).

There are two main differences between the original and upgraded versions of the RAMS configuration in ERDAS. First, the original configuration of RAMS ran without cloud microphysics whereas the new configuration is run with full cloud microphysics on all grids. Second, the areal extent of the innermost, nested grid was expanded and the horizontal resolution was improved from 3 to 1.25 km. While the previous configuration of ERDAS was validated (Evans 1996), a systematic evaluation of the new configuration of ERDAS has not yet been performed. For this reason, representatives from 45th Range Safety (45 SW/SE) and 45th Weather Squadron (45 WS) requested that the upgraded version of RAMS in ERDAS be evaluated.

The prognostic gridded data from RAMS is available to ERDAS for display and input to the Hybrid Particle and Concentration Transport (HYPACT) model. The HYPACT model provides three-dimensional dispersion predictions using RAMS forecast grids to represent the environmental conditions. Thus, the accuracy of dispersion predictions using the HYPACT model is highly dependent upon the accuracy of RAMS forecasts. As a result, the primary goal of this evaluation is to determine the accuracy of RAMS forecasts during all seasons and under various weather regimes.

The evaluation protocol is based on the operational needs of 45 SW/SE and 45 WS and designed to provide specific information about the capabilities, limitations, and daily use of ERDAS RAMS for operations at KSC/CCAFS. The ERDAS RAMS evaluation primarily concentrates on wind and temperature (stability) forecasts that are required for dispersion predictions using the HYPACT model. The RAMS evaluation is divided into two segments, an objective and subjective component. The objective component focuses on model point error statistics at a number of observational locations. Since point error statistics cannot adequately evaluate meteorological phenomena and mesoscale patterns such as sea breezes and precipitation, there is also a subjective portion of the evaluation. The subjective component involves the manual examination of forecasts and observations to determine how RAMS predicts fine-scale phenomena such as sea breezes, precipitation, and thunderstorms.

This report provides a summary of the AMU's evaluation of the RAMS component of ERDAS for the 1999–2000 cool season, and 1999 and 2000 warm seasons, focusing on local results at KSC/CCAFS and the immediate surrounding area. This report continues the work from the ERDAS RAMS interim report, which presented evaluation results from the 1999 Florida warm season (Case 2000). Therefore, this report will focus primarily on the 1999-2000 cool- and 2000 warm-season results.

Table 1.1.   A summary of the grid parameters for all four RAMS grids. The model parameters include the number of grid points in the x, y, and z directions (nx, ny, and nz), horizontal resolution (dx), minimum and maximum vertical resolutions (dzmin and dzmax), and time steps (dt).

Grid	nx	ny	nz	dx (km)	dzmin (m)	dzmax (m)	dt (s)
1	36	40	33	60	50	750	45
2	38	46	33	15	50	750	45
3	41	50	36	5	25	750	22.5
4	74	90	36	1.25	25	750	7.5

1.3 RAMS Forecast Cycle

RAMS is initialized twice-daily at 0000 and 1200 UTC using the Eta 12-h forecast grids and operationally-available observational data including the CCAFS rawinsonde (XMR), Aviation Routine Weather Reports (METAR), buoys, and KSC/CCAFS wind-tower, and 915-MHz and 50-MHz Doppler Radar Wind Profiler (DRWP) data.   No variational data assimilation or nudging technique is applied when incorporating observational data. Instead, RAMS is initialized from a cold start by integrating the model forward in time from a gridded field without any balancing or data assimilation steps.   Observational data are analyzed onto hybrid coordinates using the RAMS Isentropic Analysis (ISAN) package (Tremback 1990).   The ISAN hybrid coordinate consists of a combination of constant potential temperature (isentropes) and terrain-following surfaces on which data are analyzed within the RAMS model domain, similar to the NCEP Rapid Update Cycle (RUC) model (Benjamin et al. 1998).

The ERDAS RAMS forecast cycle is illustrated in Figure 1.2. The RAMS cycle is run in real-time for a 24-h forecast period on a Hewlett Packard (HP) K460 workstation cluster with 12 processors (with 1 of these processors serving as the master node).   The model run-time performance is optimized by using a message-passing interface (MPI) on the 12 processors.   In MPI, the run-time is significantly reduced compared to a single processor because each processor simultaneously performs computations on a portion of the domain (Tremback et al. 1998).

The operational cycle requires approximately 15 minutes to analyze observational data for the initial conditions using ISAN and 10-12 h to complete the 24-h forecast cycle.   On many occasions when the model produced extensive convection (primarily during the summer months), a 24-h forecast could not complete in 12 h due to the calculations associated with the microphysics scheme. In these instances, the existing RAMS run is terminated before the 24-h simulation is completed, and the new simulation begins.   Consequently, RAMS data are occasionally missing from the 22-24-h forecasts, primarily due to extensive model convection.   In the event of a 1-cycle failure, prognostic data are still available from the previous forecast cycle.

RAMS forecast output is available once per hour for display and analysis purposes due to disk-space limitations of the operational hardware.   Thus, all portions of this model verification study are limited in time to a frequency of 1 hour, regardless of the frequency of available observational data.   This frequency of model output presents a limiting factor in the verification since warm-season weather phenomena in Florida can develop over time scales much shorter than 1 hour (particularly convection).   Nonetheless, hourly forecast output at high spatial resolution has the potential to provide valuable guidance in forecasting warm-season phenomena in east-central Florida.

2. Methodology

The AMU evaluation of RAMS during the 1999–2000 cool, and 1999 and 2000 warm seasons includes both an objective and subjective component, following the methodology used in the interim ERDAS RAMS report. The objective component is designed to present a representative set of model errors of winds, temperature, and moisture for both the surface and upper-levels. The goal of the subjective verification is to provide an assessment of the forecast timing and propagation of the east-central Florida East Coast Sea Breeze (ECSB), daytime forecast precipitation, and forecast thunderstorm initiation by examining selected RAMS forecast fields. Since the 1999 warm-season objective and subjective results were thoroughly discussed in the interim report, this final report will focus on results from the 1999-2000 cool and 2000 warm seasons.

2.1 Objective Component

The objective component of the RAMS evaluation consists of five separate segments listed below that compute point error statistics:

- Verification of the operational 4-grid configuration of RAMS.

- Surface wind regime classification.

- Thunderstorm day regime classification.

- Comparison of point error statistics between the operational configuration and a RAMS configuration with a coarser horizontal resolution

- Comparison of RAMS errors to the Eta model errors.

Each portion of the objective component focuses on point error statistics at many different observational locations on all four forecast grids with emphasis placed on stations in grid 4.

2.1.1 Standard Evaluation

The standard objective evaluation consists of point forecast error statistics for the operational RAMS configuration during the 1999-2000 cool and 2000 warm seasons in Florida. Zero to 24-h point forecasts of wind, temperature, and moisture were compared with surface METAR and buoy stations, the XMR rawinsonde, KSC/CCAFS wind-tower, 915-MHz, and 50-MHz DRWP data at all available observational locations on grid 4, and selected surface and rawinsonde stations on grids 1–3. This report will focus on point error statistics at sensors within RAMS grid 4, particularly the KSC/CCAFS wind tower network, the XMR rawinsonde and the 50-MHz profiler. The locations of all the observations used for point verification are given in Figure 2.1.

The point statistics presented include the root mean square (RMS) error, bias, and error standard deviation (SD) of wind direction, wind speed, temperature, and dew point temperature for November 1999–March 2000 (cool-season months), and for May–September 2000 (warm season months). In addition, the average values of forecasts and observations for these variables were computed as a function of forecast hour at all observational sites for the entire evaluation period. Special care was exercised when computing the mean and SD of wind direction errors following Turner (1986). However, in general, the mean seasonal observed and forecast wind direction quantities have little meaning because the distributions of the wind direction were nearly uniform, particularly during the warm season. Therefore, only plots of RMS error and bias are provided for wind direction. Error statistics for all other variables were calculated in the manner as outlined below.

If Φ represents any forecast variable, then forecast error is defined as $\Phi' = \Phi_f - \Phi_o$, where the subscripts f and o denote forecast and observed quantities, respectively. The bias represents the average model error and is computed as

$$\text{Bias} = \frac{1}{N}\sum_{i=1}^{N}\Phi', \tag{2.1}$$

5

For purposes of interpretation in this report, we have assumed that the magnitude of the observational error is negligible compared to the model error. The total model error (RMS error) includes contributions from both systematic and random errors. Systematic error (bias) can be caused by a consistent misrepresentation of physical parameters such as radiation or model-generated convection. Random or nonsystematic errors, given by the error SD, represent the errors caused by uncertainties in the model initial condition or unresolveable differences in scales between the forecasts and observations. Note that the error standard deviation contains a component of natural variability since the model value is an average over a grid volume whereas the observed value is usually a point measurement.

A quality control (QC) check was performed on all point error statistics to remove any errors greater than 3 standard deviations from the mean error (bias). This QC check was performed to screen out bad observations or corrupted model forecasts and generally resulted in the rejection of less than 2 percent of all possible errors.

2.1.2   Regime Classifications

The second and third segments of the objective evaluation involve the computation of point error statistics under various weather regimes for the operational RAMS configuration during the 2000 warm season. Specifically, two types of regimes are examined in this report, surface winds and thunderstorm days. During each day, the surface wind regime was identified according to the early morning wind flow observed across the KSC/CCAFS wind-tower network. The days were then grouped into three classes of wind-flow patterns: westerly (offshore), easterly (onshore), and light or light and variable, where light wind regimes were defined as sustained speeds less than 5 knots. The RAMS forecasts were grouped together according to the similar surface wind regimes and error statistics were compiled for the similar wind regimes.

For the thunderstorm regime classification, the RAMS point forecasts were computed for all combinations of forecast and observed thunderstorms on grid 4. Every day was categorized according to the occurrence of observed or forecast thunderstorms within the area of the RAMS grid 4. Each RAMS forecast fell into one of four categories: both observed and forecast thunderstorms, observed but no forecast thunderstorms, forecast but no observed thunderstorms, and no observed or forecast thunderstorms. Point error statistics were computed for each of these four combinations of thunderstorm days during the 2000 warm season. The results of the regime classification experiments are presented in Section 5.2.3.

2.1.3   Benchmark Experiments

The fourth and fifth segments of the objective evaluation consist of two benchmark experiments. One benchmark experiment compares the RAMS 4-grid operational configuration to a 3-grid configuration by simply excluding grid 4 and rerunning RAMS with only grids 1, 2, and 3. The statistics were computed separately for the 3-grid and 4-grid data for the forecast cycles when both models runs were available (refer to Appendix A). Section 4.5 presents the results of this comparison for observational data within the grid 4 domain. The goal of this experiment is to measure the impact from a decrease in horizontal resolution of the innermost grid on the resulting forecast errors.

The second benchmark experiment compares the Eta point forecasts at 14 surface stations in the southeastern United States and 4 upper-air stations in the Florida peninsula to RAMS forecasts interpolated to the same stations (refer to Fig. 2.1 and Table 2.1). This important benchmark compares RAMS forecasts to the widely-used NCEP Eta model and quantifies any added value that may be provided by the RAMS over the Eta model, based on an objective comparison. This report will focus on the RAMS/Eta comparison at TTS (surface only), since this station is the only available location on RAMS grid 4. The results from the Eta model benchmark are discussed in Section 4.6.

traces (meteograms) of hourly temperature, dew point temperature, wind direction, wind speed, and mean sea-level pressure observations and RAMS forecasts were examined at seven selected surface stations on the east coast of the Florida peninsula (Jacksonville (JAX), Daytona Beach (DAB), the Shuttle Landing Facility (TTS), Melbourne (MLB), Vero Beach (VRB), West Palm Beach (PBI), and Miami (MIA)). Frontal passages were verified for both the 0000 UTC and 1200 UTC RAMS forecast cycles whenever the 24-h forecast overlapped an observed frontal passage and sufficient archived forecast and observed data were available. The discontinuities in winds, temperature, and dew point temperature were each verified independently because the wind shifts and temperature/dew point temperature gradients often occurred at different times with a frontal passage.

The forecast errors associated with frontal passages were examined for three criteria: pre-frontal conditions, the frontal transition zone, and post-frontal maximum wind speed. The pre-frontal forecast wind direction, temperature, and dew point temperature errors were obtained by differencing the observations from the RAMS forecast values at each surface station that experienced both a forecast and observed frontal passage. The errors in forecast frontal timing were computed to the nearest hour, limited by the frequency of available RAMS output. The intensity of the frontal zone was verified by comparing the observed and forecast 3-h changes in each meteorological quantity following the initial observed or forecast discontinuity. Finally, the maximum forecast post-frontal wind speed was verified against the maximum observed post-frontal wind speed for each forecast that experienced a frontal passage. The results of the frontal verification are presented in Section 5.1.1.

2.2.1.2 Verification of Precipitation

The 1999-2000 cool season offered only a small number of cases for frontal-associated precipitation verification. Very few significant frontal passages occurred with substantial frontal or pre-frontal rain bands, thereby preventing a robust verification of RAMS forecast precipitation during the cool season. The two most significant frontal events with precipitation across the Florida peninsula occurred on 2 November 1999 and 24 January 2000, but each case had problems in the RAMS forecast. The 0000 UTC RAMS forecast cycle failed on 2 November. On the 24 January case, the NCEP Eta model poorly predicted the development of an Atlantic coastal cyclone prediction, and thus did not provide adequate boundary conditions for the RAMS forecasts. Additional cases with weak or broken squall lines occurred on a few days in March.

Section 5.1.2 summarizes the most significant precipitation events for which sufficient forecast and observational data were available for subjective verification. In addition, a few RAMS forecasts are compared to observed satellite and rain-gauge data for the 24 January and 11 March 2000 events. To compare rain-gauge data to RAMS forecast precipitation, archived rainfall data from the St. John River, south Florida, and KSC networks were obtained from the Goddard Space Flight Center. An objective analysis was performed on the accumulated hourly rain-gauge data at every hour for the entire 1999-2000 cool season to obtain observed rainfall on RAMS grids 2, 3, and 4. RAMS forecast rainfall was then compared to these gridded rain-gauge data overlaid on infrared satellite imagery, primarily focusing on grid-2 for peninsula-scale rainfall verification associated with fronts and troughs.

2.2.1.3 Verification of Low-level Temperature Inversions

For all five cool-season months, the occurrence of observed and forecast temperature inversions at XMR were recorded in the lowest 3 km of the atmosphere, including both surface-based radiational inversions and elevated subsidence inversions. Approximately 80% of the cases examined were surface-based radiational inversions. Both the 0000 UTC and 1200 UTC RAMS forecast cycles were examined and verified against the observed morning XMR sounding, which was typically released at 1115 UTC. Therefore, the 11-h forecast from the 0000 UTC RAMS cycle and the 23-h forecast from the previous day's 1200 UTC RAMS cycle are the verifying forecast hours.

The number of model forecast "hits" and "misses" were compiled to determine how well RAMS can predict the occurrence of a temperature inversion. When both an observed and forecast inversion occurred, specific parameters were verified including the intensity of the temperature inversion in °C, the height of the inversion base in meters, and the depth of the inversion layer in meters.

In addition to the evaluation of the RAMS predicted ECSB at the 12 selected towers, the AMU conducted two benchmark/sensitivity tests within the sea-breeze verification. The first sensitivity study compares the RAMS 4-grid sea-breeze forecasts to RAMS 3-grid forecasts, where grid 4 is simply excluded in the model predictions. The sea-breeze verification is conducted at the 12 wind towers (Figure 2.2) for all common 4-grid and 3-grid RAMS forecasts only during the 2000 warm season (refer to Appendix A for available RAMS forecasts). The second sensitivity experiment compares the RAMS 4-grid sea-breeze forecasts to the Eta point forecasts at the Shuttle Landing Facility (TTS, shown in Fig. 2.1d). The TTS sea-breeze verification was performed for all common RAMS and Eta point forecasts during the 1999 and 2000 warm seasons. The same onshore versus offshore criterion as used for the KSC/CCAFS wind-tower evaluation was applied when verifying the RAMS and Eta sea-breeze forecasts at TTS.
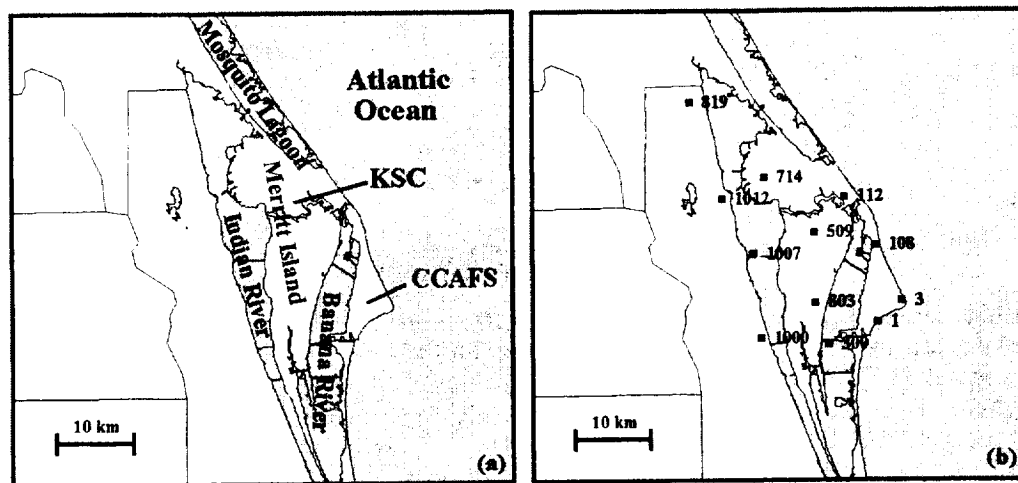
Figure 2.2. A plot of the geographic locations of KSC, CCAFS, the local water bodies surrounding KSC/CCAFS, and the 12 KSC/CCAFS wind towers used for the east coast sea-breeze subjective verification. The labels of geographical locations are given in a) and the wind tower locations are shown in b). The wind towers were chosen to examine the timing of the ECSB along the immediate Atlantic coastline, Merritt Island, and mainland Florida.

A 2 × 2 contingency table was used to summarize the ECSB verification statistics based on the occurrence of both an observed and forecast ECSB at any of the 12 KSC/CCAFS towers. A "hit" is defined as the occurrence of both an observed and forecast sea-breeze passage at a particular KSC/CCAFS tower. Because RAMS forecast output is available once per hour, the AMU verified the timing of the onset and movement of the sea breeze to the nearest hour at each of the 12 KSC/CCAFS towers. Table 2.2 is a sample 2 × 2 contingency table from which a variety of categorical and skill scores can be computed to measure forecast performance. The total number of correct forecasts is given by x in the upper left corner (forecast and observed = yes) and w in the lower right corner (forecast and observed = no). The number of forecast failures is given in the lower left portion of the table (forecast = no, observed = yes) and the number of false alarm forecasts is given in the upper right corner (forecast = yes, observed = no).

Table 2.2. A sample 2 × 2 contingency table for the evaluation of a forecast element is shown from which categorical and skill scores are computed (see text).

	Observed = Yes	Observed = No
Forecast = Yes	x	z
Forecast = No	y	w

Number of correct forecasts = (x+w)
Number of false alarm forecasts = z
Number of forecast misses = y

Because convective precipitation is often localized and fleeting across east-central Florida, the AMU applied an alternative technique to verify precipitation on RAMS grid 4 during the 2000 Florida warm season. Based on the methodology described in Manobianco and Nutter (1999), the RAMS grid 4 was divided into six separate zones to identify locations of forecast and observed precipitation (Fig. 2.3). The original intent was to verify hourly accumulated forecast precipitation; however, the AMU discovered late in the study that instantaneous precipitation rates were being archived once per hour rather than RAMS accumulated rainfall. As a result, only instantaneous precipitation rates were verified against instantaneous observed precipitation once per hour. Consequently, this precipitation verification will be quite stringent compared to a technique that utilizes accumulated observed and forecast precipitation fields. The effects of this instantaneous rainfall verification compared to a verification of accumulated precipitation were not estimated.

In order to perform the precipitation verification adequately, the AMU could rerun RAMS forecasts from May to September 2000 and extract the accumulated precipitation fields from the model. In addition, the AMU could obtain archived WSR-88D rainfall estimates from the MLB radar site for the entire warm season to serve as a validation for the predicted precipitation. However, the level of effort required to perform this analysis is beyond the available resources of the current task.

Hourly forecast precipitation rates ≥ 5 mm h^{-1} (0.2 in h^{-1}) were identified on a daily basis for both the 0000 and 1200 UTC RAMS runs in each verification zone between 1500–2300 UTC (peak convective hours). The technique used composite reflectivity at 2,000 ft from the WSR-74C to verify the location of observed precipitation at each hour. A "hit" was defined as the occurrence of both forecast and observed precipitation within a specific zone at a given hour, with intensity ≥ 5 mm h^{-1}. To obtain an approximate reflectivity threshold corresponding to a 5 mm hr^{-1} rain rate, the AMU utilized the tropical reflectivity/rain rate relationship derived in the Global Atmospheric Research Program (GARP) Atlantic Tropical Experiment (GATE, Hudlow 1979),

$$Z = 230R^{1.25},$$ (2.9a)

$$dBZ = 10\log_{10} 230 + 12.5\log_{10} R,$$ (2.9b)

where Z is reflectivity and R is rain rate in mm h^{-1}. Using this relationship yields a reflectivity factor of about 32 dBZ corresponding to a rain rate of 5 mm h^{-1}.

The AMU also verified precipitation in two and three-hourly verification bins in order to identify any improvement in precipitation forecast skill with a larger verification time interval. Increasing the verification time interval and reapplying skill-score thresholds can help to determine a predictable limit of RAMS precipitation forecasts. For the two-hour forecast bins, a hit is defined as the occurrence of observed and forecast precipitation in the same zone for either hour of the two-hour bin. Similarly for three-hourly bins, a hit is defined as the occurrence of both observed and forecast precipitation at any hour within the three-hour time interval. To measure the accuracy of RAMS hourly precipitation forecasts, the AMU computed the POD, FAR, CSI, and HSS for each zone in Figure 2.3.

In this study, precipitation is verified according to the occurrence of precipitation at only 1 threshold (≥ 5 mm hr^{-1}) anywhere within the six separate zones of Figure 2.3. Thus, the methodology used in this study is less stringent than threat score techniques in terms of spatial and intensity verification. However, this methodology is more stringent temporally based on the small time windows used to verify the forecast precipitation (1–3 h). In addition, this study looks at instantaneous precipitation rates rather than accumulated precipitation. Most current operational techniques still verify model precipitation for 24-h periods; however, NCEP recently began routine 3-h precipitation verification for many national-scale operational models (Baldwin 2000). Section 5.2.2 summarizes the categorical and skill scores of RAMS forecast precipitation and includes verification scores for 1-, 2-, and 3-h verification windows.

correctly predicted the initiation time exactly (0-h difference between observations and forecast), within 1 h (-1 to +1 h error), within 2 h (-2 to +2 h error), and within 3 h (-3 to +3 h error) of the observed time, irrespective of spatial accuracy. In addition, the spatial and timing accuracy of thunderstorm initiation were examined in combination by developing contingency tables and determining categorical and skill scores for each individual grid-4 zone based on specific timing thresholds. The results of the thunderstorm initiation verification are presented in Section 5.2.3.

DRWP was out of service or unreliable for a significant portion of the season due to damage inflicted by two hurricanes during the fall of 1999 (Floyd and Irene). As a result, less than half the possible verification points were available for the 1999-2000 cool season (Fig. 3.2a), and these data will not be used for upper-air wind verification in the cool season. However, the data were much more reliable during the 2000 warm season, with > 70% of the maximum verification points available in much of the mid-upper troposphere (Fig. 3.2b).
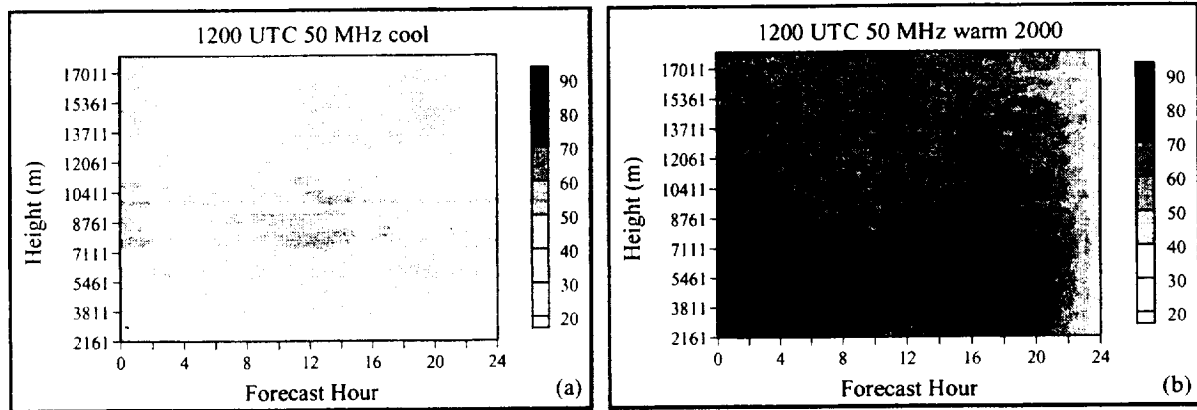
Figure 3.2. Time-height plot of the percentage of available 50-MHz DRWP verification data for the 1200 UTC forecast cycle during the a) 1999-2000 cool season (November–March) and b) 2000 warm season (May–September).

The XMR rawinsonde standard launch times are typically 0615 and 1815 local time year-round, with an additional sounding launch at 1100 local during the convective season (May–September). Thus, XMR rawinsonde observations were available at 1115 and 2315 UTC during the 1999-2000 cool season, and 1015, 1500, and 2215 UTC during the warm season. Since RAMS forecast output was available only once per hour, the observations were used for verification at both hours surrounding the observation, when appropriate.

The distribution of available XMR verification data for the 1200 UTC RAMS forecast cycle is shown in Figures 3.3 and 3.4 for wind direction and temperature, respectively. During the cool season, the 1200 UTC RAMS predictions interpolated to the XMR site were verified for forecast hours 0, 11, 12, 23, and 24 (corresponding to universal times 1200, 2300, 0000, 1100, and 1200 UTC). The theoretical maximum number of verification points at a particular time and sounding level is equal to the number of possible verification days, 152 in the cool season and 153 in the warm season. However, the largest number of verification points is about 130 in conjunction with the late-morning sounding launches during 2000 warm season. A combination of missing sounding data and failed RAMS forecasts (see next section and Appendix A) account for the loss of data during the two seasons.

The available wind verification data extends from the surface to ~10–12 km (Fig 3.3) whereas the temperature verification data extend from the surface to about 8 km (Fig. 3.4). Available dew point temperature verification data only reached ~6–7 km (not shown). The cause of this lack of data above certain levels for each variable is not known. A bug may exist in the RAMS data extraction routine since sounding data are readily available above these levels.

The operational RAMS configuration is designed to provide each forecast cycle with 12 hours to complete a 24-h forecast (see Section 1.3). Due to limitations in the processing speed associated with the operational hardware, the current configuration of RAMS cannot always complete all 24 forecast hours within the prescribed time of 12 hours. If the RAMS prediction takes longer than 12 hours to complete, the current cycle is terminated prematurely, and the subsequent cycle begins. Thus, a recurring issue with the operational RAMS configuration is the termination of the current forecast cycle before it completes all 24 forecast hours. This loss of data was most prevalent during the warm seasons when extensive convection generated by the model slowed down the system due to the intensive computations associated with the microphysical cloud scheme.

Figure 3.5 illustrates the availability of RAMS data as a function of forecast hour for both the 1999-2000 cool season and 2000 warm season. Since widespread precipitation only occurred rarely during the 1999-2000 cool season, most RAMS forecasts completed all 24 hours of integration as only about 10–25 forecasts from each cycle failed to complete the 24th hour (Fig. 3.5a). The 2000 warm season statistics depict quite a different story since well over half of all successful forecasts did not complete the 24th forecast hour (Fig. 3.5b). In fact, a substantial drop in available data begins at 22 hours and continues to drop sharply out to 24 hours. The variations of RAMS data availability between the cool and warm seasons clearly indicate the slower RAMS performance during the active convective months.
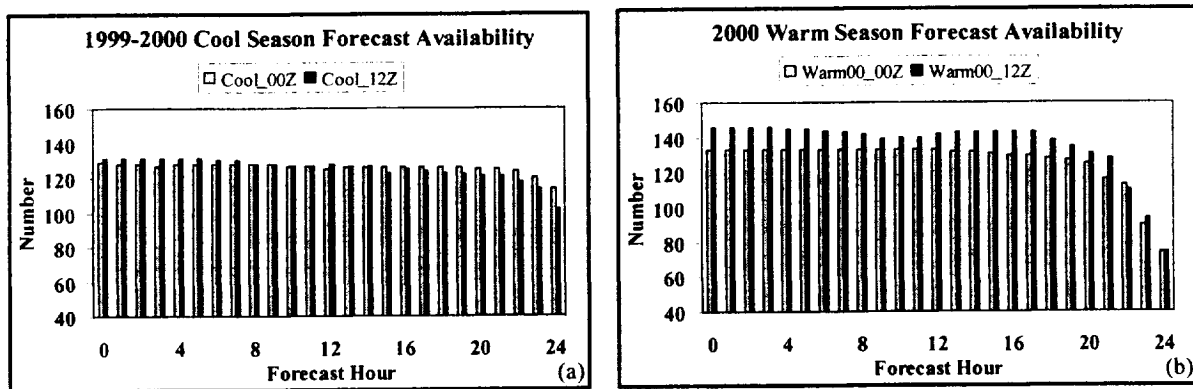
Figure 3.5. A display of the number of available RAMS forecasts as a function of forecast hour for the a) 1999-2000 Florida cool season (November–March) and b) 2000 Florida warm season (May–September). The gray bars represent the number of days of available 0000 UTC cycle forecasts whereas the black bars are the number of days of available 1200 UTC cycle forecasts. The theoretical maximum numbers at each hour are 152 for the 1999-2000 cool season and 153 for the 2000 warm season.

4.1.2 Summary of Upper-level Errors (XMR rawinsonde)

Table 4.2. Summary of the 4-grid RAMS upper-air error statistics for the 0000 and 1200 UTC forecast cycles during the 1999-2000 Florida cool season. Upper-level conditions are verified at the XMR rawinsonde for the 1115 UTC and 2315 UTC standard launch times (11-h and 23-h forecasts, respectively).

Variable	Forecast Cycle	RMS Error	Bias	Notable Errors
Temp (°C)	0000 UTC 1200 UTC	1 to 3.5 1 to 4	-3 to 1 -3 to 1	• Too cold below 650 mb in both cycles. • During the early morning hours, RAMS is too warm at the surface and much too cold just above the surface, indicating that the lowest levels are not stable enough. • Slightly too warm above 650 mb. • Largest RMS error near the surface.
Dew Point (°C)	0000 UTC 1200 UTC	4 to 8 3 to 8	-4 to 3 -4 to 2.5	• Too moist at low levels below 900 mb. • Largest RMS error near 850 mb. • Tendency to be too dry at mid and upper levels.
Wind Direction (deg.)	0000 UTC 1200 UTC	15 to 60 15 to 55	-20 to 20 -15 to 25	• Largest errors below 950 mb. • Smallest errors between 300–400 mb. • Positive bias near the surface; negative bias above 950 mb. • In the 0000 UTC cycle, an easterly bias (negative u-wind bias) increases with time at all levels. • In both cycles, a southerly bias (positive v-wind bias) occurs at both times and all levels.
Wind Speed (m s^{-1})	0000 UTC 1200 UTC	2.5 to 4.5 2.5 to 5.5	-2 to 1.5 -2 to 2	• Smallest errors near the surface, largest at upper levels. • Positive bias near the surface, negative bias above 950 mb.

4.1.3 Discussion of 1999-2000 Cool-season Results

Because the diurnal variations in objective error statistics were quite similar for the operational 0000 and 1200 UTC forecast cycles, a brief discussion of the RAMS point forecasts is provided here for only the 1200 UTC forecast cycle surface and upper-level error statistics on RAMS grid 4. The analysis of surface errors focuses on the results from the KSC/CCAFS wind towers, but also supplements these results with standard METAR observational errors from grid 4 and the errors at the two buoys of Cape Canaveral, FL (refer to Fig. 2.1 for station locations). All referenced graphical plots and figures in this section can be found in Appendix B.

4.1.3.1 Surface errors from 1200 UTC Cycle (KSC/CCAFS towers, METAR, buoys)

a. Temperature and dew point temperature

During the 1999-2000 Florida cool season, a pronounced daytime cold temperature bias was prevalent at all verification sensors of interest, including the KSC/CCAFS wind-tower network, METAR observations on grid 4, and the two offshore buoys. At the KSC/CCAFS wind towers, a slight warm bias (~2°C) occurs in the initial condition, but quickly switches to a cold bias by the 2-h forecast, reaching a maximum magnitude of -4°C at 6 h (Fig. B1c). The bias dissipates to 0°C during the overnight hours after 18 h. The combination of the random error (SD) and the bias yields a maximum RMS error close to 5°C at the 6-h forecast (Fig. B1b). As shown in Figure B2, the surface cold bias is also quite significant, as well as constant throughout all 24 forecast hours at the offshore buoys. The mean forecast temperature at the buoys is about 3–4° too cold compared to the observed temperatures yielding a bias of the same magnitude (Fig. B2a). The combination of the cold bias and

21

a. Temperature and dew point temperature

RAMS generally produced a forecast temperature profile that is too stable throughout the troposphere for both XMR launch times. At 2315 UTC (11-h forecast), a cold bias occurs from the surface to about 625 mb whereas a slight warm bias is found above 625 mb (Fig. B6a). In the early morning forecast (23 h compared with the 1115 UTC sounding), RAMS still has a temperature profile that is too stable from about 950 mb to 625 mb; however, at the very lowest levels (surface to 950 mb), the bias profile shows that RAMS is not stable enough (Fig. B6b). A slight warm bias exists at the surface while at 950 mb the temperatures are too cold by nearly 3°C. This result suggests that on average, RAMS does not adequately predict the occurrence and/or intensity of nocturnal and early morning surface-based temperature inversions during the 1999-2000 cool season. This conclusion implied by the low-level bias profile is supported by the subjective verification of RAMS low-level temperature inversions, presented in Section 5.1.3.

In the dew point temperature forecasts, RAMS had the largest RMS errors at mid-levels (600–850 mb), the largest moist bias near the surface, and the largest dry bias in the 450–600 mb layer (11-h forecast shown in Fig. B7). The 23-h forecast exhibited similar characteristics but with a larger moist bias near the surface and a larger dry bias above 600 mb (not shown).

b. Winds

As a rule of thumb, the wind direction RMS errors decrease with height whereas the wind speed RMS errors increase with height. The 11-h RAMS forecast wind direction RMS error in Figure B8a shows a 50° RMS error near the surface, decreasing to about 10° near 300 mb. Meanwhile, a positive bias occurs at the surface with a general small negative bias above 950 mb (Fig. B8b). Consist with previous studies (Manobianco *et al.* 1996; Nutter and Manobianco 1999; Case 2000), the wind speed errors increase as wind speed increases. At 11 h (2300 UTC), the strongest mean wind speeds occur above 400 mb (Fig. B9a) corresponding to the greatest magnitude of errors (Figs. B9b-d). A positive bias in wind speed is evident very close to the surface while a negative wind speed bias prevails above 950 mb (Fig. B9c). Similar error patterns occur in the 23-h RAMS wind forecasts as well (not shown).

The individual wind component errors (not shown) indicate that RAMS consistently over-predicted the southerly (v-wind) component above 950 mb by 2 m s^{-1} or more for both the 11-h and 23-h forecasts. The predicted u-wind component experienced a negative (easterly) bias above 700 mb at 11 h, but exhibited no significant bias at 23 h (not shown).

4.1.4   Low Temperature Verification

As part of the 1999-2000 cool-season evaluation, the AMU was tasked to verify the RAMS forecast low temperatures on the innermost forecast grid. To accomplish this verification, the AMU developed an algorithm that identifies the lowest hourly forecast and observed surface temperature at the 1.8-m (6-ft) level for all available KSC/CCAFS wind towers. In addition, the lowest hourly observed and forecast temperature was identified at selected surface METAR stations, including Orlando (MCO), Daytona Beach (DAB), Melbourne (MLB), and the Shuttle Landing Facility (TTS). The subsequent lowest forecast hourly temperature was verified for every available station during all successful RAMS forecasts (both 0000 and 1200 UTC cycles). Only the results from the 0000 UTC forecast cycle are presented in this section.

The low temperature algorithm works as follows. The daily point forecast and observed temperatures at individual wind towers or METAR stations were examined between the hours of 0000 and 1200 UTC. Prior to identifying the lowest hourly temperature, data availability and QC checks were established to ensure a sufficient amount of quality data. For data availability, over half of the hourly data in the 0000–1200 UTC range must be present, and at least half of these existing files must contain the station of interest. For QC checks, a realism test and a simple temporal buddy check were used to ensure that unrealistic data values were not used in the statistics.

Table 4.3 summarizes the results of the low-temperature verification on RAMS grid 4 for the 0000 UTC RAMS cycle. The RMS errors for forecast low temperature range from 1.7°C at MLB to 2.5°C at DAB and the KSC/CCAFS wind towers. No significant bias occurs at any of the locations. The timing RMS errors fall between 3.0 h at MCO and 3.9 h at both DAB and MLB. The forecast low temperatures are typically reached too early at each of the METAR stations, indicated by the negative timing bias. However, the only timing biases comparable in magnitude to the frequency of available output (once per hour) occurred at DAB and MLB (-2.0

4.2.2 Summary of Upper-level Errors (XMR rawinsonde and 50-MHz profiler)

Table 4.5. Summary of the 4-grid RAMS upper-air error statistics for the 0000 and 1200 UTC forecast cycles during the 2000 Florida warm season. Upper-level winds were verified at the KSC/CCAFS 50 MHz profiler and XMR rawinsonde whereas the upper-level temperatures and dew point temperatures were verified at XMR only.

Variable	Forecast Cycle	RMS Error	Bias	Notable Errors
Temp (°C)	0000 UTC	1 to 4	-3.5 to 0.5	• Early morning is not stable enough in the lowest 50 mb (as in cool season). • A general cold bias at all levels, but largest at low levels. • The magnitudes of errors decrease with height.
	1200 UTC	1 to 3	-2.5 to 0.2	
Dew Point (°C)	0000 UTC	1.5 to 7	-2.5 to 1.5	• The largest RMS errors occur in mid-levels (600–800 mb). • Tendency towards a negative (dry) bias at low- and upper-levels with comparable magnitudes.
	1200 UTC	1 to 5.5	-2 to 0.5	
Wind Direction (deg.)	0000 UTC	20 to 60	-15 to 10	• At 50-MHz profiler: the largest errors occur during the afternoon hours between 2–6 km. • At XMR: the largest errors are found near the surface during the early morning hours. • An easterly (negative u-wind) bias is found at low levels. • A general southerly (positive v-wind) bias occurs at all levels, especially above 12 km at the 50-MHz profiler.
	1200 UTC	20 to 70	-20 to 20	
Wind Speed (m s⁻¹)	0000 UTC	1.5 to 7	-2 to 2	• The largest errors occur at upper-levels where wind speeds are strongest. • At XMR: a positive bias occurs in the lowest 100 mb. • A negative bias occurs above 850 mb.
	1200 UTC	1.8 to 7	-2 to 2	

4.2.3 Discussion of 2000 Warm Season Results

A brief discussion of the RAMS point forecasts is provided here for the 1200 UTC forecast cycle surface and upper-level error statistics on RAMS grid 4. Again, the analysis of surface errors focuses on the results from the KSC/CCAFS wind towers, but are also supplemented with standard METAR observational errors from grid 4 and the errors at the two buoys of Cape Canaveral, FL. All referenced graphical plots and figures in this section can be found in Appendix C.

4.2.3.1 Surface errors from 1200 UTC Cycle (KSC/CCAFS towers, METAR, buoys)

a. Temperature and dew point temperature

As in the 1999-2000 cool season, RAMS exhibits a surface-based cold temperature bias at all observational sensors on grid 4. The maximum magnitude of the cool bias during the 2000 warm season is about 1°C smaller than during the cool season, and predominantly a daytime phenomenon as well (particularly over land). Figures C1 and C2 summarize the evolution of the 1200 UTC surface temperature errors over the KSC/CCAFS wind towers and offshore buoys, respectively. The RMS error at the KSC/CCAFS wind towers peaks at the 8-h forecast (Fig. C1b) and the cold bias peaks between 8–11 h (Fig. C1c). At the offshore buoys, the RMS error and cold bias steadily increase from 1–9 h, then maintain a constant error thereafter (Fig. C2b,c). Interestingly,

the RMS error also increases from 650 mb down to the surface (Fig. C7b). The temperature errors are nearly constant above 650 mb in the 10-h forecast as well as the 3-h and 22-h forecasts (not shown). Except for the surface, the SD of the errors is nearly constant at about 1°C as a function of height for all three forecast times at about 1°C. Thus, the primary contributor to the growth of the total error at low levels is the model's systematic cold error.

The profile of dew point temperature errors during the 2000 warm season is also quite similar to the error profile during the 1999-2000 cool season. In all three forecast times verified at XMR, the dew point errors are smallest near the surface (1.5–3.0°C) and increase with height reaching a maximum of 5–6°C between 600–800 mb, then decrease above 600 mb (not shown). The errors are composed of primarily random variability since the SD is quite similar to the RMS error and the biases are small in magnitude relative to the RMS error.

b. *Winds*

The errors in wind speed and wind direction exhibit a similar pattern to the 1999-2000 cool-season errors, but the change in magnitude of the errors as a function of height is not as pronounced as the cool season, particularly with wind direction. In the lowest 2 km (roughly surface to 800 mb) at XMR, the magnitude of the wind speed errors increase slightly with time from about 2 m s^{-1} at the 3-h forecast to 2.5 m s^{-1} at the 10-h and 22-h forecasts (not shown). The wind speed errors are nearly constant with height in the lowest 2 km as well.

Above 2 km, the wind speeds can be verified against the 50-MHz DRWP on an hourly basis. Figure C8 shows a time-height cross section of RAMS wind speed errors at the 50-MHz DRWP location. By comparing the mean observed and forecast wind speeds in Figures C8a and b, it appears that the RAMS wind speeds are slightly weaker than the observed speeds. The plot in Figure C8d reveals a 1–2 m s^{-1} negative bias at nearly all levels particularly after the 12-h forecast. Meanwhile, the total error in Figure C8c depicts an increase in RMS error with height reaching a maximum between 12–14 km, corresponding to the axis of maximum observed wind speed.

The wind direction errors verified at XMR in the lowest 2 km (roughly surface to 800 mb) indicate that RAMS forecasts have the largest errors near the surface for the 3-h and 22-h forecasts (1500 and 1000 UTC respectively shown in Figs. C9a and C11a). At these times, the RMS error decreases with height from the surface to 800 mb. Meanwhile, the wind direction errors during the late afternoon, post-sea breeze regime have a much different profile between the surface and 800 mb (Fig C10). During the mean post-sea breeze regime, the wind direction RMS errors increase from about 30° near the surface to about 50–55° between 800–900 mb. This late-afternoon error structure could result from consist accurate predictions of the sea-breeze onset and propagation across east-central Florida near the surface (refer to the results of the east-coast sea-breeze subjective verification in Section 5.2.1), combined with uncertainty in the depth of the sea-breeze circulation.

The wind direction verification above 2 km at the 50-MHz profiler is shown in Figure C12. A general increase in the RMS error occurs in the first 6 forecast hours at nearly all vertical levels (Fig. C12a). Most of the errors are between 30–50° for all levels and forecast hours at the 50-MHz DRWP. The magnitude of the bias is typically 10° or less (Fig. C12b) and thus, substantially less than the magnitude of the RMS error. As a result, most of the errors are composed of random variability.

The wind component errors do not have many extraordinary characteristics that are substantially different from the wind speed and direction errors. The RMS errors increase with height for both wind components (as in the wind speed) and only a 1 m s^{-1} easterly bias occurs below 950 mb in the 10-h forecast at XMR (not shown). The v-wind component tends to have the largest bias at all times and levels, especially in the lowest levels of the atmosphere. Generally, a 1–2 m s^{-1} southerly bias is evident with the greatest bias occurring in the 10-h forecast below 800 mb at XMR (not shown).
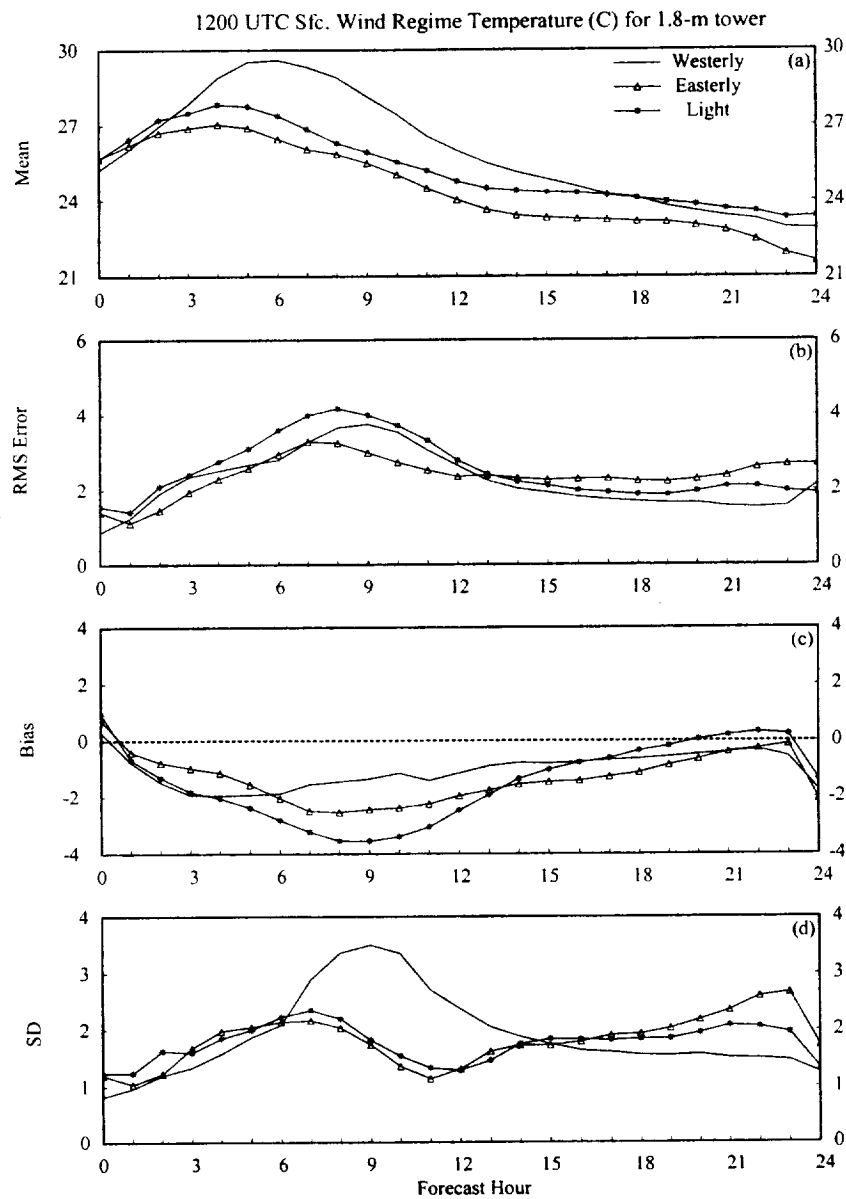
Figure 4.1. A meteogram plot of the 1200 UTC RAMS temperature errors (°C) during westerly, easterly, and light surface wind regimes for the 2000 Florida warm season. The temperature is verified at the 1.8-m level of the KSC/CCAFS wind-tower network. Parameters plotted as a function of forecast hour are a) mean forecast temperature under each wind regime, b) RMS error, c) bias, and d) error standard deviation.

Wind Direction

The results of the wind-regime classification reveal two very apparent characteristics of the wind direction errors. First, the westerly wind regime contains the largest RMS error during the afternoon and evening hours, likely associated with the higher frequency of convection under low-level westerly flow. Second, the light wind regime is the primary contributor to the relatively large RMS errors during the late night and early morning hours, as anticipated. Figures 4.2 and 4.3 show the wind direction RMS errors and biases for the 0000 and 1200 UTC forecast cycles, respectively. In both forecast cycles, the daytime errors are substantially larger associated with westerly wind flows compared to light or easterly winds. Under surface westerly wind flow, the 0000 UTC

1200 UTC Sfc. Wind Cycle Wind Dir (deg) for 16.5-m towers
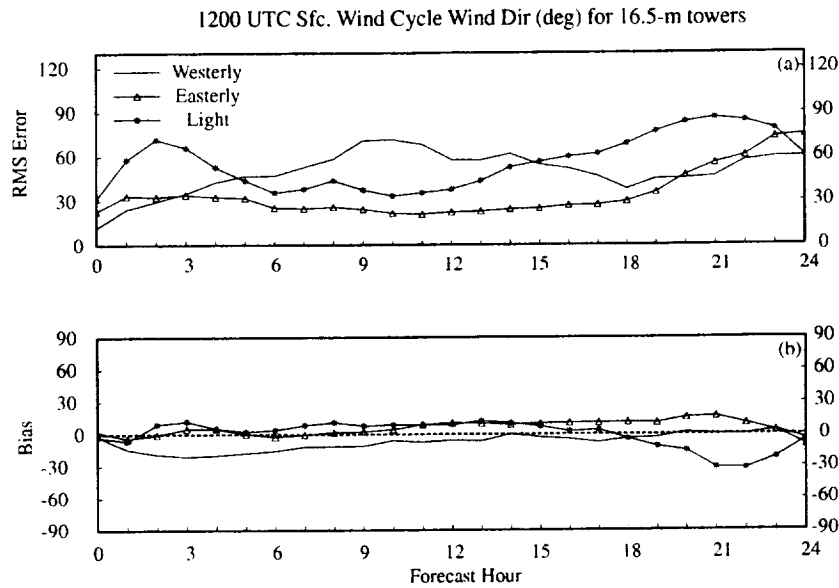
Figure 4.3. A meteogram plot of the 1200 UTC RAMS wind direction errors (deg.) during westerly (solid line), easterly (△), and light surface wind regimes (*) for the 2000 Florida warm season. The wind direction is verified at the 16.5-m level of the KSC/CCAFS wind-tower network. Parameters plotted as a function of forecast hour are a) RMS error, and b) bias.

Wind Components

The distribution of mean u-winds in the KSC/CCAFS wind tower network during the 0000 UTC cycle is shown in Figure 4.4a. By examining each of these mean wind flows, the mean forecast sea-breeze passage is evident at ~1300 UTC under easterly flow, ~1400 UTC under light flow, and ~1600–1700 UTC under westerly flow. Under westerly wind flow, the mean u-wind is between 0–2 m s^{-1} from 2–16 h, then becomes negative with the mean passage of the sea breeze thereafter. In light regimes, the u-wind approaches zero at about 12 h, but generally maintains an easterly component at all hours. Meanwhile under easterly surface flow, the mean u-wind remains under -2 m s^{-1} at all hours. RAMS predicts easterly flow following the mean sea-breeze passage with nearly the same intensity in both the light and easterly wind regimes (Fig. 4.4a).

While no dramatic variations are evident in the v-wind errors under different wind regimes (not shown), the u-wind errors show some interesting behavior in both the 0000 and 1200 UTC forecast cycles. In the 0000 UTC cycle, the largest u-wind RMS errors occur after 15 h under westerly flow (Fig. 4.4b). The light wind regime has somewhat smaller errors while the easterly wind flow has the smallest errors of all three regimes during the afternoon and evening hours. All three regimes have comparable errors between 0–15 h. A similar pattern is evident in both the bias and SD plots in Figures 4.4c and d. A negative (easterly) bias occurs in all regimes, especially after 15 h, but is largest under westerly flow and smallest in easterly flow. Similarly, the SD (random) errors are by far the largest under westerly flow and smallest in easterly flow. The v-wind random errors are generally largest under westerly flow during the afternoon hours as well (not shown).

This relatively large random u-wind error during westerly flow could be the result of two factors. First, when surface winds are sufficiently strong from the west, the ECSB typically remains close to the east coast of Florida within the KSC/CCAFS wind-tower domain. If the RAMS model has just a small error in the location or timing of the ECSB then large random errors in the u-wind can result in the wind-tower network. Second, as mentioned previously, convection is most prevalent in east-central Florida under westerly flow since the focusing mechanism for convection (i.e. the ECSB) remains near KSC/CCAFS. Errors between observed and model-predicted convection can also lead to large random wind errors. Similar features in the u-wind errors are also found in the 1200 UTC cycle (Fig. 4.5); however, the biases are nearly identical compared to the 0000 UTC forecasts. Again, the random u-wind errors are largest under westerly flow in the 1200 UTC cycle (Fig. 4.5d).

31

1200 UTC Sfc. Wind Regime u-wind (m/s) for 16.5-m towers
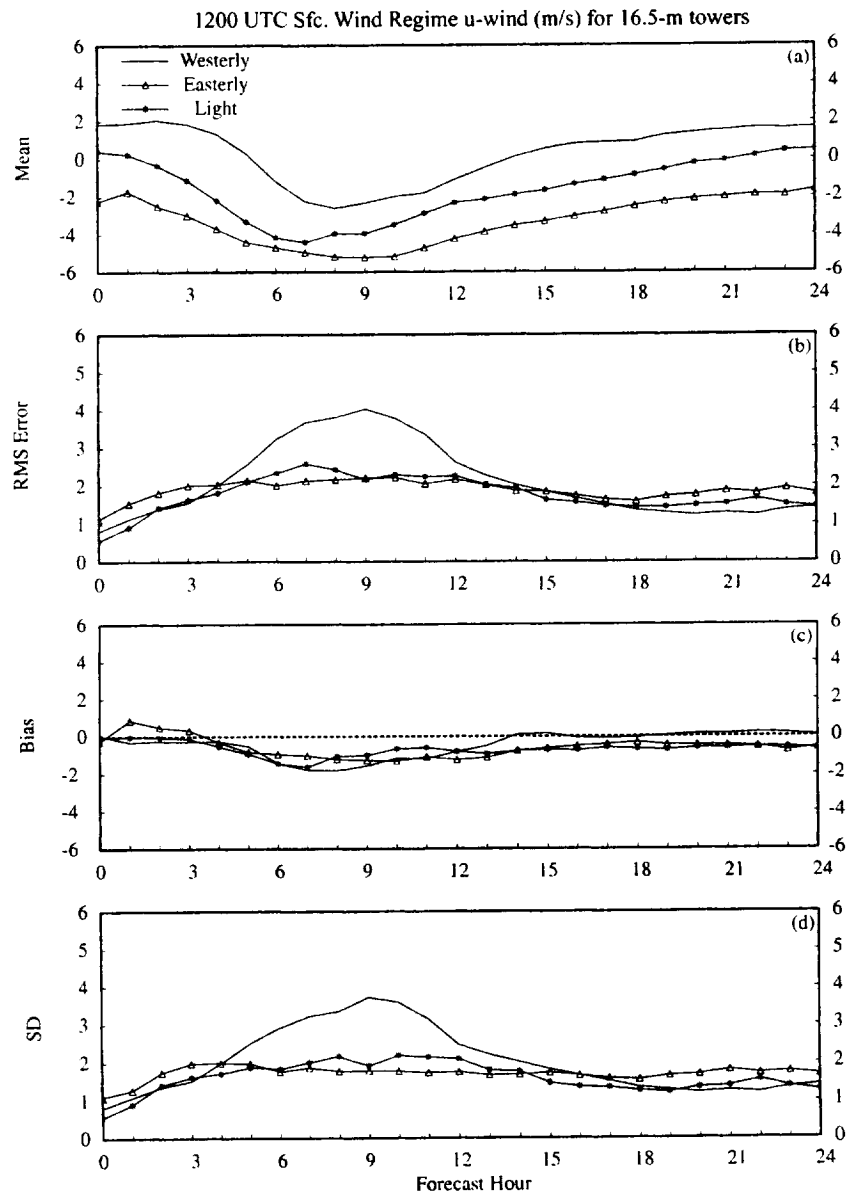
Figure 4.5. A meteogram plot of the 1200 UTC RAMS u-wind component errors (m s^{-1}) during westerly (solid line), easterly (△), and light surface wind regimes (*) for the 2000 Florida warm season. The u-wind is verified at the 16.5-m level of the KSC/CCAFS wind-tower network. Parameters plotted as a function of forecast hour are a) mean forecast u-winds under each wind regime, b) RMS error, c) bias, and d) error standard deviation.

4.3.2 Thunderstorm Regime

For the thunderstorm day regime classification, the RAMS forecasts were grouped together according to the observed versus forecast thunderstorm days using the subjective thunderstorm verification results (Section 5.2.3). A contingency table of the daily thunderstorm occurrence during the 1500–2300 UTC time frame was developed for both the 0000 and 1200 UTC forecast cycles as part of the subjective evaluation scheme (Table 4.7). The forecasts composing each quadrant of the 0000 and 1200 UTC contingency tables were grouped together and point forecast error statistics at the KSC/CCAFS wind towers were calculated separately for each

1200 UTC Thunder Regime Temperature (C) for 1.8-m towers
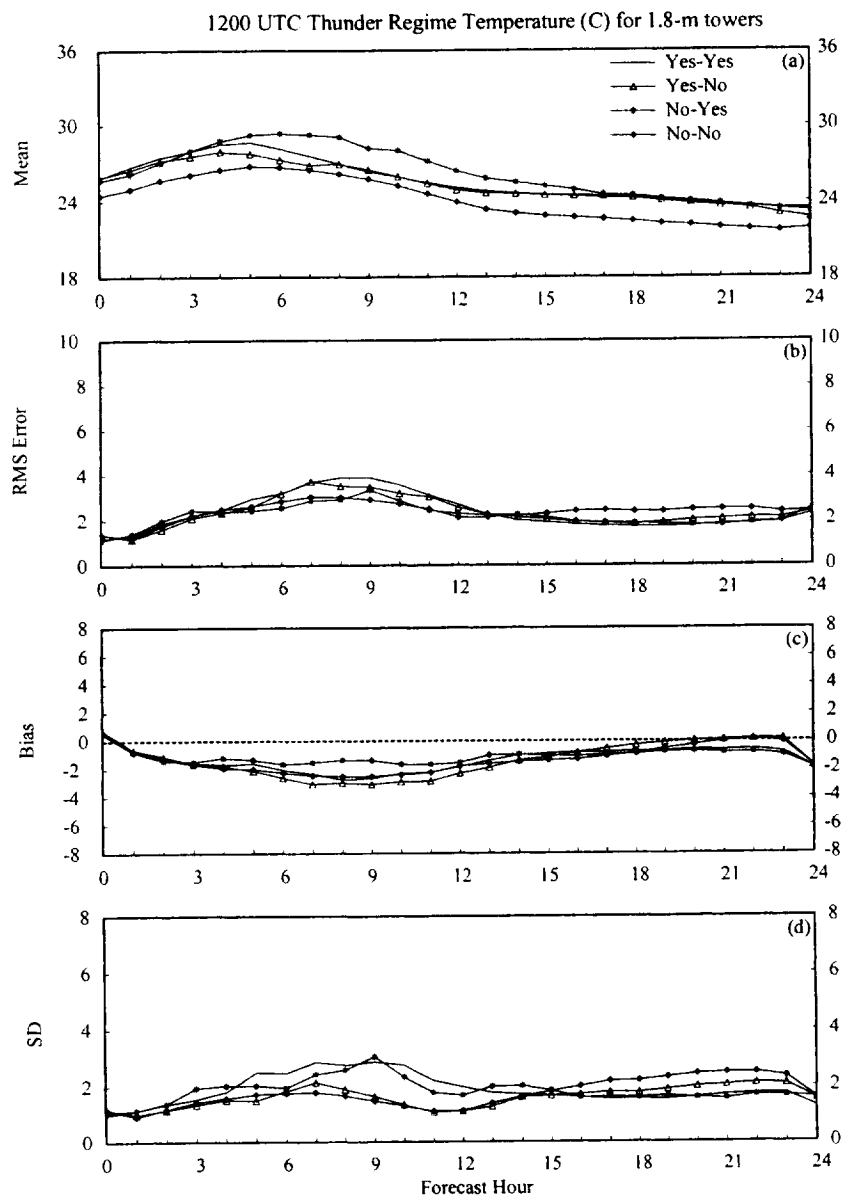
Figure 4.6. A meteogram plot of 1200 UTC RAMS temperature errors (°C) during the four contingency combinations of thunderstorm forecasts (yes-yes, yes-no, no-yes, no-no) for the 2000 Florida warm season. The temperatures are verified at the 1.8-m level of the KSC/CCAFS wind-tower network. Parameters plotted as a function of forecast hour are a) mean forecast temperatures, b) RMS error, c) bias, and d) error standard deviation (SD).

4.4 Comparison between 4-grid and 3-grid RAMS Configurations

This section presents the results from a comparison between the 4-grid RAMS and a 3-grid configuration of RAMS, where grid 4 was withheld. This experiment was conducted to determine the impact of a reduction in horizontal resolution of the innermost grid on objective error statistics. The error statistics are compared at the KSC/CCAFS wind towers for the surface, and at XMR and the 50-MHz DRWP for upper-levels. Since the 50-MHz DWRP data were not of sufficient quality during the 1999-2000 cool season, these errors are not shown.

4.4.1 1999-2000 Cool Season

4.4.1.1 Summary of 1200 UTC Surface Errors (KSC/CCAFS wind towers)

Table 4.8. Summary of the 4-grid/3-grid RAMS error comparison at the KSC/CCAFS wind towers for the 1200 UTC forecast cycle during the 1999-2000 Florida cool season. Temperature and dew point errors are valid at 1.8 m whereas wind direction and speed errors are valid at 16.5 m.

Variable	Config.	RMS Error	Bias	Notable Errors
Temp (°C)	4-grid	1.5 to 4.5	-3.5 to 1	• Similar errors at all times, but slightly larger in the 3-grid forecasts during the day.
	3-grid	1.5 to 5	-4 to 1	• Both configurations have notable daytime cold biases.
Dew Point (°C)	4-grid	1.5 to 3.5	-1.5 to 1	• A slightly larger daytime RMS error and dry bias occurs in the 3-grid forecasts.
	3-grid	1.5 to 3.5	-2 to 0.5	• The 4-grid has a slightly more moist bias during the nocturnal hours.
Wind Direction (deg.)	4-grid	15 to 60	-20 to 15	• Errors are virtually identical at all forecast hours.
	3-grid	15 to 60	-20 to 20	
Wind Speed (m s⁻¹)	4-grid	1.2 to 2	-0.5 to 0.8	• A slightly higher positive bias occurs in the 3-grid forecasts; otherwise, the errors are nearly the same.
	3-grid	1.2 to 2.3	0 to 1.5	

4.4.1.2 Summary of 1200 UTC Upper-level Error (XMR rawinsonde)

Table 4.9. Summary of the 4-grid/3-grid RAMS error comparison at the XMR rawinsonde site for the 1200 UTC forecast cycle during the 1999-2000 Florida cool season.

Variable	Config.	RMS Error	Bias	Notable Errors
Temp (°C)	4-grid	1 to 4	-3 to 1	• Slightly larger errors occur in the 3-grid forecasts below 900 mb.
	3-grid	1 to 4.5	-4 to 1	• All other errors are very similar.
Dew Point (°C)	4-grid	1 to 8	-4 to 2	• A larger error occurs in the 4-grid forecasts below 900 mb, due to greater moist bias.
	3-grid	1 to 8	-3 to 2	• Both configurations tend to have a dry bias above 900 mb. • Largest errors are in the 600–800 mb layer.
Wind Direction (deg.)	4-grid	10 to 55	-15 to 25	• Both forecasts have the smallest errors at upper levels and largest errors at low levels.
	3-grid	10 to 55	-15 to 20	• Largest RMS error differences are ~10–15° between 800–1000 mb.
Wind Speed (m s⁻¹)	4-grid	2.5 to 6	-2.5 to 2	• Errors increase with height in both forecasts. • The 3-grid forecasts have a more negative bias in the upper levels at the 11-h forecast.
	3-grid	2.5 to 5.5	-3.5 to 1.5	

1200 UTC 3/4-grid Cycle Temperature (C) for 1.8-m towers

Figure 4.8. A meteogram plot that displays a comparison between the 1200 UTC forecast cycle surface temperature errors (°C) from the 4- and 3-grid RAMS configurations during the 1999-2000 Florida cool season. Surface temperatures are verified at the 1.8-m level of the KSC/CCAFS wind tower network. Parameters plotted as a function of forecast hour are a) mean observed, mean 4-grid forecast, and mean 3-grid forecast temperature, b) RMS error, c) bias, and d) error standard deviation (SD). The plotting convention is a solid line for the 4-grid forecasts, dot-dashed line for the 3-grid forecasts, and a dashed line for observed values.

1200 UTC 3/4-grid Cycle Wind Dir (deg) for 16.5-m towers

Figure 4.10. A meteogram plot that displays a comparison between the 1200 UTC forecast cycle near-surface wind direction errors (degrees) from the 4-grid and 3-grid RAMS configurations during the 1999-2000 Florida cool season. Wind direction is verified at the 16.5-m level of the KSC/CCAFS wind tower network. Parameters plotted as a function of forecast hour are a) RMS error and b) bias. The plotting convention is a solid line for the 4-grid errors and a dot-dashed line for the 3-grid errors.

b.   Upper-level Errors from 1200 UTC Cycle (XMR rawinsonde)

As in Section 4.1.3.2, the XMR soundings taken at 2315, and 1115 UTC are used to verify temperature and dew point temperature forecasts for the 11-h, and 23-h forecasts, respectively. The 50-MHz DRWP is not used to verify winds because of the unreliable data during the 1999-2000 cool season. This brief discussion will only examine error statistics at XMR for the 11-h forecast valid at 2300 UTC.

1.   Temperature and dew point temperature

Similar to the surface error statistics, only minor differences occur in the upper-level temperature and dew point temperature error statistics. Figure 4.11 shows that the vertical profiles of the temperature RMS error and bias for the 4-grid and 3-grid forecasts generally exhibit small differences. Both configurations contain a low-level cold bias below 600 mb, reaching a maximum at about 975 mb (Fig. 4.11c). The greatest differences in RMS error occur above 800 mb where the 3-grid errors are about 0.5°C smaller than the 4-grid errors (Fig. 4.11b), resulting from differences in the random error component (SD in Fig. 4.11d). The temperature error profiles do not change substantially by 23 h in either model configuration (not shown).

The profiles of dew point temperature errors indicate that the 4-grid RAMS forecasts tend to have a greater moist bias at the lowest levels below 950 mb whereas the 3-grid forecasts tend to have larger RMS errors between 600–700 mb (not shown). Both plots are quite noisy with widely changing errors with height. The largest errors are found between 600–800 mb in both forecasts and the patterns are generally quite similar (not shown).

2.   Winds

Once again, only minor differences occur between the 4-grid and 3-grid error statistics of upper-level winds. The wind direction RMS errors in both RAMS configurations decrease with height at the 11-h and 23-h forecast times (not shown). These errors are typically within 10° of each other at all levels. The wind speed errors have the greatest variation at upper levels where the errors are largest in both model configurations; however, these

41

Figure 4.12. Vertical profiles of wind speed errors (m s⁻¹) at XMR for the 11-h forecast displaying a comparison between the 4- and 3-grid configurations of RAMS from the 1200 UTC forecast cycle during the 1999-2000 Florida cool season. Parameters plotted as a function of pressure are a) mean observed, mean 4-grid forecast, and mean 3-grid forecast wind speed, b) RMS error, c) bias, and d) error standard deviation (SD). The plotting convention is a solid line for the 4-grid forecasts, dot-dashed line for the 3-grid forecasts, and a dashed line for observed values.

43

4.4.2.3 Discussion of 4-grid/3-grid Comparison

a. Surface Errors from 1200 UTC Cycle (KSC/CCAFS wind towers)

1. Temperature and dew point temperature

Unlike the 1999-2000 cool-season results, the 4-grid/3-grid comparison during the 2000 warm season yields some substantial differences between the model configurations. The most significant difference between the operational 4-grid and the 3-grid forecasts is the much larger surface temperature and dew point temperature errors of the 3-grid configuration caused in part by a more substantial cold, dry bias in the 3-grid forecasts. The differences between the two forecasts begin during the daylight hours and continue to increase during the remaining time out to 24 forecast hours. Figure 4.13 shows the error comparison between the 4-grid and 3-grid forecast temperatures at the KSC/CCAFS wind towers. After 3 h, the magnitude of the 3-grid RMS error, bias, and SD all exceed the 4-grid forecasts, typically by 1–2°C or more. Whereas the 4-grid errors decrease somewhat in magnitude during the overnight hours after 12 h, the 3-grid forecast errors do not taper as significantly overnight. In fact, after 20 h, the 3-grid RMS error increases further due to the increase in random errors (Figs. 4.13b and d).

The differences in dew point temperature errors are even more substantial than the temperature errors. Figure 4.14 illustrates the dramatic growth in the 3-grid dew point temperature errors after 2 h. Between 2–5 h, the dew point RMS error jumps from 2–8°C in the 3-grid forecasts while staying at about 2°C in the 4-grid forecasts (Fig. 4.14b). This 3-grid RMS error is composed of a dry bias of -5° to -6°C (peaking at 5 h and 24 h in Fig. 4.14c) and a random error peaking at 6–7.5°C at 5 h, and again after 20 h (Fig. 4.14d). Meanwhile, the 4-grid dew point temperature errors are considerably smaller during all forecast hours, with a maximum RMS error slightly greater than 2°C, a bias near -1°C, and a SD at about 2°C (Figs. 4.14b-d). The cause of these much larger errors in the 3-grid forecasts is not known.

2. Winds

In general, the surface wind errors are quite similar in the 4-grid and 3-grid RAMS forecasts during the 2000 warm season. The RMS errors in wind direction are nearly identical during the first 4 h and afterwards, the 3-grid RMS errors are generally 5–10° larger (Fig. 4.15a). The wind direction biases are virtually the same until 13 h, after which they deviate by 10–20° (Fig. 4.15b); however, this deviation after 13 h is small compared to the magnitude of the RMS error during these hours. The only substantial difference in the wind speed errors is a slightly larger positive wind speed bias by 0.5–1.0 m s^{-1} in the operational 4-grid forecasts during the daylight hours (not shown). This difference in wind speed bias is caused by a greater easterly bias in the 4-grid forecasts (negative u-wind bias, also not shown).
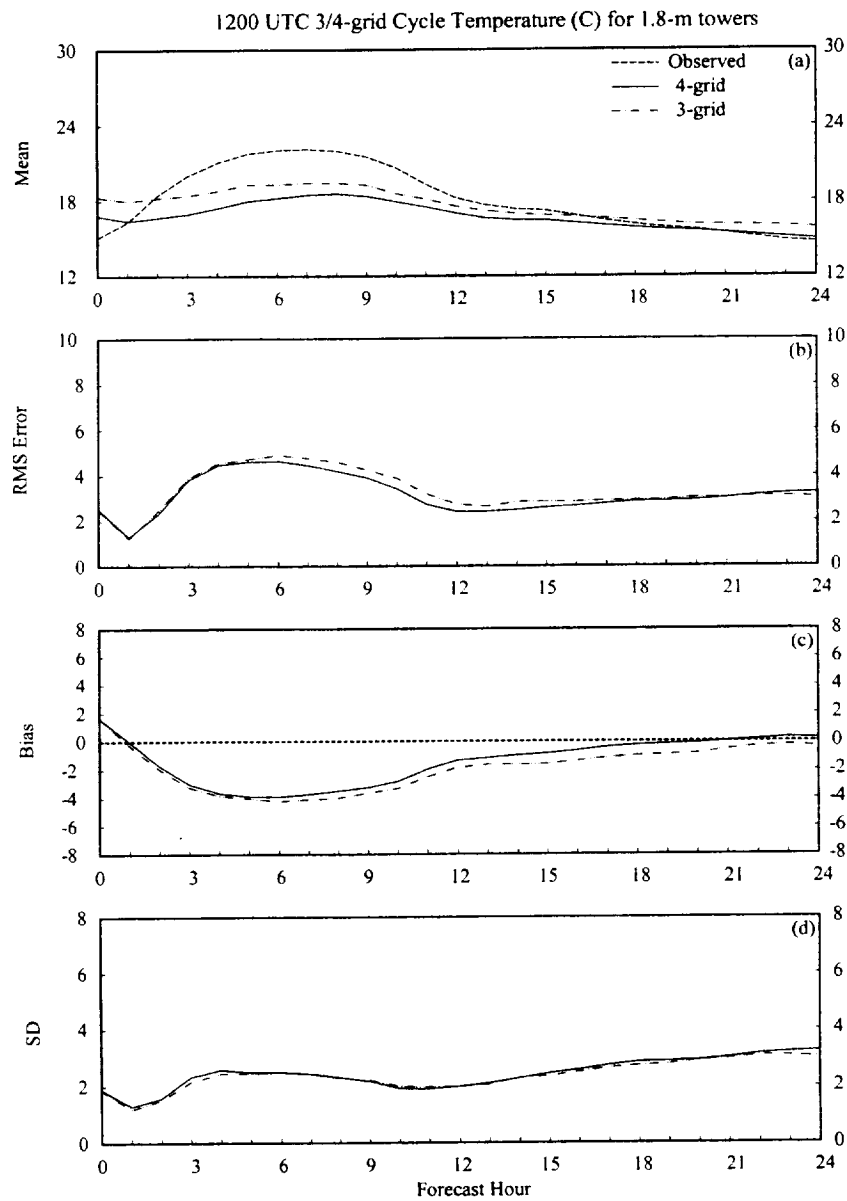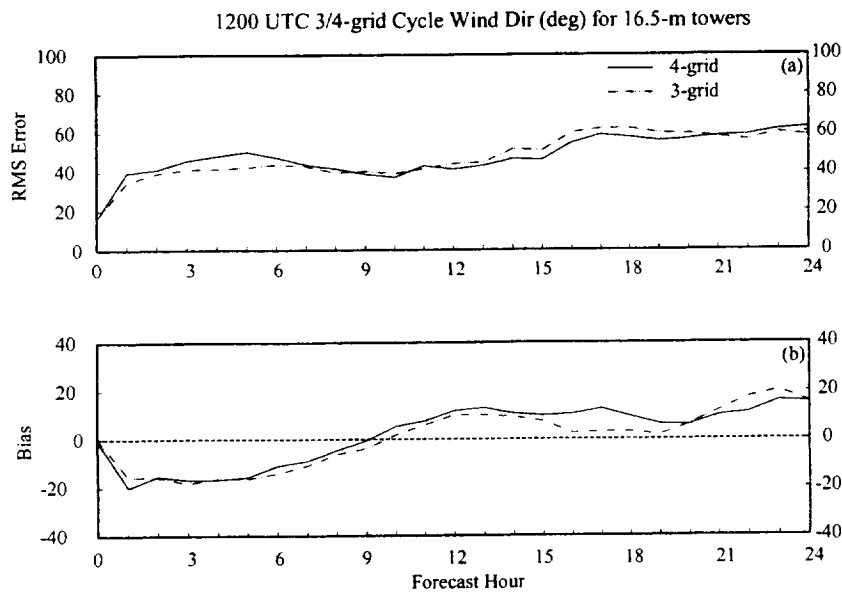
1200 UTC 3/4-grid Cycle Dew point (C) for 1.8-m towers

Figure 4.14. A meteogram plot that displays a comparison between the 1200 UTC forecast cycle surface dew point temperature errors (°C) from the 4- and 3-grid RAMS configurations during the 2000 Florida warm season. Surface dew point temperatures are verified at the 1.8-m level of the KSC/CCAFS wind tower network. Parameters plotted as a function of forecast hour are a) mean observed, mean 4-grid forecast, and mean 3-grid forecast dew point temperature, b) RMS error, c) bias, and d) error standard deviation (SD). The plotting convention is a solid line for the 4-grid forecasts, dot-dashed line for the 3-grid forecasts, and a dashed line for observed values.

47

The only substantial differences in errors occurs below 900 mb where a larger RMS error by about 1 m s^{-1} is found in the operational 4-grid forecasts (Fig. 4.17b). This difference in RMS error is almost entirely attributed to a larger positive wind speed bias in the 4-grid forecasts compared to the 3-grid configuration (Fig. 4.17c).

The upper-level wind direction errors are within 0–10° of each other at all times and levels for both the 50-MHz DRWP and the XMR rawinsonde (not shown). Also not shown are the individual wind component errors, which have only minor differences throughout the troposphere.

4.4.3   Summary of 4-grid/3-grid Error Comparison

The collective results from the 4-grid/3-grid comparison during the 1999-2000 cool, and 1999 and 2000 warm seasons suggest the following about the RAMS model in east-central Florida:

- Running a higher-resolution configuration of RAMS results in a significant improvement in the surface temperature and moisture error statistics during the warm season, but not during the cool season.

- The error comparison does not yield a noticeable improvement in the surface and upper-level wind error statistics during both seasons.

- During the warm season, the higher resolution configuration of RAMS tends to over predict wind speeds at the surface and lower levels of the atmosphere.

Additional subjective evaluations in Section 5 will help to illustrate the total benefit of running the higher resolution, operational configuration of RAMS, particularly with respect to sea-breeze forecasts within the KSC/CCAFS wind-tower network.
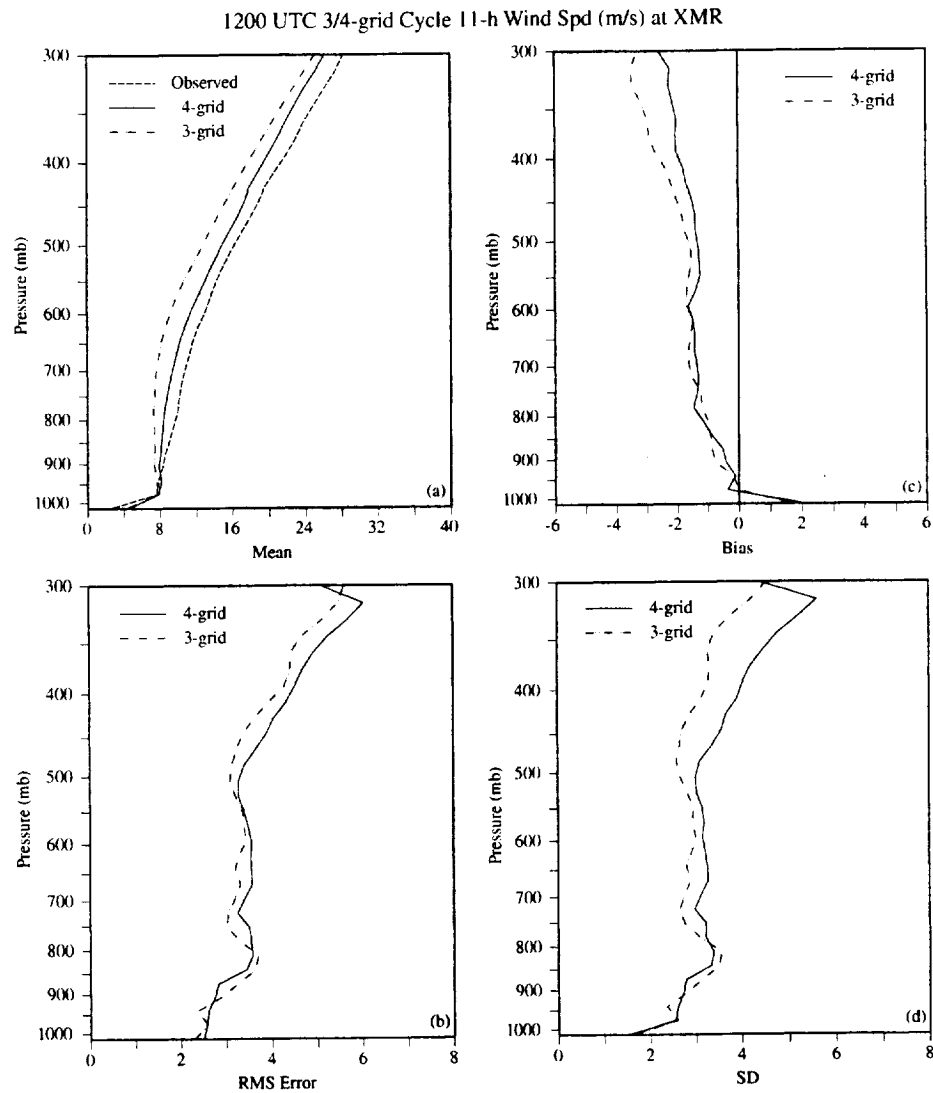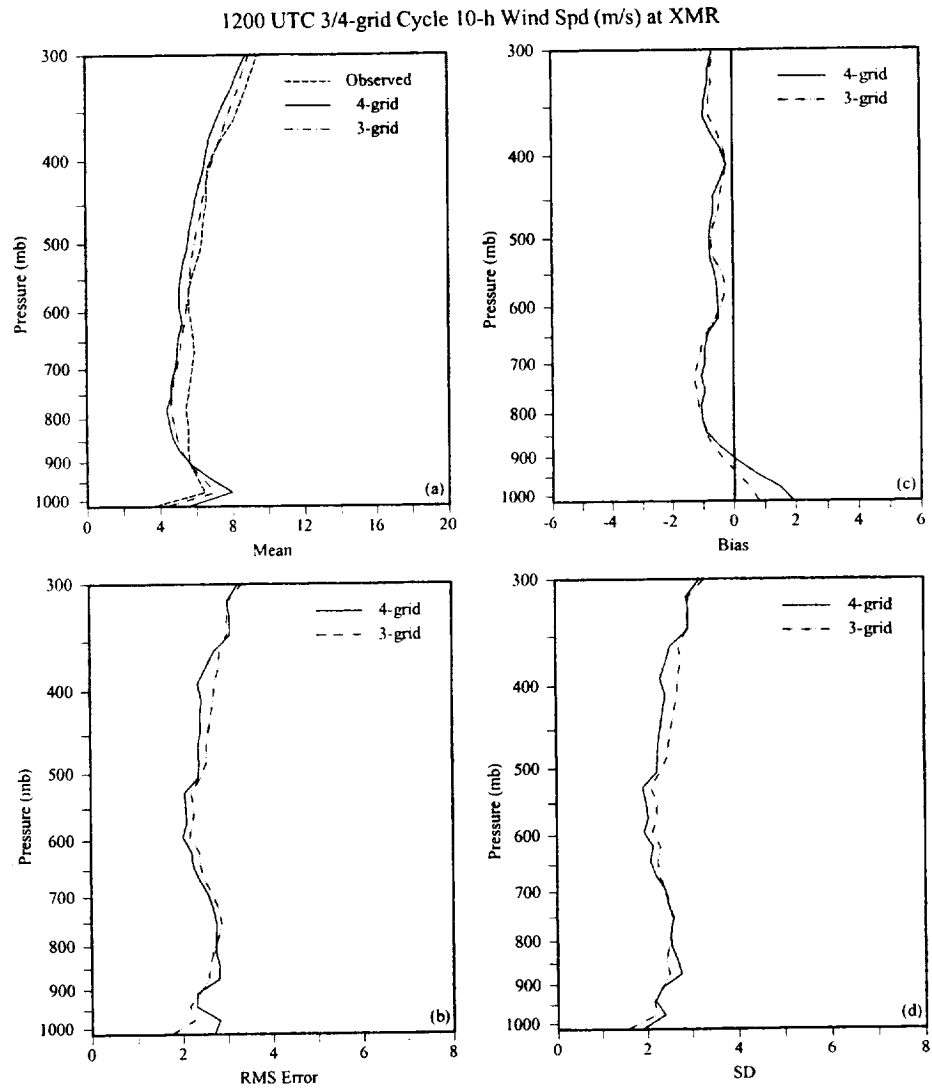
Figure 4.17. Vertical profiles of wind speed errors (m s^{-1}) at XMR for the 10-h forecast displaying a comparison between the 4- and 3-grid configurations of RAMS from the 1200 UTC forecast cycle during the 2000 Florida warm season. Parameters plotted as a function of pressure are a) mean observed, mean 4-grid forecast, and mean 3-grid forecast wind speed, b) RMS error, c) bias, and d) error standard deviation (SD). The plotting convention is a solid line for the 4-grid forecasts, dot-dashed line for the 3-grid forecasts, and a dashed line for observed values.

(Fig. 4.18b). At all other forecast hours, the RMS errors are nearly identical, generally 2–3°C. The larger RAMS RMS errors are attributed to the marked daytime cold bias (Fig. 4.18c) and a larger random error component as well (Fig. 4.18d). Unlike the meso-Eta evaluation results in Nutter and Manobianco (1999), the Eta model exhibits a warm bias of about 1–2°C at most forecast hours, but the magnitude of the Eta warm bias is significantly less than the magnitude of the RAMS daytime cold bias. However, the Eta retains its warm bias at night while the RAMS bias diminishes to zero by 17 h (Fig. 4.18c).

Both models generally have a slight moist bias in forecast dew point temperature as indicated by Figure 4.19. During all 24 forecast hours, the RAMS and Eta models have nearly identical RMS errors and biases (Figs. 4.19b-c). The most notable differences are found in the random error between 12–24 h. The RAMS SD is about 1–2°C larger than the Eta during these forecast hours (Fig. 4.19d). Other than this minor difference, the errors are nearly the same during all forecast hours.

b. Winds

The major difference in the wind errors is due to a substantial positive bias in the Eta wind speed forecasts at 10 m. Since about November 1999, NCEP has experienced a post-processing problem that resulted in a significant positive wind speed bias in the Eta point forecasts, especially for stations at low elevations near sea level. This problem has resulted in wind speed biases on the order of 3–4 m s^{-1} in the Eta point forecast at TTS for both the 1999-2000 cool and 2000 warm season. These wind speed biases are not representative of the actual Eta forecasts since this problem is purely a post-processing issue. Because of this problem in the Eta wind speed forecasts, the wind speed error plots will not be shown in this report. Please refer to http://www.emc.ncep.noaa.gov/mmb/research/nearsfc/statsbyvblmod.html for additional information and bias plots for the Eta 48-h forecasts.

The wind direction errors show that RAMS generally has slightly larger RMS errors by about 5–15°, mainly after 3 h (Fig. 4.20a). The most significant differences in wind direction RMS errors occur between 18–21 h (overnight hours). The biases indicate that the Eta model typically has a near zero or small positive bias whereas RAMS experiences a negative bias during the first 8 hours (Fig. 4.20b). After 8 h, the RAMS and Eta biases are very similar. The magnitudes of the bias in both models are small relative to the total error and thus, do not indicate any substantial systematic error in wind direction.

The u-wind plots in Figure 4.21 show the tendency for RAMS to develop more of an easterly bias (negative u-wind bias) compared to the Eta model during the 1999-2000 cool season. Between 9–24 h, RAMS has about a -1 m s^{-1} u-wind bias whereas the Eta model has only a slight negative bias (Fig. 4.21c). The much larger RMS error and SD in the Eta model are indicative of the wind speed problem mentioned above (Figs. 4.21b and d). The v-wind biases are near zero for both the RAMS and Eta models (not shown).
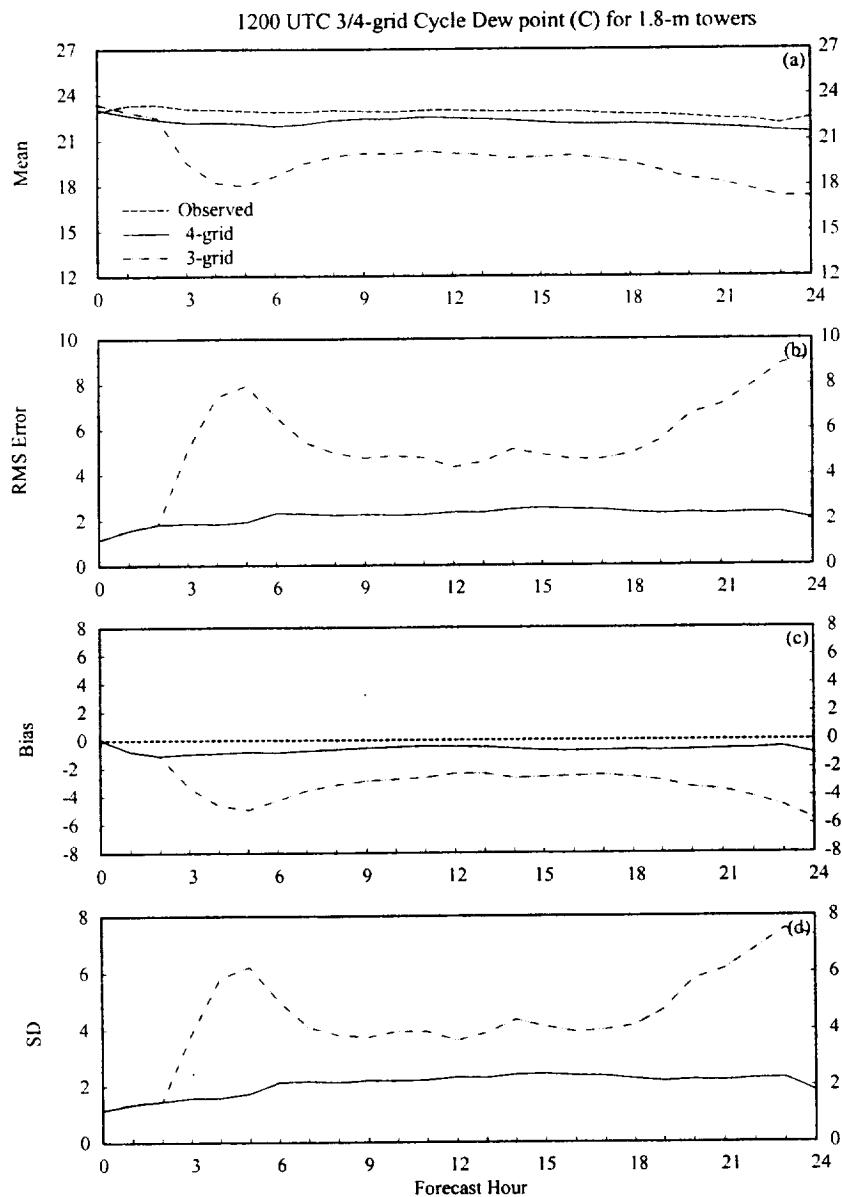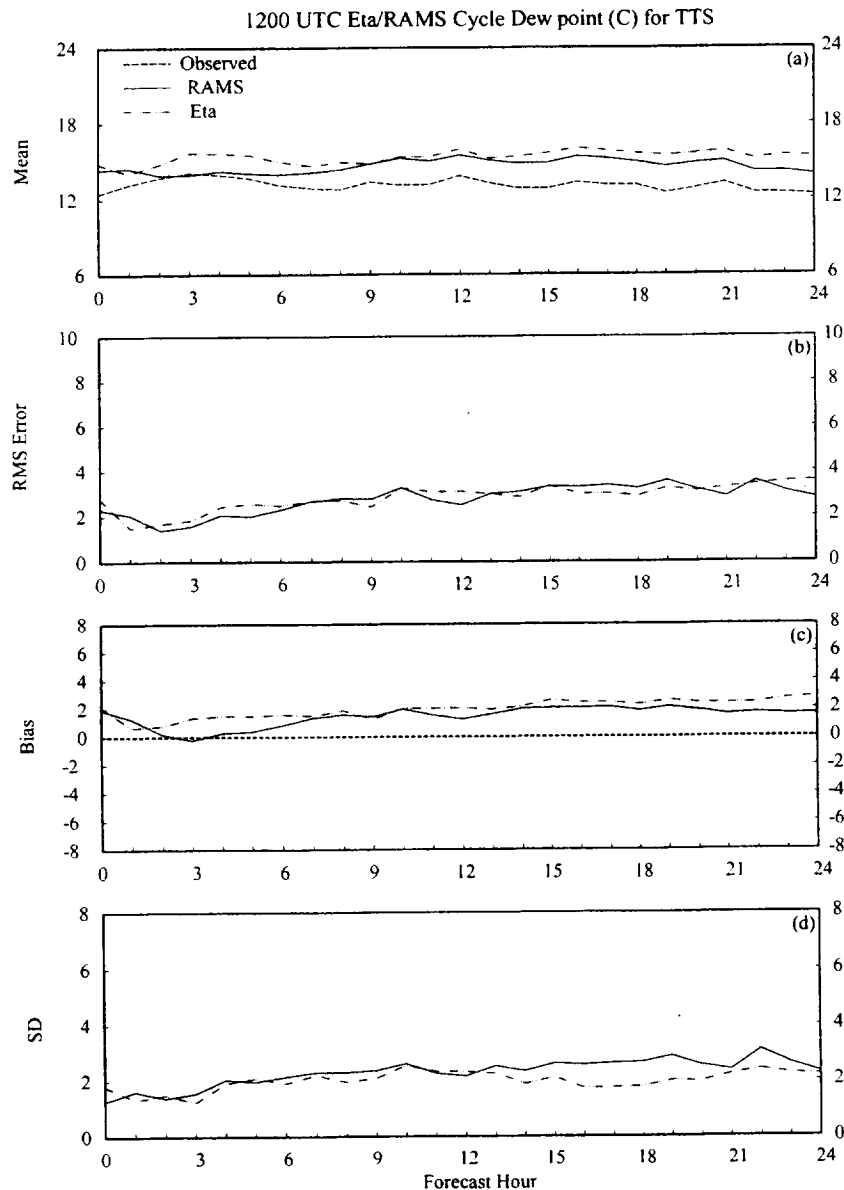
Figure 4.19. A meteogram plot that displays a comparison between the 1200 UTC forecast cycle surface dew point temperature errors (°C) from the RAMS operational configuration and the Eta model during the 1999-2000 Florida cool season. Surface dew point temperatures are verified at TTS only. Parameters plotted as a function of forecast hour are a) mean observed, mean RAMS forecast, and mean Eta forecast dew point temperature, b) RMS error, c) bias, and d) error standard deviation (SD). The plotting convention is a solid line for the RAMS forecasts, dot-dashed line for the Eta model, and a dashed line for observed values.

1200 UTC Eta/RAMS Cycle u-wind (m/s) for TTS
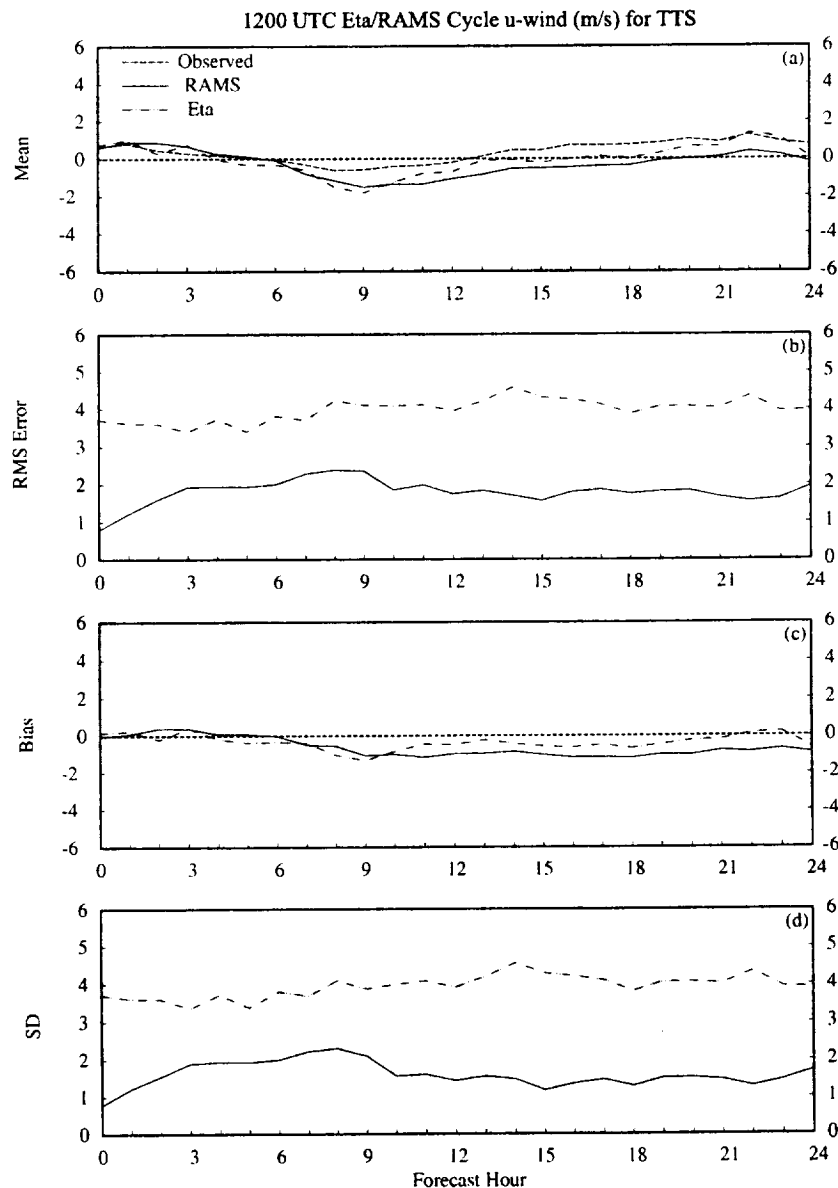
Figure 4.21. A meteogram plot that displays a comparison between the 1200 UTC forecast cycle u-wind component errors (m s⁻¹) from the RAMS operational configuration and the Eta model during the 1999-2000 Florida cool season. The u-wind component is verified at TTS only. Parameters plotted as a function of forecast hour are a) mean observed, mean RAMS forecast, and mean Eta forecast u-wind, b) RMS error, c) bias, and d) error standard deviation (SD). The plotting convention is a solid line for the RAMS forecasts, dot-dashed line for the Eta model, and a dashed line for observed values.

The biases of the u- and v-wind components are shown in Figure 4.25 and indicate that the Eta model has a substantial southerly and easterly bias compared to RAMS. The magnitudes of the Eta point forecast biases are likely exaggerated due to the high wind speed bias resulting from the post-processing problem. Nonetheless, the Eta model exhibits an easterly bias between forecast hours 0 and 18 (Fig. 4.25a), and a southerly bias after the 6-h forecast (Fig. 4.25b). The RAMS u-wind plot shows a small bias of 0.5–1.0 m s^{-1} between 5–14 h (Fig. 4.25a) and virtually no bias in the v-wind component (Fig. 4.25b). Thus, at the very least, the RAMS point forecasts at TTS result in an improvement in the v-wind component bias that occurs in the Eta model.
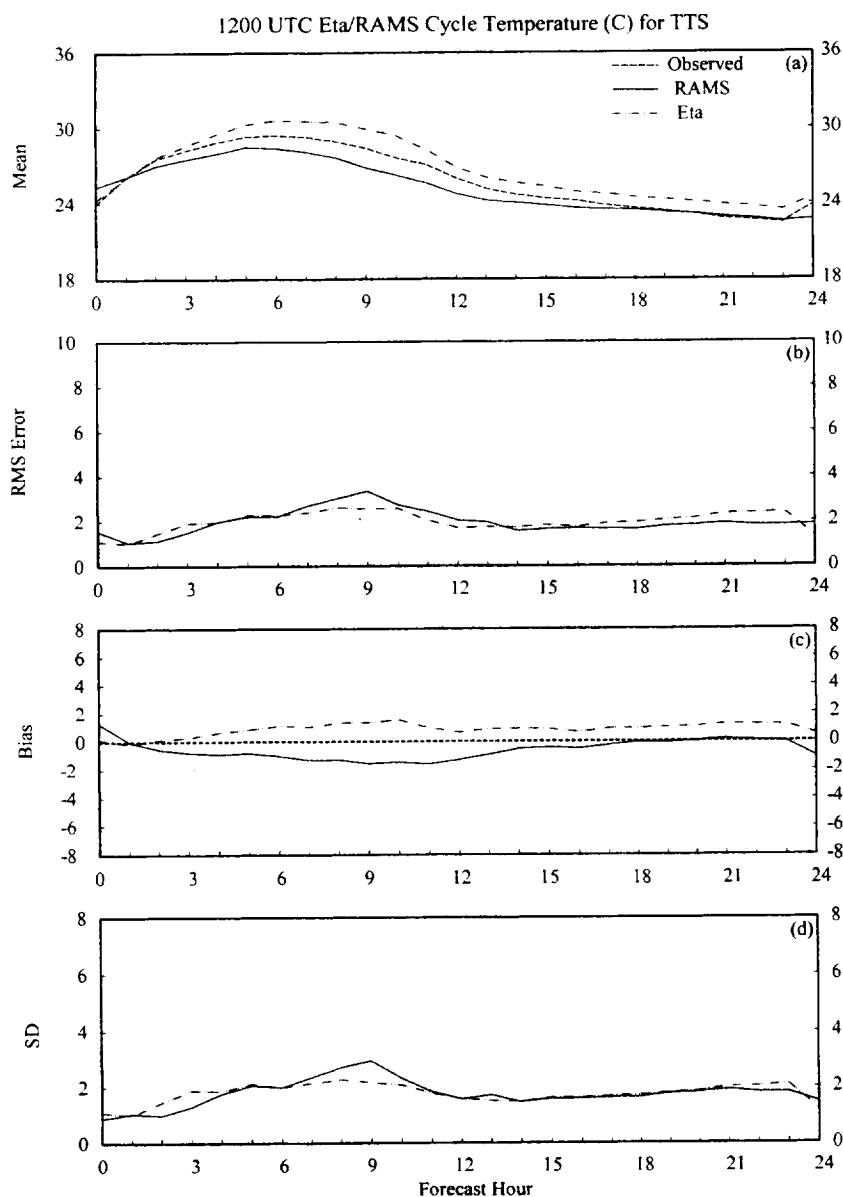
Figure 4.22. A meteogram plot that displays a comparison between the 1200 UTC forecast cycle surface temperature errors (°C) from the RAMS operational configuration and the Eta model during the 2000 Florida warm season. Surface temperatures are verified at TTS only. Parameters plotted as a function of forecast hour are a) mean observed, mean RAMS forecast, and mean Eta forecast temperature, b) RMS error, c) bias, and d) error standard deviation (SD). The plotting convention is a solid line for the RAMS forecasts, dot-dashed line for the Eta model, and a dashed line for observed values.

59

1200 UTC Eta/RAMS Cycle Wind Dir (deg) for TTS
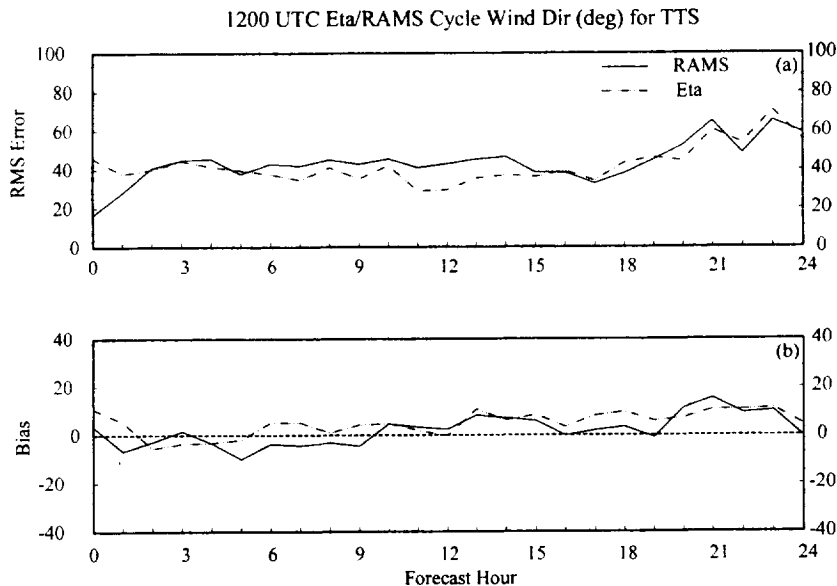
Figure 4.24. A meteogram plot that displays a comparison between the 1200 UTC forecast cycle surface wind direction errors (degrees) from the RAMS operational configuration and the Eta model during the 2000 Florida warm season. Surface wind direction is verified at TTS only. Parameters plotted as a function of forecast hour are a) RMS error and b) bias. The plotting convention is a solid line for the RAMS errors and a dot-dashed line for the Eta model errors.

1200 UTC Eta/RAMS Cycle u/v-wind Bias (m/s) for TTS
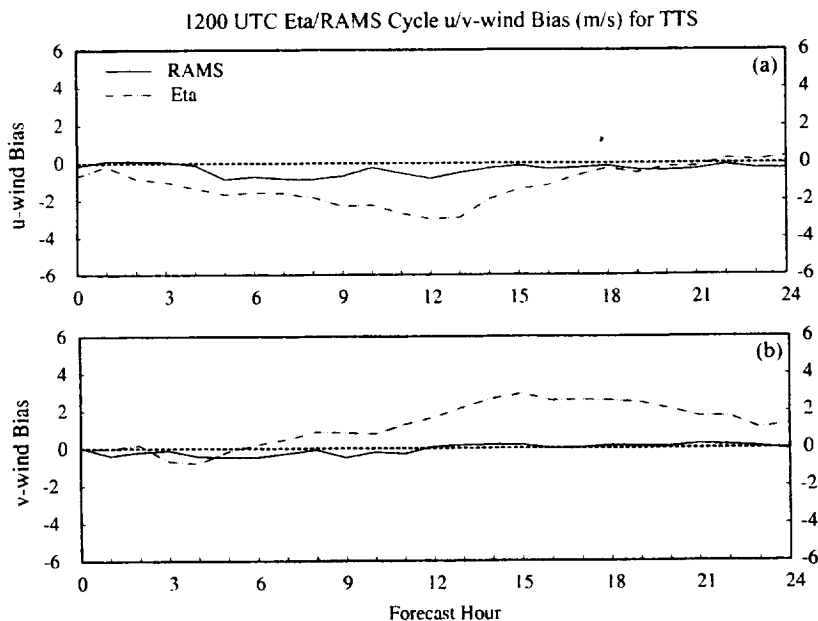
Figure 4.25. A meteogram plot that displays a comparison between the 1200 UTC forecast cycle u- and v-wind component biases (m s⁻¹) from the RAMS operational configuration and the Eta model during the 2000 Florida warm season. The wind component biases are verified at TTS only. Parameters plotted as a function of forecast hour are a) u-wind bias, and b) v-wind bias. The plotting convention is a solid line for the RAMS forecasts and a dot-dashed line for the Eta model.

5. Subjective Evaluation Results

This section presents results from an extensive number of subjective verification experiments for both the 1999-2000 cool, and 1999 and 2000 warm seasons. The 1999-2000 cool-season subjective verification results include:

- Frontal passages at seven east coast stations in Section 5.1.1.

- Cool-season precipitation verification in Section 5.1.2. During the 1999-2000 cool season, very few significant precipitation events occurred and thus, Section 5.1.2 includes only a brief summary of the events that occurred along with two precipitation examples.

- Low-level temperature inversions at the XMR rawinsonde in Section 5.1.3.

The warm season results also include three components:

- Sea-breeze verification at the KSC/CCAFS wind towers and at TTS for 1999 and 2000 forecasts presented in Section 5.2.1.

- Precipitation validation on RAMS grid 4 for the 2000 months shown in Section 5.2.2.

- Thunderstorm initiation verification for the 2000 months given in Section 5.2.3.

Even though the ERDAS RAMS interim report contained the 1999 warm season sea-breeze verification results, the AMU evaluated these sea-breeze forecasts again for two reasons. First, the AMU modified the evaluation technique to include all available archived forecast data for both the 1999 and 2000 warm seasons compared to data only during AMU working days, as was done in the interim report on the 1999 data. Second, by performing the evaluation for all available archived forecasts, the AMU could build a database of sea-breeze verification statistics for two Florida warm seasons, thereby increasing the robustness of the results. It is important to note that the 1999 database contains forecasts during the months of May–August whereas the 2000 warm season database contains forecasts for May–September.

The precipitation and thunderstorm initiation verifications are performed on the 2000 warm season forecasts only, as tasked in the ERDAS RAMS extension evaluation. The precipitation verification closely follows the technique used in the ERDAS RAMS interim report, but with a few modifications (refer to Section 2.2.2.2 and Case 2000). As with the sea-breeze evaluation, the precipitation verification was modified from the technique used for the 1999 warm season to include all available archived forecasts during the 2000 warm season in order to maximize the verification data base. However, the appropriate WSR-74C reflectivity fields for the precipitation verification were not archived until late May 2000. Thus, the precipitation verification is performed only for the months of June–September 2000. The thunderstorm initiation verification was conducted for all 2000 warm season months (May–September).

5.1 1999-2000 Cool Season

The results from the 1999-2000 Florida cool-season subjective verification are presented in this section. All three components of the cool-season subjective verification were conducted from November 1999 to March 2000. Refer to Section 2.2.1 for the methodology used in each experiment.

5.1.1 Verification of Fronts

During the five cool-season months, the AMU documented all occurrences of any type of observed frontal discontinuities (wind shifts, temperature, or dew point temperature gradients). Graphical traces (meteograms) of observed and forecast hourly temperature, dew point temperature, wind direction, wind speed, and pressure observations were examined at seven selected surface stations in the Florida peninsula [Jacksonville (JAX), Daytona Beach (DAB), the Shuttle Landing Facility (TTS), Melbourne (MLB), Vero Beach (VRB), West Palm Beach (PBI), and Miami (MIA)]. Figure 5.1 shows a sample meteogram from 22 December 1999 illustrating the evolution of forecast and observed variables during the passage of a weak front at TTS. Note the smooth transition in the forecast wind shift compared to the observed wind shift in Figure 5.1b. From 1400–1500 UTC, the observed wind direction changes sharply from southwesterly (~240°) to northwesterly (> 300°). Meanwhile, the RAMS forecast has a very gradual shift from south-southwesterly winds at 1400 UTC to northwesterly by

Figure 5.2 shows an example of a RAMS forecast at JAX during the passage of a strong cold front. In this instance, RAMS did a particularly poor job in forecasting the intensity of this cold front. The observed cold front was accompanied by a notable increase in wind speed from 3 to 7 m s⁻¹ (Fig. 5.2a), a sharp wind shift from southerly to northwest (Fig. 5.2b), a 3-h temperature drop of 11°C (from 23 to 12°C in Fig. 5.2c), and a more gradual decrease in dew point temperature (Fig. 5.2d). In this case the frontal intensity increased dramatically due to evaporational cooling caused by post-frontal precipitation that fell over southern Georgia and northern Florida (not shown).
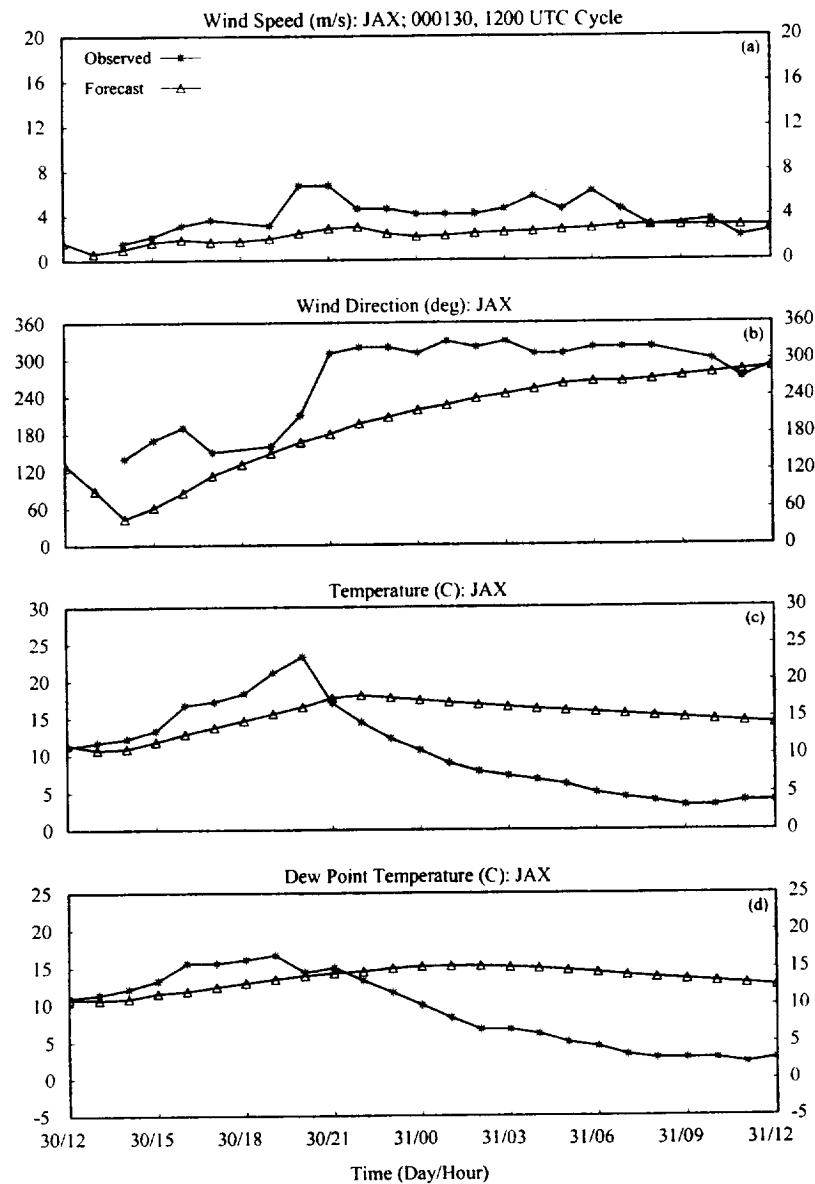
Figure 5.2. A plot of surface variables at JAX used for verifying RAMS forecast frontal passages/discontinuities during the 1999–2000 Florida cool season. This example shows the RAMS forecast during the passage of a strong cold front on 30-31 January 2000. The variables plotted are a) wind speed, b) wind direction, c) temperature, and d) dew point temperature.

Table 5.2 summarizes the seven most substantial precipitation events during the 1999-2000 cool season. Based on these events, RAMS performed with variable accuracy when forecasting cool-season precipitation events across the Florida peninsula. RAMS generally did not accurately predict the timing and location of pre-frontal rain bands, but could handle the rain bands associated with the actual cold front better. With some events such as 17 December 1999 and 31 January 2000, RAMS did not predict any substantial precipitation despite the occurrence of fairly widespread observed rainfall. In the 2 November 1999 cold front and associated squall line, the timing of the frontal passage was substantially in error and thus, the rainfall was not predicted well at all. In the 12 March and 27 March 2000 frontal events, RAMS did not predict the significant convection that occurred over southern Florida, but accurately predicted the lighter precipitation over central Florida.

Figure 5.3 shows an example of how RAMS missed the pre-frontal rain band during the 24 January 2000 strong frontal passage over the Florida peninsula. This figure also illustrates the accurate prediction of the frontal band; however, most of the precipitation fell with the pre-frontal squall line, so the forecast rainfall rates are much too high associated with the frontal passage. At 0900 UTC, a substantial amount of convection is prevalent across the Florida peninsula, especially concentrated over the southern and eastern portions (Fig. 5.3a). RAMS does not indicate forecast precipitation in any portion of the grid-2 domain at this time. The squall line has cleared much of the peninsula by 1200 UTC when a second band of convection becomes prevalent across the northwestern portions of grid 2 (Fig. 5.3b). Between 1500–1800 UTC, the frontal band quickly moves into central Florida and weakens noticeably by 1800 UTC (Figs. 5.3c-d). At these times, RAMS predicts a fairly intense rain band associated with the second observed cloud band with rainfall rates exceeding 40 mm h^{-1} in some instances. However, only light precipitation occurred with the passage of the frontal band since most of the heaviest rainfall occurred with the pre-frontal rain band. This case shows how RAMS had difficulty in predicting pre-frontal squall lines during the 1999-2000 cool-season precipitation events.
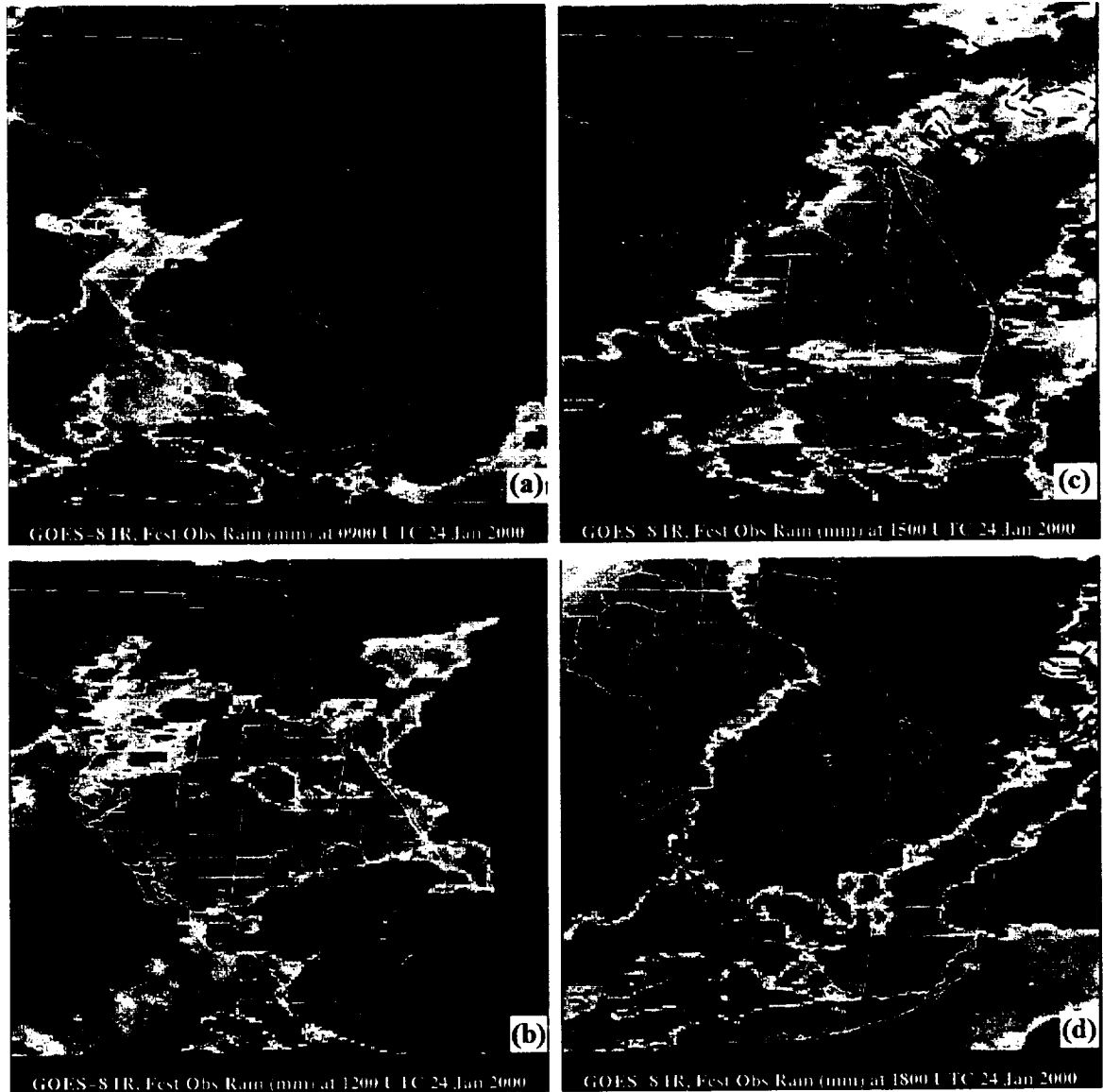
Figure 5.3. The RAMS grid-2 forecast versus observed precipitation features during the 0000 UTC 24 January 2000 forecast cycle. Enhanced GOES-8 infrared (IR) imagery is plotted along with contoured observed hourly precipitation across eastern and southern Florida (blue lines, units of mm h^{-1}) and forecast precipitation rate (dashed green lines, units of mm h^{-1}). Valid times on 24 January are: a) 0900 UTC (9-h forecast), b) 1200 UTC (12-h forecast), c) 1500 UTC (15-h forecast), and d) 1800 UTC (18-h forecast). The dark red colors represent the coldest cloud-top temperatures and deepest convection.

Figure 5.4 depicts a 4-h evolution of clouds and scattered rain showers in advance of a cold front during the afternoon hours of 11 March 2000. In this case, the 1200 UTC cycle of RAMS performed quite well in generating scattered shower activity during the afternoon hours across the eastern portions of the Florida peninsula. The timing of the forecast precipitation is accurate to the nearest hour and the location is slightly north and west of the observed precipitation. At 2000 UTC, scattered convection develops across southern and eastern Florida close to the Atlantic coast whereas RAMS develops showers just to the west of the observed rain areas (Fig. 5.4a). The rainfall continues to develop over the next 2-3 hours as the entire disorganized band pushes offshore to the north and east (Figs. 5.4b-d). Meanwhile, RAMS develops additional rainfall across central and portions of southern Florida in Figures 5.4b-d and these showers move northeast and consolidate over east-central Florida, to the north and west of the observed convection. The results from this case illustrate that RAMS can offer some utility in predicting scattered rainfall activity in advance of a cold front.

When RAMS successfully forecasts a low-level inversion, the model typically underestimates the intensity of the inversion by 2.5°C (bias of -2.5°C in Table 5.4). The RMS errors in forecast inversion depth and height of the inversion base are 202 m and 516 m, respectively (2nd and 3rd rows of Table 5.4). The model has a slight tendency to spread the inversion through a deeper layer than observed (59 m bias). Not directly indicated in these tables is the difficulty that RAMS demonstrated in its ability to consistently predict surface-based inversions. Many surface-based inversions were either not forecast by RAMS, or the predicted inversion occurred above the surface in the lowest 1 km.

Table 5.3. A contingency table of the number of the combined 0000 and 1200 UTC RAMS forecast versus observed occurrences of low-level temperature inversions at the CCAFS rawinsonde during the period of November 1999 to March 2000. The categorical scores derived from this table are shown below.

0000/1200 UTC Cycles	Observed Inversion	No Observed Inversion
Forecast Inversion	86	3
No Forecast Inversion	103	15
Probability of Detection: 0.46 Bias: 0.47		
False Alarm Rate: 0.03 CSI: 0.45		

Table 5.4. A summary of the root mean square (RMS) error and bias statistics of the RAMS forecast temperature inversion intensity (°C), depth of the inversion (m), and height of the inversion base (m), using the CCAFS rawinsonde from November 1999 to March 2000.

Parameter	RMS Error	Bias
Intensity (°C)	4.1	-2.5
Depth (m)	202	59
Height (m)	516	22

5.2 1999 and 2000 Warm Seasons

The AMU conducted an extensive sea-breeze verification for the 1999 and 2000 Florida warm seasons to determine the potential utility of using RAMS for surface wind forecast guidance during the warm season. In addition, the AMU benchmarked the skill of RAMS sea-breeze predictions to the NCEP Eta model point forecasts at TTS and compared the skill of the operational configuration to the coarser 3-grid configuration of RAMS. Furthermore, the AMU conducted a precipitation and thunderstorm initiation verification during the 2000 warm season months. This section presents the results from the sea-breeze, precipitation, and the thunderstorm initiation verifications during the 1999 and 2000 warm seasons.
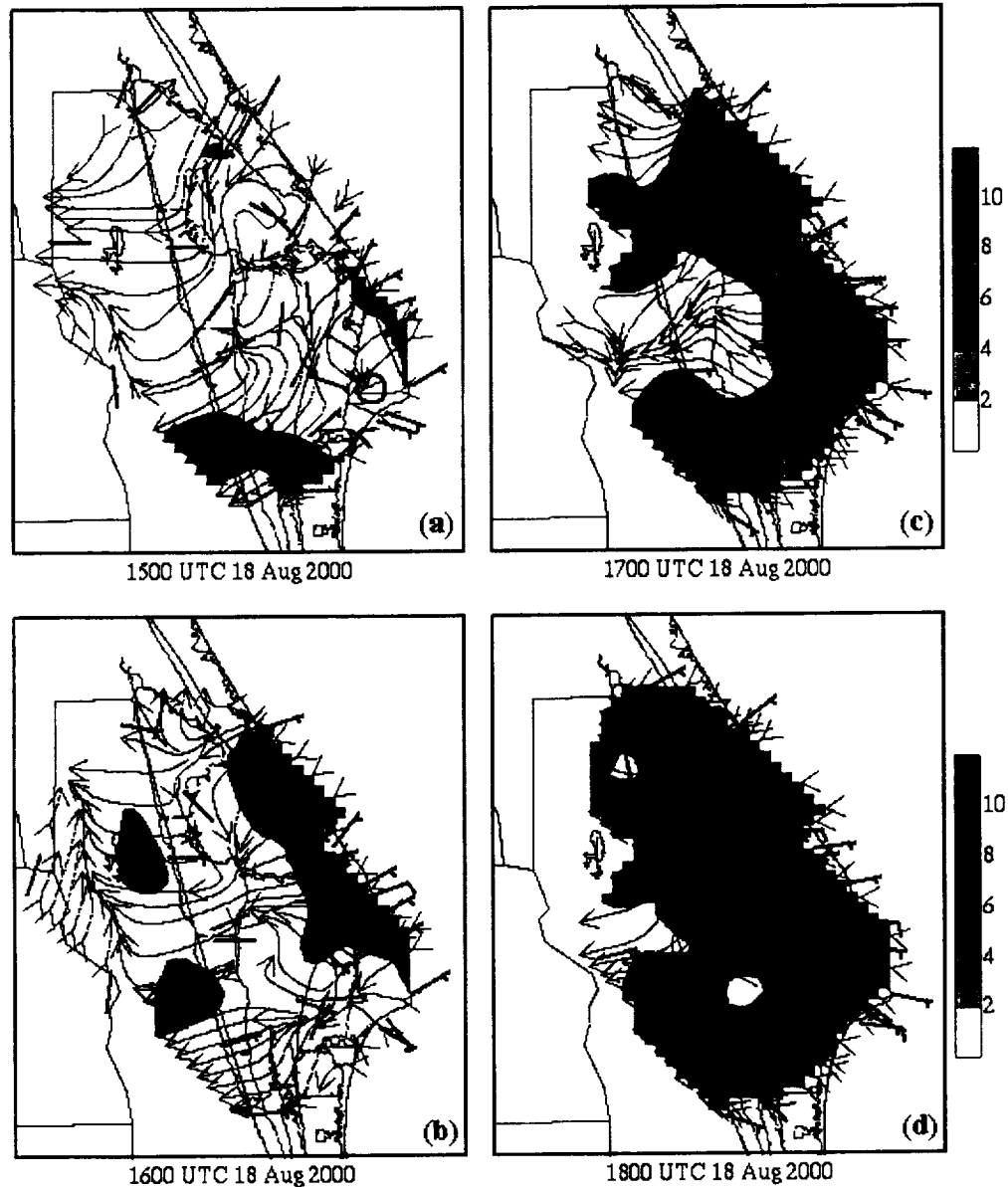
Figure 5.5. A plot of observed KSC/CCAFS 16.5-m wind flow on 18 August 2000 illustrating the interaction between local river and ocean breezes. The valid times for each panel are a) 1500 UTC, b) 1600 UTC, c) 1700 UTC, and d) 1800 UTC.

In Figures 5.7 and 5.8, graphical traces (meteograms) of wind direction and wind speed are used to verify subjectively the sea-breeze passage at each of the 12 KSC/CCAFS wind towers given in Figure 2.2b. In both figures, the 12 meteograms representing each of the 12 wind towers are arranged to follow the north-south, and east-west spatial layout of the wind towers in east-central Florida. For example, the meteograms of the 4 westernmost wind towers of Figure 2.2b (819, 1012, 1007, and 1000) are arranged on the far left (west) portion of the figure. In addition, their north-south orientation is preserved and plotted top-bottom in Figures 5.7 and 5.8. This plotting convention facilitated the subjective sea-breeze verification since these meteograms were examined for every day of 9 months worth of data. To determine an observed or forecast sea-breeze passage at an individual station, the wind direction is first examined to see if a shift from offshore to onshore occurs. Wind directions between the dashed lines on each meteogram of Figure 5.7 represent offshore winds whereas wind directions outside the dashed lines are onshore. Under light or easterly flow, the wind speed plots are also examined to identify the accompanying wind speed increase with the sea-breeze passage.

73

With the exception of the wind speeds being too strong, this case illustrates how remarkably well RAMS can predict the interaction between river and sea breezes during a light and variable wind regime. The development of the circulations and the timing of these wind features are excellent at each hour between 1500 and 1800 UTC. Since the river and sea breezes often serve as the focal points for warm-season convective initiation, it is critical that a model such as RAMS can predict these local interactions at sufficiently high resolutions on a regular basis. The remaining portion of this section presents the collective statistics and skill scores from the 1999 and 2000 warm-season sea-breeze evaluations.
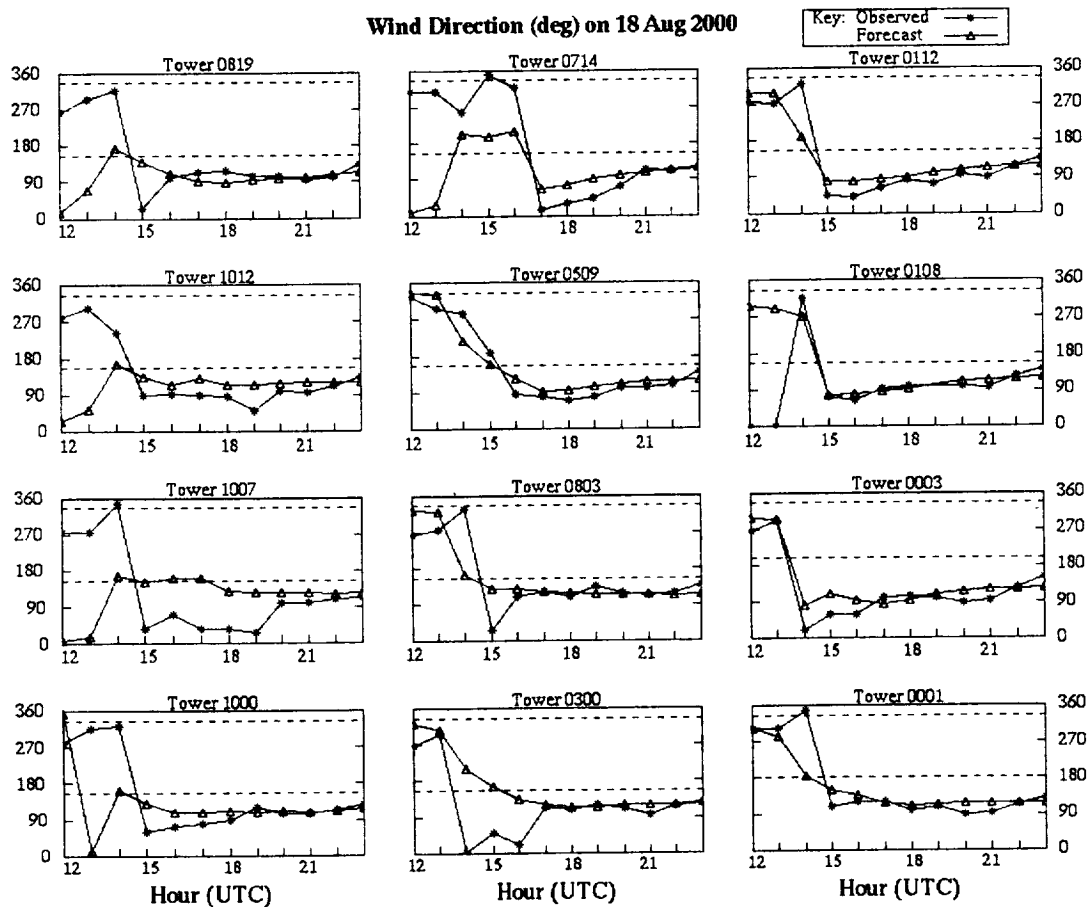
Figure 5.7. A meteogram plot of RAMS forecast versus observed wind direction (deg) for the 0000 UTC forecast cycle of 18 August 2000. Observed points are given by an asterisk whereas a triangle represents forecast values. The KSC/CCAFS towers used for verification (Fig. 2.2, and labeled above each graph) are arranged according to the spatial location in east-central Florida. The left/center/right-hand columns are the mainland/Merritt Island/coastal towers, and each are arranged in a north-south orientation from the top-bottom.

and 1200 UTC forecasts are statistically significant. Refer to Appendix D for more details regarding the statistical significance tests.

In the instances when a correct yes forecast of a sea breeze occurred, the timing errors were determined at each of the wind towers during the 9-month evaluation period. Table 5.7 summarizes the timing error statistics for all the correct yes forecasts of a sea breeze for both the 0000 and 1200 UTC cycles. In general, the RMS error ranges from 1.5–2.1 h for each category of wind towers. The errors are smallest at the coastal towers and largest at the mainland towers, but the variation is less than 0.5 h, which is smaller than the data sampling rate of once per hour. In all instances the bias is -0.2 or -0.3 h, which is negligible compared to the sampling rate.

Table 5.5.   Contingency tables of the occurrence of the operational RAMS forecast versus observed sea breeze, verified at each of the 12 selected KSC/CCAFS towers of Figure 2.2b during the 1999 and 2000 Florida warm seasons.

0000 UTC Forecast Cycle	Observed Sea Breeze	No Observed Sea Breeze
Forecast Sea Breeze	1381	261
No Forecast Sea Breeze	228	599

1200 UTC Forecast Cycle	Observed Sea Breeze	No Observed Sea Breeze
Forecast Sea Breeze	1575	293
No Forecast Sea Breeze	34	567

Table 5.6.   Categorical and skill scores of RAMS forecast versus observed sea breeze during the 1999 and 2000 Florida warm seasons, associated with the contingencies in Table 5.5.

Parameter	0000 UTC Forecast Cycle	1200 UTC Forecast Cycle
Probability of Detection	0.86	0.98
False Alarm Rate	0.16	0.16
Bias	1.02	1.16
Critical Success Index	0.74	0.83
Heidke Skill Score	0.56	0.69

Table 5.7.   A summary of timing error statistics for the May–August 1999 and May–September 2000 evaluation periods are given for the subjective sea breeze verification performed for the 12 KSC/CCAFS tower locations of Figure 2.2b. The RMS error and bias are shown in units of hours for the 0000 UTC and 1200 UTC forecast runs.

Location	Statistic	0000 UTC Cycle	1200 UTC Cycle
Coastal Towers	RMS Error	1.8	1.5
	Bias	-0.3	-0.3
Merritt Island Towers	RMS Error	1.9	1.7
	Bias	-0.3	-0.2
Mainland Towers	RMS Error	2.1	1.9
	Bias	-0.3	-0.2

Finally, Tables 5.12 and 5.13 compare the skill between the 4-grid and 3-grid RAMS forecasts only at the mainland wind towers west of the Indian river. This group of wind towers exhibited the greatest discrepancy in skill between the 4-grid and 3-grid RAMS forecasts during the 2000 warm season. Table 5.12 shows that there were 70 more missed ECSB forecasts in the 3-grid compared to the 4-grid RAMS. As a result, the POD is 14% higher in the 4-grid forecasts, resulting in a 9% higher CSI and 11% higher HSS (Table 5.13). Contrary to the comparison of wind objective error statistics, these results suggest that the 4-grid configuration better resolves the interactions between the river and sea breezes, providing a dramatic improvement in the ECSB forecasts. The 5-km horizontal resolution of RAMS grid 3 is simply not sufficient to resolve river breeze circulations adequately since theoretically, it cannot resolve features whose wavelengths are less than 20 km (4 times the horizontal grid spacing). Meanwhile, the 1.25-km grid can resolve features with wavelengths as small as 5 km, which is comparable to or smaller than the scale of river-breeze circulations [CHECK FOR REFERENCE].

These results also show that objective error statistics alone are not sufficient to evaluate the potential utility that a high-resolution model can provide to forecasters. The warm-season objective comparison between the 4-grid and 3-grid configurations of RAMS showed little difference in the errors during the 2000 warm season (refer to Section 4.4.2). However, the phenomenological verification presented in this section clearly shows that the higher resolution RAMS configuration has greater skill in predicting the ECSB over the course of a 5-month warm season. The accurate prediction of phenomenological features are quite important in determining the added value of a modeling system for everyday forecasting at the 45 WS and dispersion modeling for the 45 SW/SE.

Table 5.10. Contingency tables of the occurrence of the 1200 UTC 4-grid and 3-grid configurations of RAMS versus observed sea breeze, verified at each of the 12 selected KSC/CCAFS towers of Figure 2.2b during the 2000 Florida warm season.

1200 UTC RAMS 4-grid	Observed Sea Breeze	No Observed Sea Breeze
Forecast Sea Breeze	767	135
No Forecast Sea Breeze	15	286

1200 UTC RAMS 3-grid	Observed Sea Breeze	No Observed Sea Breeze
Forecast Sea Breeze	719	126
No Forecast Sea Breeze	63	295

Table 5.11. Categorical and skill scores of the 1200 UTC RAMS 4-grid and 3-grid configurations versus observed sea breeze during the 2000 Florida warm season, associated with the contingencies of Table 5.10.

Parameter	1200 UTC RAMS 4-grid	1200 UTC RAMS 3-grid
Probability of Detection	0.98	0.92
False Alarm Rate	0.15	0.15
Bias	1.15	1.08
Critical Success Index	0.84	0.79
Heidke Skill Score	0.71	0.64

Even though RAMS dramatically outperformed the Eta model during the 0000 UTC forecast cycle, the same cannot be said for the 1200 UTC cycle. Tables 5.16 and 5.17 indicate that RAMS still correctly predicts the occurrence of the ECSB at a higher percentage than the Eta model; however, RAMS also has a significantly higher FAR than the Eta model. As a result, the CSI and HSS of Table 5.17 are only marginally better in RAMS. In fact, neither the CSI nor the HSS differences are statistically significant above the 86% confidence interval (see Appendix D). Meanwhile, the higher FAR in RAMS is statistically significant compared to the Eta model, suggesting that RAMS has a tendency to overpredict the occurrence of the ECSB in the 1200 UTC cycle compared to the Eta model. Overall though, RAMS clearly demonstrates that it has the ability the better detect the occurrence of the ECSB at TTS during the Florida warm season, especially during the 0000 UTC forecast cycle. These results indicate that, despite the comparable or slightly better objective error statistics in the Eta model, the phenomenological verification of the ECSB improves over the Eta model when running the RAMS model with fine horizontal grid spacing such as in the current configuration.

Table 5.14. Contingency tables of the occurrence of the 0000 UTC operational RAMS and Eta forecast versus observed sea breeze, verified at TTS for the 1999 and 2000 warm season months.

0000 UTC RAMS	Observed Sea Breeze	No Observed Sea Breeze
Forecast Sea Breeze	73	13
No Forecast Sea Breeze	15	47

0000 UTC Eta	Observed Sea Breeze	No Observed Sea Breeze
Forecast Sea Breeze	47	7
No Forecast Sea Breeze	41	53

Table 5.15. Categorical and skill scores of the 0000 UTC RAMS and Eta forecast versus observed sea breeze during the 1999 and 2000 Florida warm seasons, associated with the contingencies of Table 5.14.

Parameter	0000 UTC RAMS	0000 UTC Eta
Probability of Detection	0.83	0.53
False Alarm Rate	0.15	0.13
Bias	0.98	0.61
Critical Success Index	0.72	0.49
Heidke Skill Score	0.61	0.38

Table 5.16. Contingency tables of the occurrence of the 1200 UTC operational RAMS and Eta forecast versus observed sea breeze, verified at TTS for the 2000 warm season months only.

1200 UTC RAMS	Observed Sea Breeze	No Observed Sea Breeze
Forecast Sea Breeze	60	13
No Forecast Sea Breeze	5	37

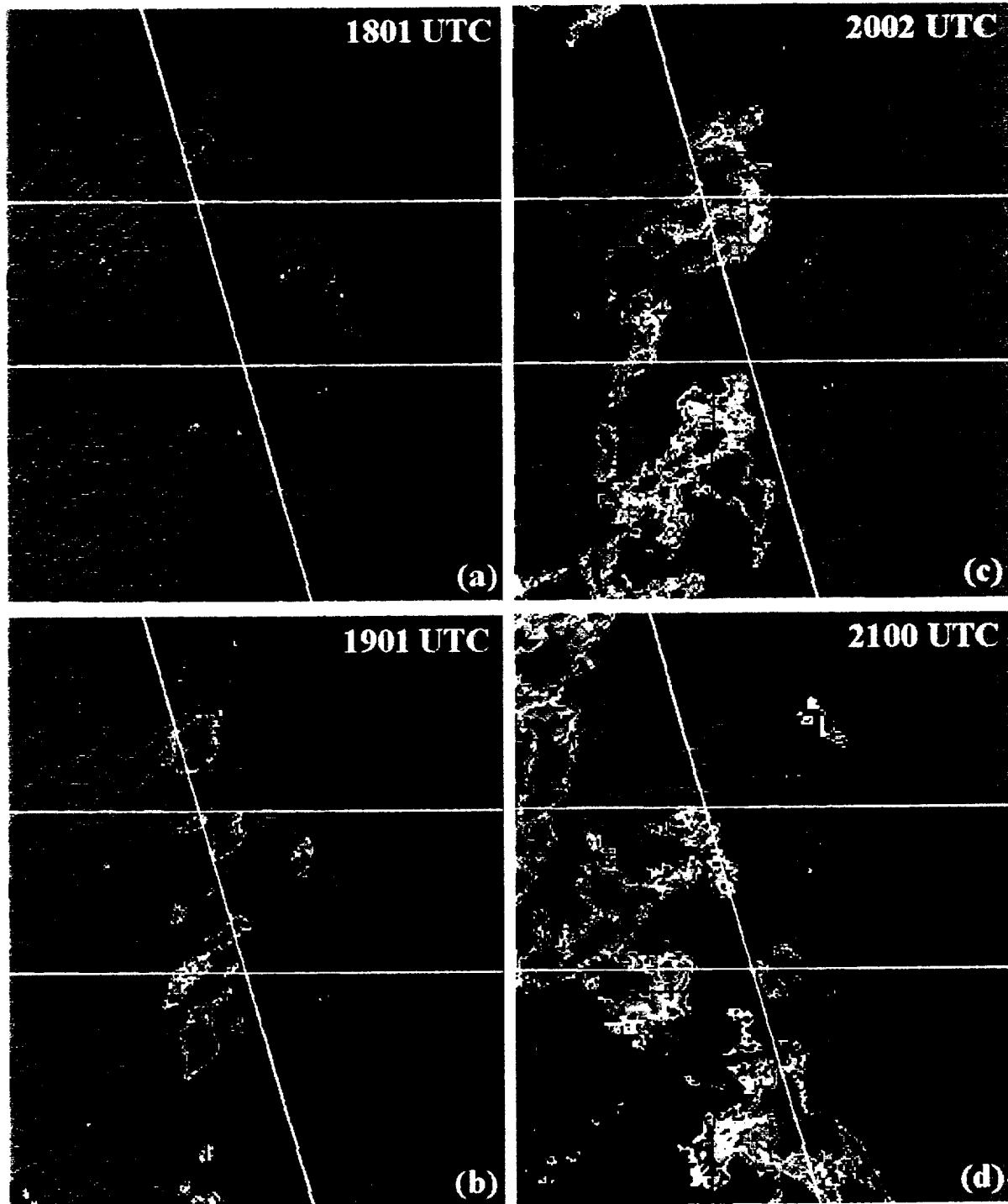| 1200 UTC Eta	Observed Sea Breeze	No Observed Sea Breeze
Forecast Sea Breeze	50	5
No Forecast Sea Breeze	15	45

Figure 5.9. Observed WSR-74C hourly reflectivity from a 2000-ft Constant Altitude Plan Position Indicator on 25 July 2000. Valid times are: a) 1800 UTC, b) 1900 UTC, c) 2000 UTC, and d) 2100 UTC. Orange and red colors represent reflectivity greater than 32 dBZ used to classify 5 mm h^{-1} rainfall rate intensities for verifying RAMS forecasts.

To obtain the seasonal precipitation verification statistics, the verification methodology described above for the specific case was repeated for both the 0000 and 1200 UTC forecast cycles during all days in the June–September 2000 time frame. The precipitation verification statistics are summarized in three ways:

- Occurrence of precipitation as a function of zone at any time within the 9-h window of 1500–2300 UTC. This test determines how well RAMS predicted precipitation occurrence within each zone anytime between the hours of 1500–2300 UTC.

- Timing and location as a function of 1-h, 2-h, and 3-h verification time windows (bins). The 1-h bins are the most stringent verification, since the observed and forecast instantaneous rainfall must occur in the same zone at the same hour for a hit. The 2-h verification bins are valid for 1600–1700, 1800–1900, 2000–2100, and 2200–2300 UTC. In these 2-h bins, a hit occurs when RAMS predicts rainfall in either one of the two hours and rainfall is observed at either hour. Finally, the 3-h windows are valid from 1500–1700, 1800–2000, and 2100–2300 UTC, and a hit occurs when forecast and observed rain occurs in one or more of the 3-h times.

- Timing and location as a function of hour within the verification window. In this validation, the performance of RAMS precipitation forecasts is verified at each hour of the 1500–2300 UTC verification window. For the 2- and 3-h bins, the precipitation statistics are presented for the first hour of the valid verification time frame.

For each scenario described above, contingency tables were developed and corresponding categorical and skill scores were calculated.

5.2.2.1   Occurrence of Daily Precipitation in each Grid-4 Zone

Figure 5.11 shows the categorical and skill scores for daily 0000 and 1200 UTC RAMS precipitation-rate predictions in each zone of grid 4 between 1500–2300 UTC. Based on these charts, RAMS has the highest skill in predicting daily precipitation over the inland zones 1–3 compared to the coastal zones 4–6. The POD is close to 0.8 on each of the inland zones whereas the POD ranges from about 0.45 to 0.70 over the coastal zones (Fig. 5.11a). RAMS generally has a lower FAR over the inland zones compared to the coastal regions (Fig. 5.11b). As a result, the CSI (analogous to precipitation threat score) in Figure 5.11c is highest at nearly 0.70 over zones 1–3, and lowest over the coastal zones 4–6, ranging from 0.35–0.55. The bias plots in Figure 5.11d indicate that RAMS has a tendency to underpredict the daily occurrence of precipitation, especially in zones 1, 4, and 6 of the 1200 UTC forecast cycle, and in all zones of the 0000 UTC cycle.

Not only does RAMS predict daily precipitation with higher skill over inland regions, it also exhibits greater skill in the 1200 UTC versus 0000 UTC forecast cycle. In every zone of grid 4, the 1200 UTC cycle has a higher POD, CSI, and bias (Fig. 5.11). The FAR is not dramatically different in any grid-4 zones. It is also interesting to note that zone 6 experiences the poorest forecast skill in both the 0000 and 1200 UTC cycles.
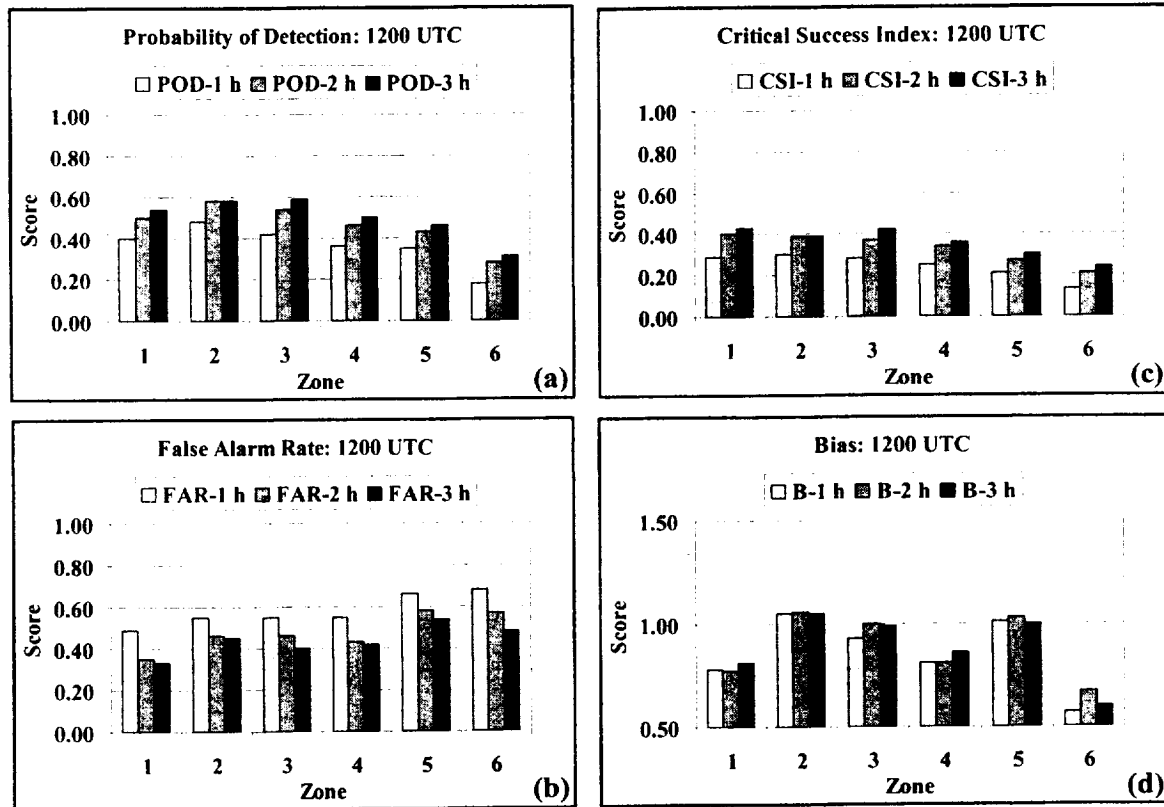
Figure 5.12. Categorical scores for the RAMS 1200 UTC precipitation forecasts plotted as a function of the 6 zones on grid 4 and time verification window. The scores shown in this figure include a) the Probability of Detection (POD), b) the False Alarm Rate (FAR), c) the Critical Success Index (CSI), and d) the Bias. The POD, FAR, CSI, and bias are each shown for 1-h, 2-h, and 3-h time verification windows. The lightest shade is the 1-h time window whereas the darkest shade is the 3-h time verification window. The 1-h window represents each instantaneous hourly time from 1500–2300 UTC. The 2-h windows are the instantaneous hours valid at 1600–1700, 1800–1900, 2000–2100, and 2200–2300 UTC. The 3-h windows are the instantaneous hours valid at 1500–1700, 1800–2000, and 2100–2300 UTC.

5.2.2.3 Timing and Location of Precipitation at each Hour

The third and final examination of the precipitation verification statistics is the timing and location validation for all six zones as a function of hour of the day, shown in Figure 5.13. For the 1-h verification bins in Figure 5.13a, 1700 UTC is the only hour when the POD is greater than the FAR, representing the peak of hourly CSI values. The lowest amount of skill occurs at 1500 UTC and especially after 2000 UTC, when the CSI drops well under 0.20 between 2100–2300 UTC. This reduction in skill is especially prevalent in the 2-h and 3-h verification bins in Figures 5.13b-c. The POD peaks at 1800 UTC in the 2-h bins and decreases sharply over the next 4 hours in conjunction with a sharp increase in the FAR during the same times (Fig. 5.13b). In the 3-h verification bins, the POD is nearly constant for the 3-h periods that begin at 1500 and 1800 UTC, and then sharply decreases in the final 3-h time frame (Fig. 5.13c).

The poor skill during the late afternoon and evening hours are likely caused by the model's inability to accurately predict the evolution of outflow boundaries and their interactions. In fact, one erroneously predicted storm can result in many subsequent erroneous storms that develop in the model along the incorrect placement of outflow boundaries. As a result, the model's skill decreases dramatically by the late afternoon hours as suggested by Figure 5.13. These model results would most likely improve dramatically with a more sophisticated data assimilation scheme that ingests continuous observational data such as WSR-88D and GOES-8 brightness temperature data. Furthermore, a data assimilation scheme where analyses and model forecasts are cycled much more frequently than the current scheme (every 12 hours) should noticeably improve the short-range precipitation forecasts.

5.2.3   Verification of Daily Thunderstorm Initiation

The last portion of the subjective verification that the AMU conducted for the 2000 warm season is the daily thunderstorm initiation verification. Following the observed and model thunderstorm definitions outlined in Section 2.2.2.3, the AMU developed a seasonal spreadsheet for May–September to tally the thunderstorm initiation results for both the 0000 and 1200 UTC forecast cycles.
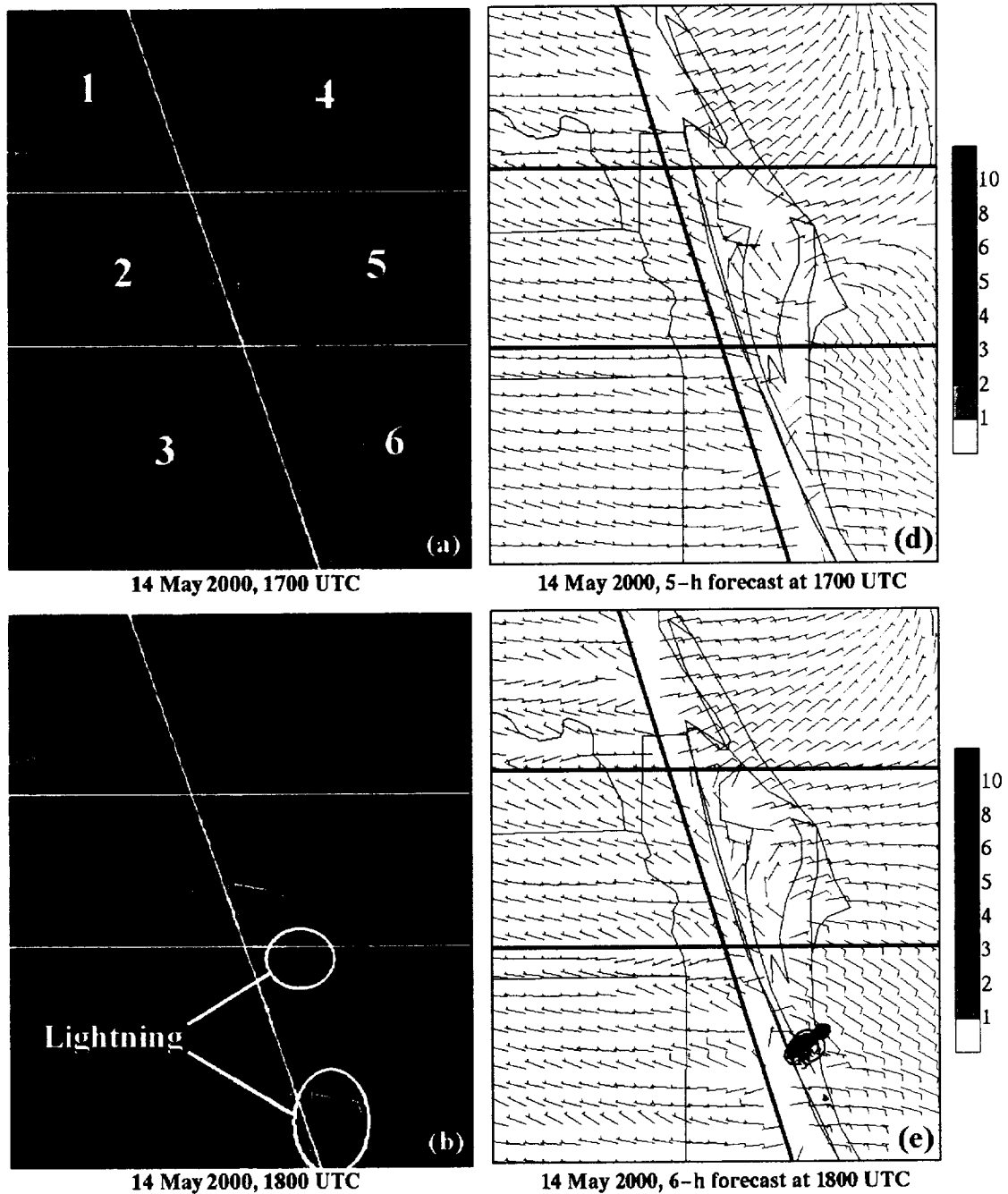
Figure 5.14. Hourly GOES-8 visible satellite imagery and surface winds overlaid with CGLSS cloud-to-ground lightning strikes (denoted by a colored 'X' in a, b, and c) compared to RAMS forecast surface winds, 7-km vertical velocity (m s^{-1}, shaded according to the scale provided), and surface instantaneous precipitation rate (mm h^{-1}) (d, e, and f) on 14 May 2000 over the area of RAMS grid 4. Valid times for the observed plots are a) 1700 UTC, b) 1800 UTC, and c) 1900 UTC and the corresponding RAMS forecast plots at d) 1700 UTC, e) 1800 UTC, and f) 1900 UTC.

5.2.3.1 Occurrence of Thunderstorm Days Anywhere on Grid 4

According to Tables 5.18 and 5.19, the 1200 UTC RAMS forecast cycle predicted the occurrence of a thunderstorm day on grid 4 much better than the 0000 UTC cycle. In the 1200 UTC cycle, the number of correctly predicted thunderstorm days is higher than the 0000 UTC cycle in combination with fewer missed forecasts (Table 5.18). As a result, the 1200 UTC cycle has a higher POD than the 0000 UTC cycle (Table 5.19); however, the 1200 UTC cycle does have a slightly greater tendency towards false alarms and over-predicting thunderstorm days as indicated by the slightly higher FAR and a bias greater than 1.0 (Table 5.19). Nonetheless, the overall skill in Table 5.19 indicates that the 1200 UTC cycle realizes a 21% higher HSS than the 0000 UTC cycle. The statistical significances of these differences were not determined.

Table 5.18. Contingency tables of the occurrence of RAMS predicted versus observed thunderstorms anywhere on grid 4, verified each day between 1500–2300 UTC during the 2000 Florida warm season.

0000 UTC Forecast Cycle	Observed T-storms	No Observed T-storms
Forecast T-storms	36	11
No Forecast T-storms	35	45

1200 UTC Forecast Cycle	Observed T-storms	No Observed T-storms
Forecast T-storms	62	21
No Forecast T-storms	9	35

Table 5.19. Categorical and skill scores of RAMS forecast versus observed thunderstorms anywhere on grid 4, associated with the contingencies of Table 5.22.

Parameter	0000 UTC Forecast Cycle	1200 UTC Forecast Cycle
Probability of Detection	0.51	0.87
False Alarm Rate	0.23	0.25
Bias	0.66	1.17
Critical Success Index	0.44	0.67
Heidke Skill Score	0.30	0.51

5.2.3.2 Timing and Spatial Accuracy of Forecast Thunderstorm Initiation

In general, both forecast cycles are comparable in terms of the spatial accuracy, whereas the 1200 UTC cycle exhibits slightly more favorable results in the timing of thunderstorm initiation. The timing RMS errors of thunderstorm initiation anywhere on RAMS grid 4 were generally between 2–3 h for both forecast cycles whereas the bias was about 1 h in the 0000 UTC cycle and 0 h in the 1200 UTC cycle (not shown). The timing error statistics for thunderstorm initiation in each individual grid-4 zone did not exhibit any trends or organized patterns that favored specific zones.

Table 5.20 summarizes the spatial and timing results of the RAMS forecast thunderstorm initiation for the 0000 and 1200 UTC cycles. Spatially, both forecast cycles correctly predicted thunderstorm initiation in one or more zones about half the time (58% in 0000 UTC cycle and 46% in 1200 UTC cycle, Table 5.20). The slightly poorer performance of the 1200 UTC cycle could be attributed to the larger sample size of correctly-forecast thunderstorm days. In the timing accuracy, only 8% (19%) of the correctly predicted thunderstorm days experienced an exact initiation time to the nearest hour in the 0000 UTC (1200 UTC) cycle. Meanwhile, RAMS correctly predicted the hourly thunderstorm initiation time to within 3 hours of the observed time about 75% of all days for both forecast cycles (slightly higher in the 1200 UTC forecasts). Note that these timing accuracies in RAMS do not reflect off-hour predictions because forecast output was available only at the top of each hour.
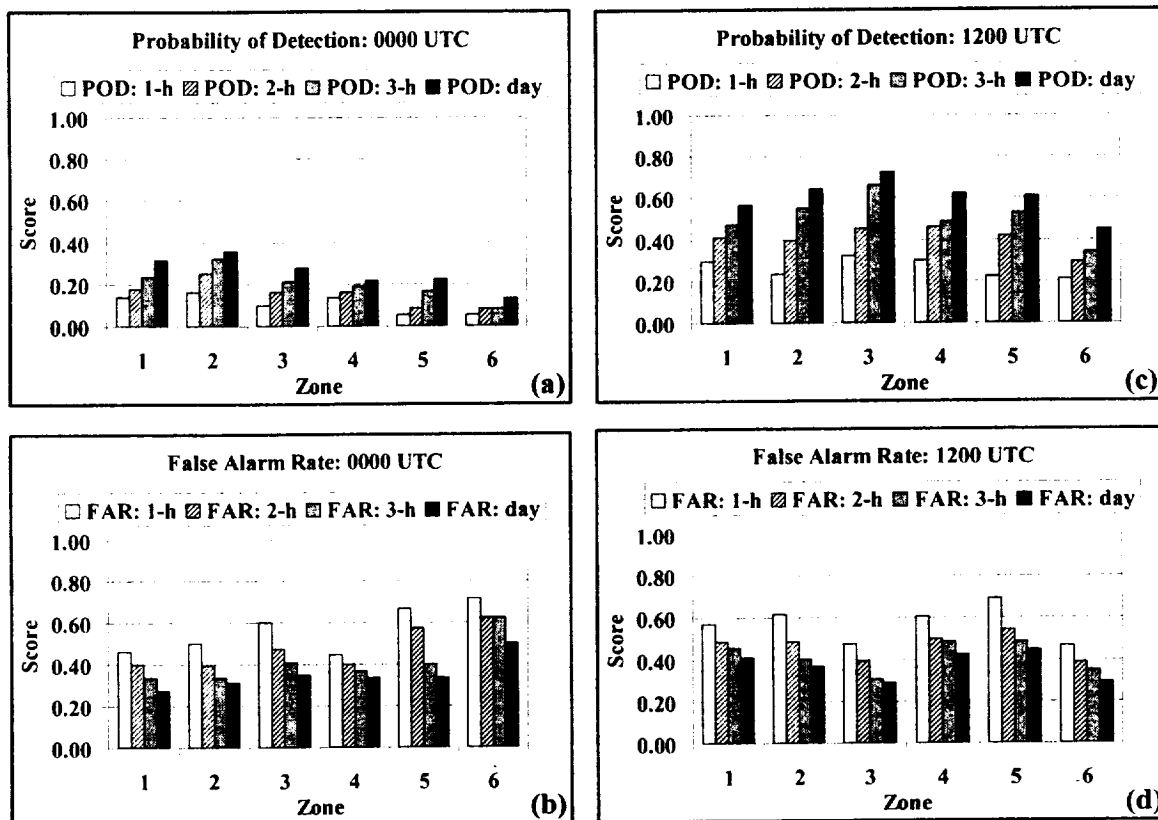
Figure 5.15. The Probability of Detection (POD) and False Alarm Rate (FAR) for the RAMS 0000 and 1200 UTC forecasts of the first daily thunderstorm occurrence in each zone of grid 4 during the hours of 1500–2300 UTC. The 0000 UTC POD and FAR are shown in a) and b) respectively, and the 1200 UTC POD and FAR are shown in c) and d) respectively. The scores were determined by verifying hourly RAMS thunderstorm occurrences to the nearest 1 h, 2 h, 3 h, and for the entire daily verification period according to the scale provided.
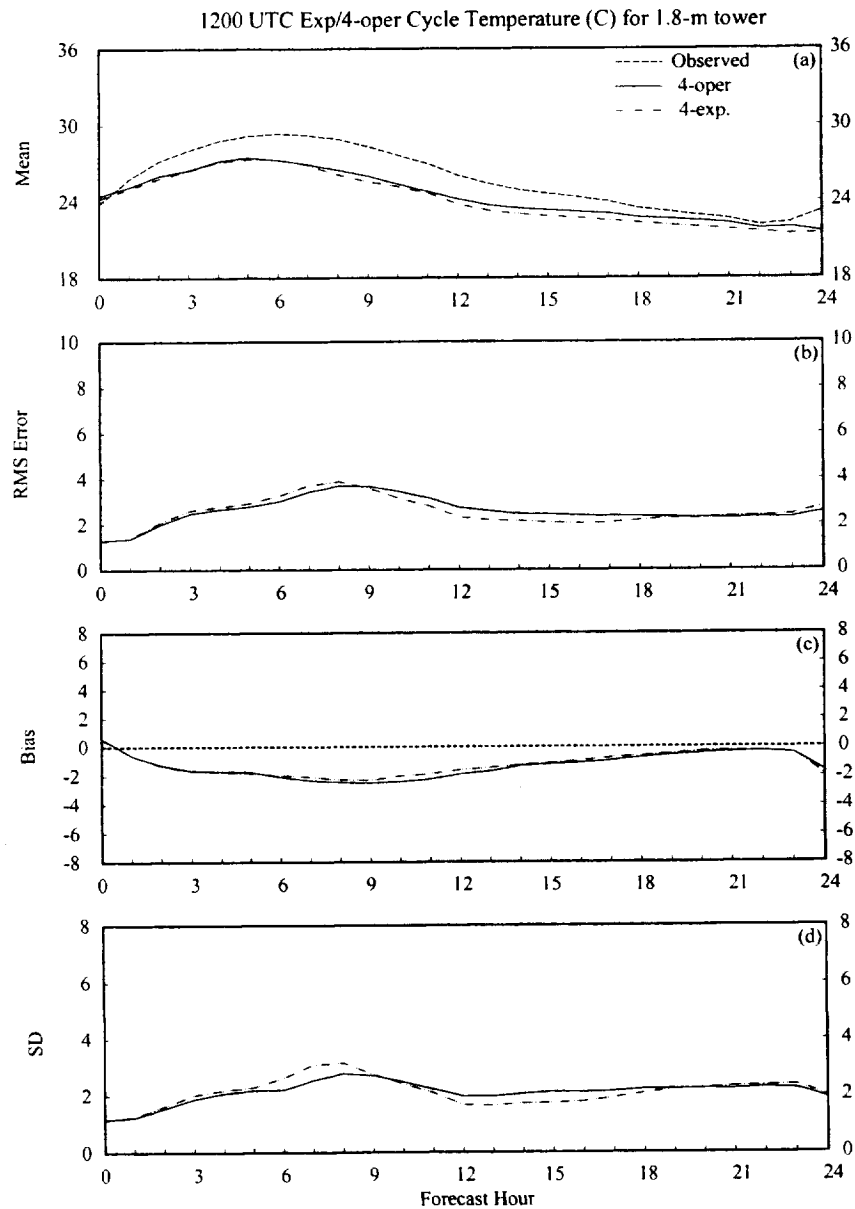
Figure 6.1. A meteogram plot of temperature errors (°C) for the experimental 1200 UTC RAMS forecasts using Eta 0-h forecasts as a background field for the initial conditions, and 0–24-h Eta forecasts as boundary conditions. The temperatures are verified at the 1.8-m level of the KSC/CCAFS wind-tower network. Parameters plotted as a function of forecast hour are a) mean observed, mean operational RAMS, and mean experimental RAMS forecast temperatures, b) RMS error, c) bias, and d) error standard deviation (SD). The labeling convention is a dashed line for observed values, a solid line for the operational RAMS, and a dot-dashed line for the experimental RAMS configuration.

7. Recommendations for Improvements

In this section, the AMU offers some recommendations for modifying and improving the existing ERDAS RAMS forecast and display system. In particular, the AMU highly recommends an improved graphics software package for routine analysis and display of RAMS forecasts. Based on the combination of the objective and subjective evaluations, RAMS clearly offers sufficient added value to short-range forecasts in support of the US Space Program.

7.1 Improve Current Graphics Capabilities

7.1.1   Replace Current RAMS Display

According to the AMU's assessment, the current graphics software within the MARSS system in the Range Weather Operations (RWO) is not a sufficient interface for displaying and analyzing RAMS forecasts in real-time. There are a number of deficiencies and problems with the display software that make it difficult for any user to efficiently access and analyze forecast data. Some of these deficiencies include:

- Frequent and unpredictable hang-ups and crashes when displaying various combinations of forecast variables.

- Occasional very slow updates when selecting new parameters or grids.

- Inadequate control and insufficient contouring and labeling of scalar fields.

- Very difficult to exit the RAMS interface cleanly without having to kill the existing session.

Other problems may exist with the interface, but these difficulties alone make it quite difficult to use in an operational setting when fast and reliable graphical products are critical.

One alternative to the current RAMS display software that the AMU recommends is the Visualization in 5 dimensions (Vis5D) software. The five dimensions of Vis5D consist of the three spatial dimensions, a dimension in time for animation, and a dimension for displaying multiple variables. Several advantages to using Vis5D as a display software are listed below:

- Vis5D is a visually appealing and easy-to-use display software that gives the user extensive control.

- Vis5D can display horizontal or vertical slices, "isosurfaces" of a constant value in three-dimensions, overlay multiple variables, and can animate all combinations of displays in three-dimensional space.

- A routine already exists within the ERDAS RAMS package to convert the RAMS forecast data into Vis5D format.

- The software is freely available from the University of Wisconsin and can be easily installed onto the existing workstations in the RWO.

- Vis5D has a shallow learning curve and is easy to use the very first time, so required training would be minimal.

Another alternative graphical package is the General Meteorological Package (GEMPAK) software. Available from the Unidata division of the University Corporation for Atmospheric Research, GEMPAK has an extensive amount of capabilities for displaying and computing derived meteorological quantities from gridded forecast fields. As a diagnostic tool, GEMPAK may be more powerful than Vis5D; however, the learning curve for GEMPAK is steeper than Vis5D. Also, in a time-restricted environment, Vis5D would likely provide a snapshot of the forecast data in a shorter time period.

7.1.2   Utilize Real-time Verification Graphical Tool

In addition to utilizing a better graphical software, the AMU also recommends that forecasters use the real-time verification Graphical User Interface (GUI) that is currently available in the RWO. Developed by the AMU, this software allows forecasters to verify RAMS predictions in real-time at both surface and upper-level observational sites. The software incorporates the point forecast data from the current RAMS simulation and

RAMS version 4.3 still contains a couple drawbacks, though. First, this version still does not incorporate fully-digital vegetation data; however, the subsequent unreleased version 4.4 should contain this digital vegetation data. Second, RAMS currently has only one cumulus/precipitation parameterization scheme, the modified Kuo scheme (Tremback 1990), for simulations on coarse grid resolutions. The Kuo cumulus scheme is the most appropriate for meso-beta grid-spacing scales of 20–200 km. Meanwhile, the current operational configuration of RAMS at CCAFS runs the Kuo cumulus scheme on grids with 15-km and 5-km horizontal resolutions. At these resolutions, an alternative hybrid cumulus scheme should be utilized rather than the Kuo scheme (Molinari and Dudek 1992). At this time, there is no identifiable date when an additional cumulus/precipitation parameterization scheme will be implemented into RAMS in the near future.

Temperature

- Daytime surface and low-level cold bias during both seasons, peaking at -4°C to -4.5°C in the cool season and -2.5°C to -3.5°C in the warm season.

- Cold bias at the buoys at all hours during both seasons, again largest in the cool season (-3°C to -4°C).

- Temperature profile too stable in the troposphere during both seasons.

- The lowest 50 mb or so of the atmosphere are not stable enough in the early morning sounding during both seasons.

- Results are consistent with the 1999 warm-season evaluation in the ERDAS RAMS interim report.

Moisture

- Nocturnal surface moist bias in the cool season of 1–2.5°C.

- Daytime surface dry bias in warm season of -1°C to -2°C.

- Largest dew point temperature errors in mid-levels (5–8°C in the 600–850-mb layer) during both seasons.

Wind Direction

- Rapid growth in surface wind direction errors from 20–40° in the first 2 hours of integration during both seasons.

- Largest errors of about 60–70° occur at the surface during the late night and early morning hours, both seasons.

- Wind direction errors decrease with height, most notably in the cool season where RMS errors are only 10–20° above 500 mb.

- Low-level easterly bias over land, both seasons (u-wind bias of -2 to -2 m s^{-1}, especially during the day in the warm season).

- Southerly bias at all levels above the surface during both seasons.

Wind Speed

- Speed errors increase with height from 2.5 m s^{-1} near the surface to 5–7 m s^{-1} at upper-levels, especially in the cool season.

- Positive bias near the surface in both seasons; negative speed bias above 950 mb in the cool season, and above 850 mb in the warm season. The magnitude of all speed biases are generally less than 2 m s^{-1}.

8.2.2   Regime Classification Results during the 2000 Warm Season

Surface Wind Classification

- The **light wind regime** experienced the largest daytime temperature RMS errors (4.5°C) and cold bias (-3.5°C). The wind direction errors were by far the largest during the late night and early morning hours (~ 80–120°) associated with this surface wind regime.

- The **westerly wind regime** contained the largest random temperature errors (3.5°C), wind direction RMS errors (75°), and u-wind component RMS errors (4.2 m s^{-1}) during the afternoon and evening hours. These errors are likely caused by the presence of the ECSB within the wind

8.3 Summary of 1999-2000 Cool-Season Subjective Evaluation

The AMU performed a frontal, precipitation, and low-level temperature inversion verification as part of the 1999-2000 cool-season subjective evaluation. For cold frontal verification, the AMU identified observed fronts using GOES-8 infrared imagery and surface stations plots. The AMU subsequently verified RAMS forecast pre-frontal conditions, the changes in temperature, dew point temperature, and wind direction associated with the frontal passage, and the maximum post-frontal wind speed at seven stations along the east coast of the Florida peninsula. During the 1999-2000 cool season, only a few significant precipitation events occurred across the Florida peninsula, so the AMU qualitatively examined each event and summarized the results in a table. The low-level temperature inversion verification was performed for forecasts at the XMR rawinsonde. Observed and forecast temperature inversions were identified and verified in the lowest 3 km of the atmosphere. The results are summarized below.

8.3.1 Frontal Verification

- RAMS pre-frontal temperatures were too cold by 1.6° due to the prevailing low-level cold bias.

- RAMS forecast fronts were generally too weak, given the fact that the average 3-h temperature and dew point temperature decreases associated with the frontal passages were 1.9°C and 4.6°C too small, respectively.

- Forecast post-frontal maximum wind speeds were typically too weak by 2.5 m s^{-1}.

8.3.2 Precipitation Verification

- RAMS demonstrated varying skill in predicting cool-season precipitation patterns.

- The model often missed significant pre-frontal rain bands.

- The problems in adequately predicting frontal-associated precipitation could be caused by large-scale timing errors associated with the Eta model boundary conditions.

8.3.3 Low-level Temperature Inversion Verification

- RAMS predicted only about half of all low-level temperature inversions.

- When successful, RAMS had a tendency to underestimate the magnitude of the temperature inversion (-2.5°C bias).

- Many predicted inversions were not based at the surface, as observed.

8.4 Summary of Subjective Evaluation during the 1999 and 2000 Warm Seasons

The AMU also performed 3 separate verifications in the warm-season subjective evaluation. These three components include a sea-breeze, precipitation, and thunderstorm initiation verification. The sea-breeze verification was composed of three segments:

- Verification of operational RAMS sea-breeze forecasts at 12 selected KSC/CCAFS wind towers for May–August 1999 and May–September 2000.

- Comparison of operational 4-grid RAMS to 3-grid RAMS sea-breeze forecasts at the same 12 KSC/CCAFS wind towers during the 2000 warm season only.

- Benchmark of the operational RAMS to the Eta model sea-breeze forecasts at TTS for the 1999 and 2000 warm season.

For the instantaneous precipitation and thunderstorm initiation verifications, RAMS grid 4 was divided into 6 zones, 3 inland and 3 coastal. In the precipitation verification, hourly forecast rain rates of 5 mm h^{-1} or greater were verified against WSR-74C reflectivities of 32 dBZ or higher. The precipitation verification was conducted during the hours of 1500–2300 UTC every day from June–September 2000.

8.4.2 Precipitation Verification

The precipitation verification results indicated the following about the operational RAMS forecasts:

- The best precipitation forecasts occurred in the inland zones of grid 4 where the POD was about 0.10–0.20 higher than the coastal zones.

- The worst predictions for both forecast cycles occurred in zone 6 (the southeastern part of grid 4) where the POD was generally under 0.30.

- The 1200 UTC cycle generally predicted precipitation better than the 0000 UTC cycle.

- In the 1200 UTC cycle, the most accurate precipitation forecasts occurred during the hours of 1600–2000 UTC when CSI scores (e.g. threat scores) were between 0.25 and 0.40. After 2000 UTC, the CSI scores decreased rapidly to well under 0.20, possibly caused by the model's inability to adequately forecast the evolution of observed convective outflow boundaries.

8.4.3 Thunderstorm Initiation Verification

The results of the thunderstorm initiation verification yielded the following conclusions:

- The 1200 UTC forecast cycle was a much better predictor of daily thunderstorm occurrence than the 0000 UTC cycle. This result is expected based on the newer initial condition of the 1200 UTC forecast cycle compared to the typical thunderstorm initiation time.

- The 0000 UTC forecast cycle underforecast the occurrence of thunderstorms in all grid-4 zones.

- Thunderstorm occurrence in zone 6 (southeastern part of grid 4) was underforecast by both cycles.

- About 50% of all RAMS forecasts correctly identified one or more zones for daily thunderstorm initiation.

- About 75% of RAMS forecasts identified the timing of thunderstorm initiation to the nearest 3 hours (± 3 h).

The results of the precipitation and thunderstorm initiation verification both could improve by:

- Expanding the lateral boundaries of grid 4 to displace errors resulting from boundary interactions further from the areas of interest.

- Replacing the modified Kuo cumulus parameterization scheme with a hybrid cumulus scheme that is more appropriate for the resolutions used on RAMS grids 2 and 3 (15 km and 5 km).

- Initializing the model soil moisture with actual soil moisture observations and/or archived precipitation data.

- Implementing a four dimensional data assimilation scheme that ingests high-resolution, continuous observational data such as WSR-88D reflectivity and radial velocity, and GOES-8 data.

8.5 Summary of Sensitivity Experiments

The AMU performed various sensitivity tests to isolate the possible cause(s) of the RAMS forecast errors, particularly the low-level cold bias. One of these experiments involved running RAMS using Eta 0-h rather than 12-h forecasts as background fields for the initial conditions. In addition, the 0–24-h rather than the 12–36-h forecasts were used as boundary conditions. This experiment resulted in nearly identical forecast errors.

An additional experiment altered the short-wave radiation scheme using the Mahrer-Pielke rather than the operational Chen and Cotton scheme. In the Mahrer-Pielke short-wave radiation scheme, the effects of clouds on short-wave radiation are ignored. In this experimental run, the surface cold bias was dramatically reduced. As a result of this experiment, the AMU discovered that RAMS routinely generates a widespread low-level fog deck across all of grid 4. The fog occurs at night over land and at all times over the ocean. The AMU has not identified the cause of this low-level fog problem.

105

9. References

Baldwin, M., 2000: Quantitative precipitation forecast verification documentation. [Available on-line from http://sgi62.wwb.noaa.gov:8080/scores/pptmethod.html.].

Benjamin, S. G., J. M. Brown, K. J. Brundage, D. Devenyi, B. E. Schwartz, T. G. Smirnova, T. L. Smith, L. L. Morone, and G. J. DiMego, 1998: The operational RUC-2. Preprints, *16th Conf. on Weather Analysis and Forecasting*, Phoenix, AZ, Amer. Meteor. Soc., 249-252.

Bloom, S. C., L. L. Takacs, A. M. DaSilvia, and D. Ledvina, 1996: Data assimilation using incremental analysis updates. *Mon. Wea. Rev.*, **124**, 1256-1271.

Bringi, V. N., K. Knupp, A. Detwiler, L. Liu, I. J. Caylor, and R. A. Black, 1997: Evolution of a Florida thunderstorm during the Convection and Precipitation/Electrification Experiment: The case of 9 August 1991. *Mon. Wea. Rev.*, **125**, 2131-2160.

Case, J., 2000: Interim report on the evaluation of the Regional Atmospheric Modeling System in the Eastern Range Dispersion Assessment System. NASA Contractor Report CR-2000-208576, Kennedy Space Center, FL, 102 pp. [Available from ENSCO, Inc., 1980 N. Atlantic Ave., Suite 230, Cocoa Beach, FL 32931].

Cetola, J. D., 1997: A climatology of the sea breeze at Cape Canaveral, Florida. M. S. Thesis, Florida State University, Tallahassee, FL, 56 pp.

Chen, S., and W. R. Cotton, 1988: The sensitivity of a simulated extratropical mesoscale convective system to longwave radiation and ice-phase microphysics. *J. Atmos. Sci.*, **45**, 3897-3910.

Cotton, W. R., M. A. Stephens, T. Nehrkorn, and G. J. Tripoli, 1982: The Colorado State University three-dimensional cloud/mesoscale model — 1982. Part II: An ice phase parameterization. *J. de Rech. Atmos.*, **16**, 295-320.

Davies, H. C., 1983: Limitations of some common lateral boundary schemes used in regional NWP models. *Mon. Wea. Rev.*, **111**, 1002-1012.

Doswell, C. A., R. Davies-Jones, and D. Keller, 1990: On summary measures of skill in rare event forecasting based on contingency tables. *Wea. Forecasting*, **5**, 576-585.

Evans, R. J., 1996: Final report on the evaluation of the Emergency Response Dose Assessment System (ERDAS). NASA Contractor Report CR-201353, Kennedy Space Center, FL, 184 pp. [Available from ENSCO Inc., 1980 N. Atlantic Ave., Suite 230, Cocoa Beach, FL 32931].

Hamill, T. M., 1999: Hypothesis tests for evaluating numerical precipitation forecasts. *Wea. Forecasting*, **14**, 155-167.

Hoke, J. E., and R. A. Anthes, 1976: The initialization of numerical models by a dynamical initialization technique. *Mon. Wea. Rev.*, **104**, 1551-1556.

Hudlow, M., 1979: Mean rainfall patterns for the three phases of GATE. *J. Appl. Meteor.*, **18**, 1656-1669.

Lin, Y., P. S. Ray, and K. W. Johnson, 1993: Initialization of a modeled convective storm using Doppler radar-derived fields. *Mon. Wea. Rev.*, **121**, 2757-2775.

López, R. E., and R. L. Holle, 1987: Distribution of summertime lightning as a function of low-level wind flow in central Florida. Technical Memorandum, NOAA Environmental Research Labs, Boulder, CO, 43 p.

Snook, J. S., P. A. Stamus, and J. Edwards, 1998: Local-domain analysis and forecast model support for the 1996 Centennial Olympic Games. *Wea. Forecasting*, **13**, 138-150.

Sun, J., and N. A. Crook, 1996: Comparison of thermodynamic retrieval by the adjoint method with the traditional retrieval. *Mon. Wea. Rev.*, **124**, 308-324.

Takano, I. and A. Segami, 1993: Assimilation and initialization of a mesoscale model for improved spin-up of precipitation. *J. Meteor. Soc. Japan*, **71**, 377-391.

Tremback, C. J., 1990: Numerical simulation of a mesoscale convective complex: model development and numerical results. Ph.D. Dissertation, Atmos. Sci. Paper No. 465, Department of Atmospheric Science, Colorado State University, Fort Collins, CO 80523, 247 pp.

Tremback, C. J., and R. Kessler, 1985: A surface temperature and moisture parameterization for use in mesoscale numerical models. Preprints, *7th AMS Conf. on Numerical Weather Prediction*, June 17-20, Montreal, Quebec, Amer. Meteor. Soc., Boston, MA, 355-358.

Tremback, C. J., I. T. Baker, M. Uliasz, and R. F. A. Hertenstein, 1998: Time domain reflectometry of soil moisture for initialization of prognostic mesoscale models. Contract No. NAS10-12264, Kennedy Space Center, FL, 339 pp. [Available from Mission Research Corporation / *ASTER Division, PO Box 466, Fort Collins, CO 80522-0466].

Turner, D. B., 1986: Comparison of three methods for calculating the standard deviation of the wind direction. *J. Climate Appl. Meteor.*, **25**, 703-707.

Warner, T. T., R. A. Peterson, and R. E. Treadon, 1997: A tutorial on lateral boundary conditions as a basic and potentially serious limitation to regional numerical weather prediction. *Bull. Amer. Meteor. Soc.*, **78**, 2599-2617.

_____, and H-M. Hsu, 2000: Nested-model simulation of moist convection: The impact of coarse-grid parameterized convection on fine-grid resolved convection. *Mon. Wea. Rev.*, **128**, 2211-2231.

Wilks, D. S., 1995: *Statistical Methods in the Atmospheric Sciences*. Academic Press, 467 pp.

Yuter, S. E., and R. A. Houze Jr., 1995a: Three-dimensional kinematic and microphysical evolution of Florida cumulonimbus. Part I: Spatial distribution of updrafts, downdrafts, and precipitation. *Mon. Wea. Rev.*, **123**, 1921-1940.

_____, and _____, 1995b: Three-dimensional kinematic and microphysical evolution of Florida cumulonimbus. Part II: Frequency distributions of vertical velocity, reflectivity, and differential reflectivity. *Mon. Wea. Rev.*, **123**, 1941-1963.

Table A2. The status of RAMS 4-grid, 3-grid, and Eta point forecasts is displayed for January and February 2000. An 'X' denotes a completed forecast whereas a blank denotes a missing forecast.

Date	0000 UTC Cycle 4-Grid	3-Grid	Eta	1200 UTC Cycle 4-Grid	3-Grid	Eta
1/1/00	X	X		X	X	
1/2/00	X	X		X	X	
1/3/00	X	X		X	X	
1/4/00		X		X		
1/5/00				X		
1/6/00				X		
1/7/00	X	X	X	X	X	X
1/8/00						X
1/9/00			X			X
1/10/00			X			X
1/11/00	X	X		X	X	
1/12/00	X	X		X	X	
1/13/00	X	X		X	X	
1/14/00	X	X		X	X	
1/15/00	X	X		X	X	
1/16/00	X	X		X	X	
1/17/00	X	X	X	X	X	X
1/18/00	X	X	X	X	X	X
1/19/00	X	X	X	X	X	X
1/20/00	X	X	X	X	X	X
1/21/00	X	X	X	X	X	X
1/22/00		X	X	X	X	X
1/23/00	X	X	X	X	X	X
1/24/00	X	X	X	X	X	X
1/25/00	X	X	X	X	X	X
1/26/00	X	X	X	X	X	X
1/27/00	X	X	X	X	X	X
1/28/00	X	X	X	X	X	X
1/29/00	X	X	X	X	X	X
1/30/00	X	X	X	X	X	X
1/31/00	X	X	X	X	X	X

Date	0000 UTC Cycle 4-Grid	3-Grid	Eta	1200 UTC Cycle 4-Grid	3-Grid	Eta
2/1/00	X	X	X	X	X	X
2/2/00	X	X	X	X	X	X
2/3/00	X	X	X	X	X	X
2/4/00	X		X	X		X
2/5/00	X		X	X		X
2/6/00	X	X	X	X	X	X
2/7/00	X	X	X	X	X	X
2/8/00	X	X	X	X	X	X
2/9/00	X	X	X	X	X	X
2/10/00	X	X	X	X	X	X
2/11/00	X	X	X	X	X	X
2/12/00	X	X	X	X	X	X
2/13/00		X	X		X	X
2/14/00	X	X	X	X	X	X
2/15/00	X	X	X	X	X	X
2/16/00	X	X	X	X	X	X
2/17/00	X	X	X	X	X	X
2/18/00	X	X	X	X	X	X
2/19/00		X	X		X	X
2/20/00		X	X		X	X
2/21/00		X	X		X	X
2/22/00		X	X	X	X	X
2/23/00	X	X	X	X	X	X
2/24/00	X	X	X	X	X	X
2/25/00	X	X	X	X	X	X
2/26/00	X	X	X	X	X	X
2/27/00	X	X	X	X	X	X
2/28/00	X	X	X	X	X	X
2/29/00	X	X	X	X	X	X

Table A4.   The status of RAMS 4-grid, 3-grid, and Eta point forecasts is displayed for June and July 2000. An 'X' denotes a completed forecast whereas a blank denotes a missing forecast.

Date	0000 UTC Cycle			1200 UTC Cycle		
	4-Grid	3-Grid	Eta	4-Grid	3-Grid	Eta
6/1/00	X	X	X	X	X	X
6/2/00	X	X	X	X	X	X
6/3/00	X		X	X		X
6/4/00	X		X	X		X
6/5/00	X	X	X	X	X	X
6/6/00	X	X	X	X	X	X
6/7/00	X		X	X		X
6/8/00	X	X	X	X	X	X
6/9/00	X	X	X	X	X	X
6/10/00			X	X	X	X
6/11/00			X	X		X
6/12/00			X	X		X
6/13/00			X	X		X
6/14/00			X	X	X	X
6/15/00	X	X	X	X	X	X
6/16/00	X	X	X	X	X	X
6/17/00	X	X	X	X	X	X
6/18/00	X	X	X	X		X
6/19/00	X	X	X	X	X	X
6/20/00	X	X	X	X	X	X
6/21/00	X	X	X	X	X	X
6/22/00	X	X	X	X	X	X
6/23/00	X	X	X	X	X	X
6/24/00	X	X	X	X	X	X
6/25/00	X	X	X	X	X	X
6/26/00	X	X		X	X	X
6/27/00				X	X	X
6/28/00	X	X	X	X	X	X
6/29/00	X	X	X	X	X	X
6/30/00	X	X	X	X	X	X

Date	0000 UTC Cycle			1200 UTC Cycle		
	4-Grid	3-Grid	Eta	4-Grid	3-Grid	Eta
7/1/00	X	X	X	X	X	X
7/2/00			X	X		X
7/3/00	X	X	X	X	X	X
7/4/00	X	X	X	X	X	X
7/5/00	X	X	X	X	X	X
7/6/00	X	X	X	X	X	X
7/7/00	X	X	X	X	X	X
7/8/00	X	X	X	X	X	X
7/9/00	X	X	X	X	X	X
7/10/00	X	X	X	X	X	X
7/11/00	X	X	X	X	X	X
7/12/00	X	X	X	X	X	X
7/13/00	X	X	X	X	X	X
7/14/00	X	X	X	X	X	X
7/15/00	X	X	X	X	X	X
7/16/00	X	X	X	X	X	X
7/17/00	X	X	X	X	X	X
7/18/00	X	X	X	X	X	X
7/19/00	X	X	X	X	X	X
7/20/00	X	X	X	X	X	X
7/21/00	X	X	X	X	X	X
7/22/00	X	X	X	X	X	X
7/23/00	X	X	X	X	X	X
7/24/00	X	X	X	X	X	X
7/25/00	X	X	X	X	X	X
7/26/00	X	X	X	X	X	X
7/27/00	X	X	X	X	X	X
7/28/00	X	X	X	X	X	X
7/29/00	X	X	X	X	X	X
7/30/00	X	X	X	X	X	X
7/31/00	X	X	X	X	X	X

Appendix B

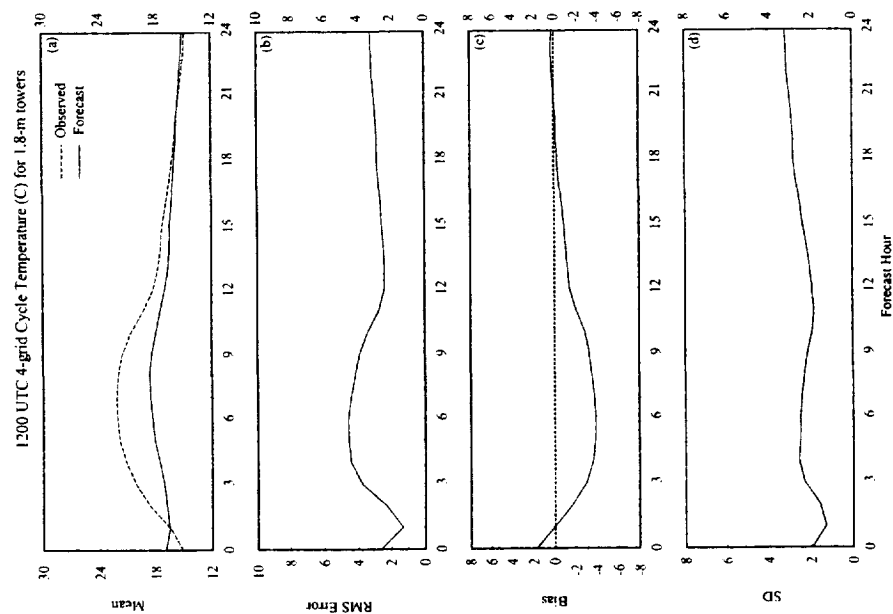## Selected Figures for the 1999-2000 Cool-season Objective Evaluation

Figure B1.   A meteogram plot of temperature errors (°C) from the 1200 UTC operational RAMS forecast cycle during the 1999-2000 cool season, verified at the 1.8-m level of the KSC/CCAFS wind-tower network. Parameters plotted as a function of forecast hour are a) mean observed (dashed) and forecast temperatures (solid), b) RMS error, c) bias, and d) error standard deviation (SD).
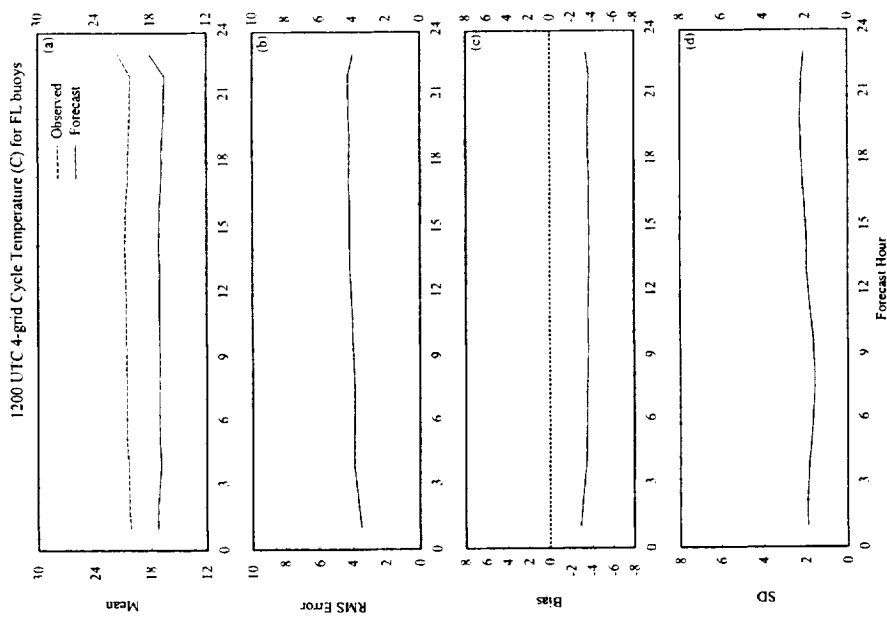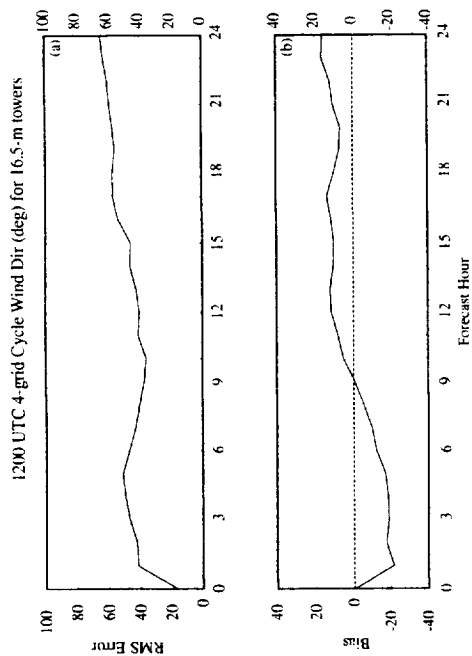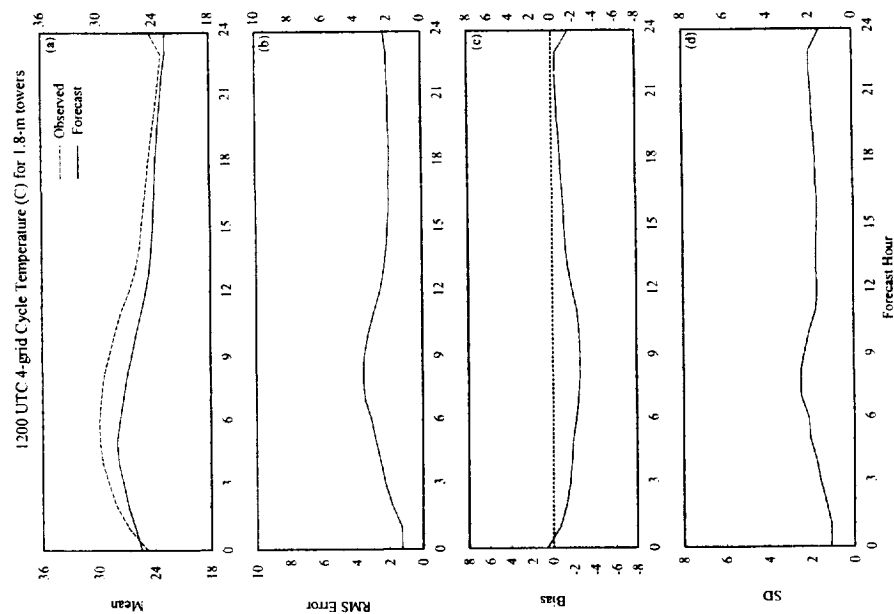

Figure B2.   A meteogram plot of temperature errors (°C) from the 1200 UTC operational RAMS forecast cycle during the 1999-2000 cool season, verified at the buoys offshore of central Florida.   Parameters plotted as a function of forecast hour are a) mean observed (dashed) and forecast temperatures (solid), b) RMS error, c) bias, and d) error standard deviation (SD).
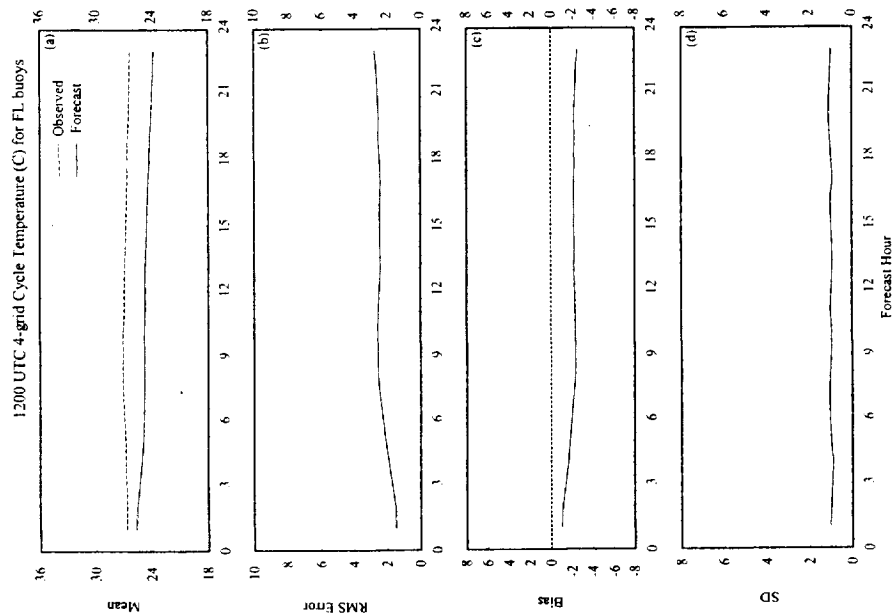
Figure B5. A meteogram plot of the wind direction errors (deg.) from the 1200 UTC operational RAMS forecast cycle during the 1999-2000 cool season, verified at the 16.5-m level of the KSC/CCAFS wind-tower network. Parameters plotted against forecast hour are a) RMS error, and b) bias.
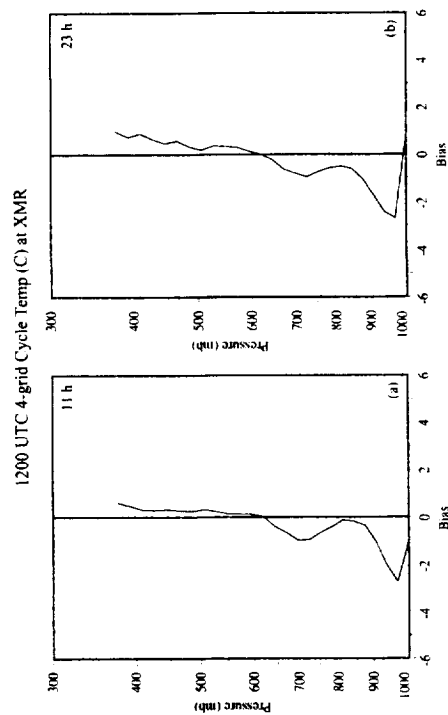
Figure B6. Vertical profiles of the temperature bias (°C) at XMR from the 1200 UTC operational RAMS forecast cycle during the 1999-2000 cool season. Biases are shown for the a) 11-h forecast and b) 23-h forecast.
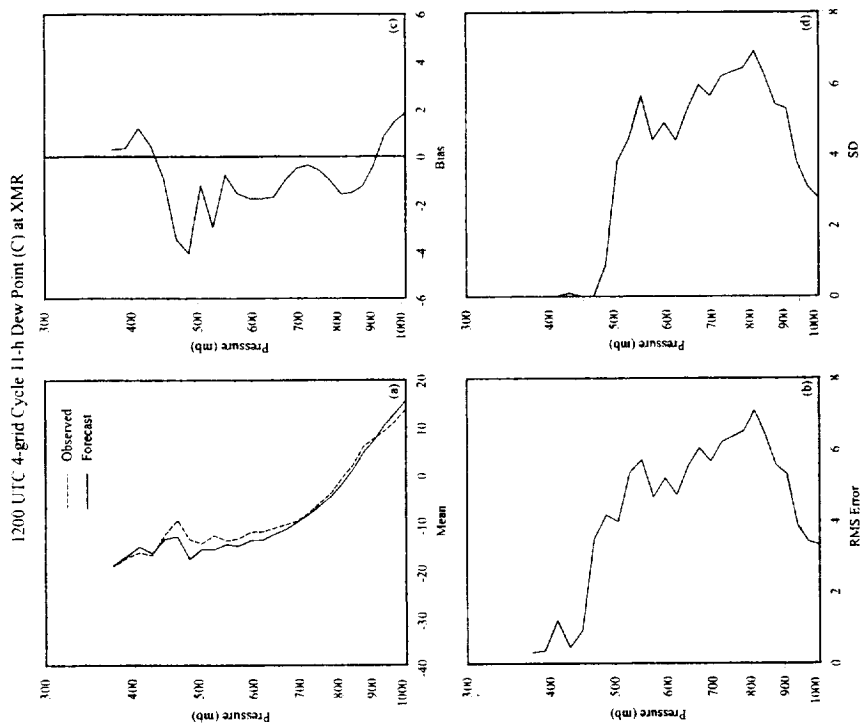
Figure B7. Vertical profiles of the dew point temperature errors (°C) at XMR for the 11-h forecast from the 1200 UTC operational RAMS forecast cycle during the 1999-2000 cool season. Parameters plotted as a function of pressure are a) mean observed (dashed) and forecast dew point temperature (solid), b) RMS error, c) bias, and d) error standard deviation (SD).

117

Appendix C

Selected Figures for the 2000 Warm Season Objective Evaluation

Figure C1. A meteogram plot of temperature errors (°C) from the 1200 UTC operational RAMS forecast cycle during the 2000 warm season, verified at the 1.8-m level of the KSC/CCAFS wind-tower network. Parameters plotted as a function of forecast hour are a) mean observed (dashed) and forecast temperatures (solid), b) RMS error, c) bias, and d) error standard deviation (SD).
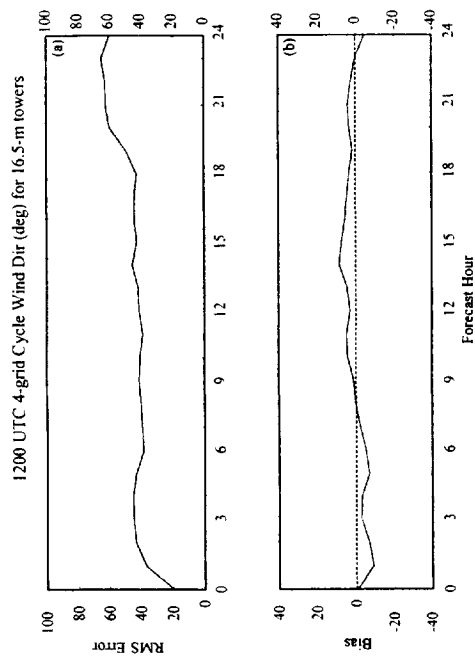
Figure C2. A meteogram plot of temperature errors (°C) from the 1200 UTC operational RAMS forecast cycle during the 2000 warm season, verified at the buoys offshore of central Florida. Parameters plotted as a function of forecast hour are a) mean observed (dashed) and forecast temperatures (solid), b) RMS error, c) bias, and d) error standard deviation (SD).

1200 UTC 4-grid Cycle Wind Dir (deg) for 16.5-m towers

Figure C5. A meteogram plot of the wind direction errors (deg.) from the 1200 UTC operational RAMS forecast cycle during the 2000 warm season, verified at the 16.5-m level of the KSC/CCAFS wind-tower network. Parameters plotted as a function of forecast hour are a) RMS error, and b) bias.
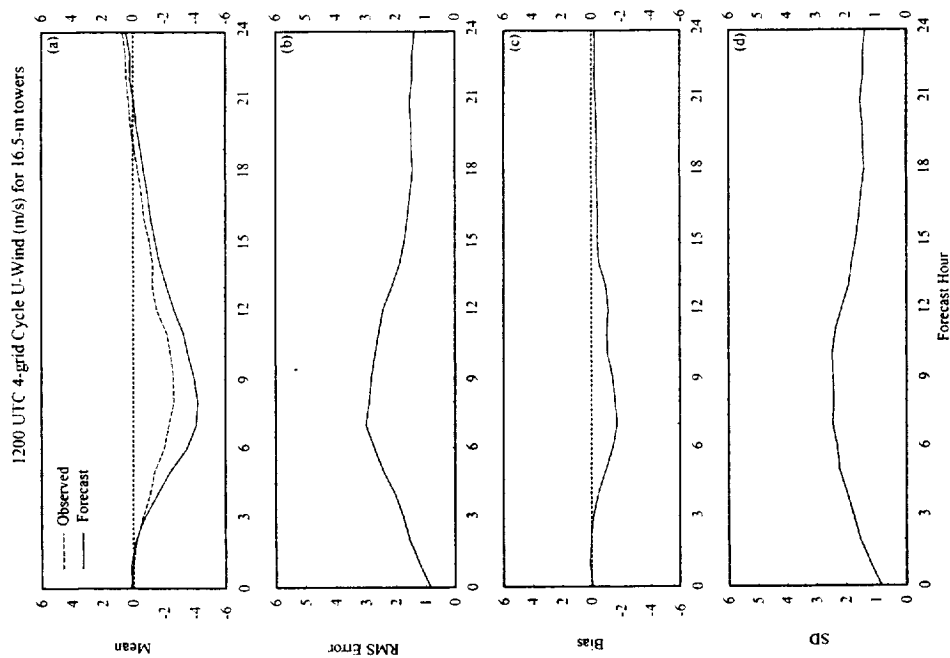

1200 UTC 4-grid Cycle U-Wind (m/s) for 16.5-m towers

Figure C6. A meteogram plot of the u-wind component errors (m s⁻¹) from the 1200 UTC operational RAMS forecast cycle during the 2000 warm season, verified at the 16.5-m level of the KSC/CCAFS wind-tower network. Parameters plotted as a function of forecast hour are a) mean observed (dashed) and forecast u-winds (solid), b) RMS error, c) bias, and d) error standard deviation (SD).
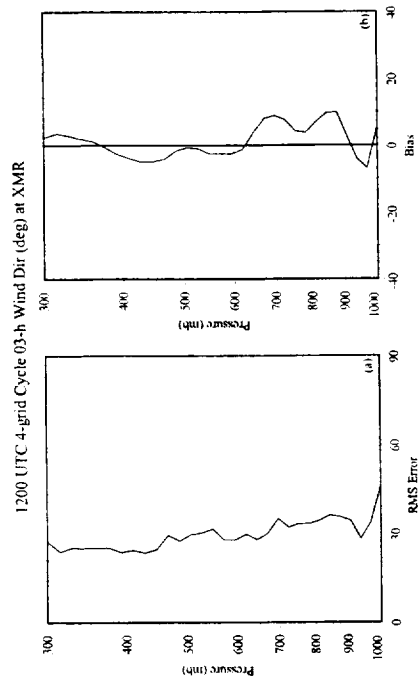
1200 UTC 4-grid Cycle 22-h Wind Dir (deg) at XMR

Figure C11. Vertical profiles of wind direction errors (deg.) at XMR for the 22-h forecast from the 1200 UTC operational RAMS forecast cycle during the 2000 warm season. Parameters plotted as a function of pressure are a) RMS error and b) bias.
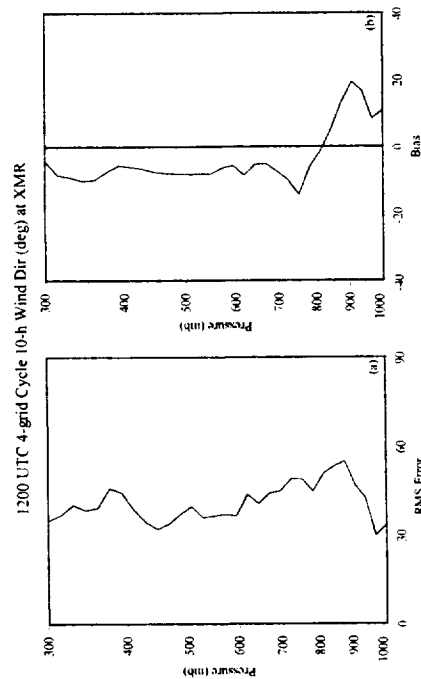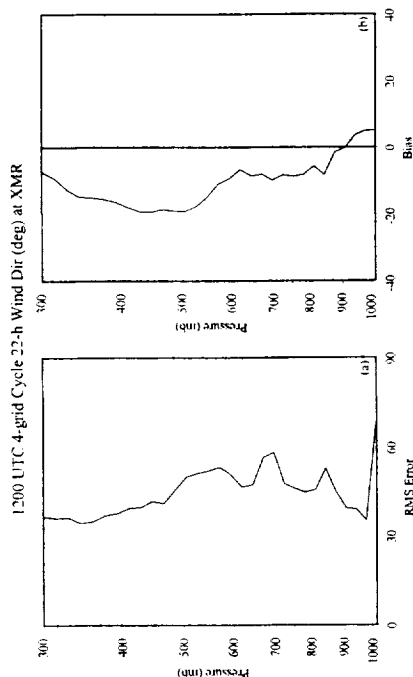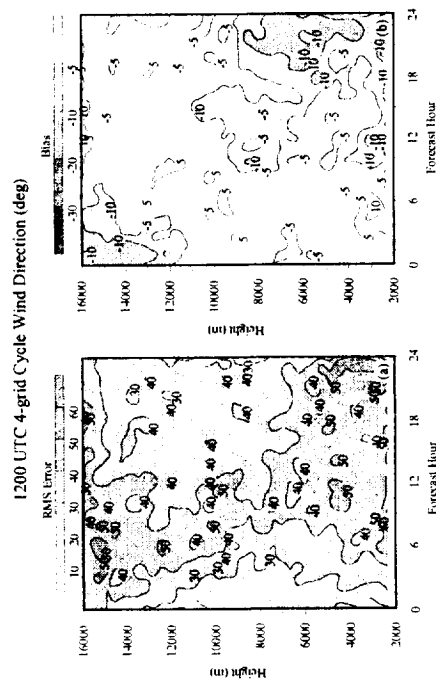

1200 UTC 4-grid Cycle Wind Direction (deg)

Figure C12. Time-height cross sections of wind direction errors at the KSC/CCAFS 50-MHz DRWP for the 1200 UTC operational RAMS forecast cycle. Parameters contoured for every hour are a) RMS error (shaded every 10°), and b) bias (contoured at ± 5°, 10°, 20°, and 30°, with negative values less than -5° shaded).

1200 UTC 4-grid Cycle 03-h Wind Dir (deg) at XMR

Figure C9. Vertical profiles of wind direction errors (deg.) at XMR for the 3-h forecast from the 1200 UTC operational RAMS forecast cycle during the 2000 warm season. Parameters plotted as a function of pressure are a) RMS error and b) bias.

1200 UTC 4-grid Cycle 10-h Wind Dir (deg) at XMR

Figure C10. Vertical profiles of wind direction errors (deg.) at XMR for the 10-h forecast from the 1200 UTC operational RAMS forecast cycle during the 2000 warm season. Parameters plotted as a function of pressure are a) RMS error and b) bias.

123

$$P * \left[\left(\hat{S}_1^* - \hat{S}_2^* \right) < \hat{t}_L \right] = \frac{\alpha}{2} = 0.025 \text{, and}$$

$$P * \left[\left(\hat{S}_1^* - \hat{S}_2^* \right) > \hat{t}_V \right] = 1 - \frac{\alpha}{2} = 0.975 \text{,} \tag{D6}$$

where $P*$ represents probabilities calculated from the resampled distribution. Finally, the null hypothesis, H_0, is rejected if $\left(\hat{S}_1 - \hat{S}_2 \right) < \hat{t}_L$ or $\left(\hat{S}_1 - \hat{S}_2 \right) > \hat{t}_V$. The results of this resampling method are shown in Table D1 for most individual categorical and skill scores presented in the main report. The interpretation is as follows. Each column in Table D1 represents a significance test by subtracting one forecast or configuration from another. The convention is (Forecast 1 – Forecast 2). If the test statistic is greater than 97.5%, then the skill of Forecast 1 is significantly higher than Forecast 2. Conversely, if the test statistic is less than 2.5%, then the skill of Forecast 2 is significantly higher than the skill of Forecast 1.

Table D1. Levels of statistical significance (%) for various comparisons of the RAMS and Eta sea-breeze categorical and skill scores using a two-tailed, resampling method following Hamill (1999). The RAMS versus Eta tests are valid for the sea-breeze evaluation at TTS while the comparisons of different configurations and initializations of RAMS are valid at the 12 KSC/CCAFS wind towers in Figure 2.2b. Scores that are statistically significant at 95% confidence or higher are highlighted in bold italic font.

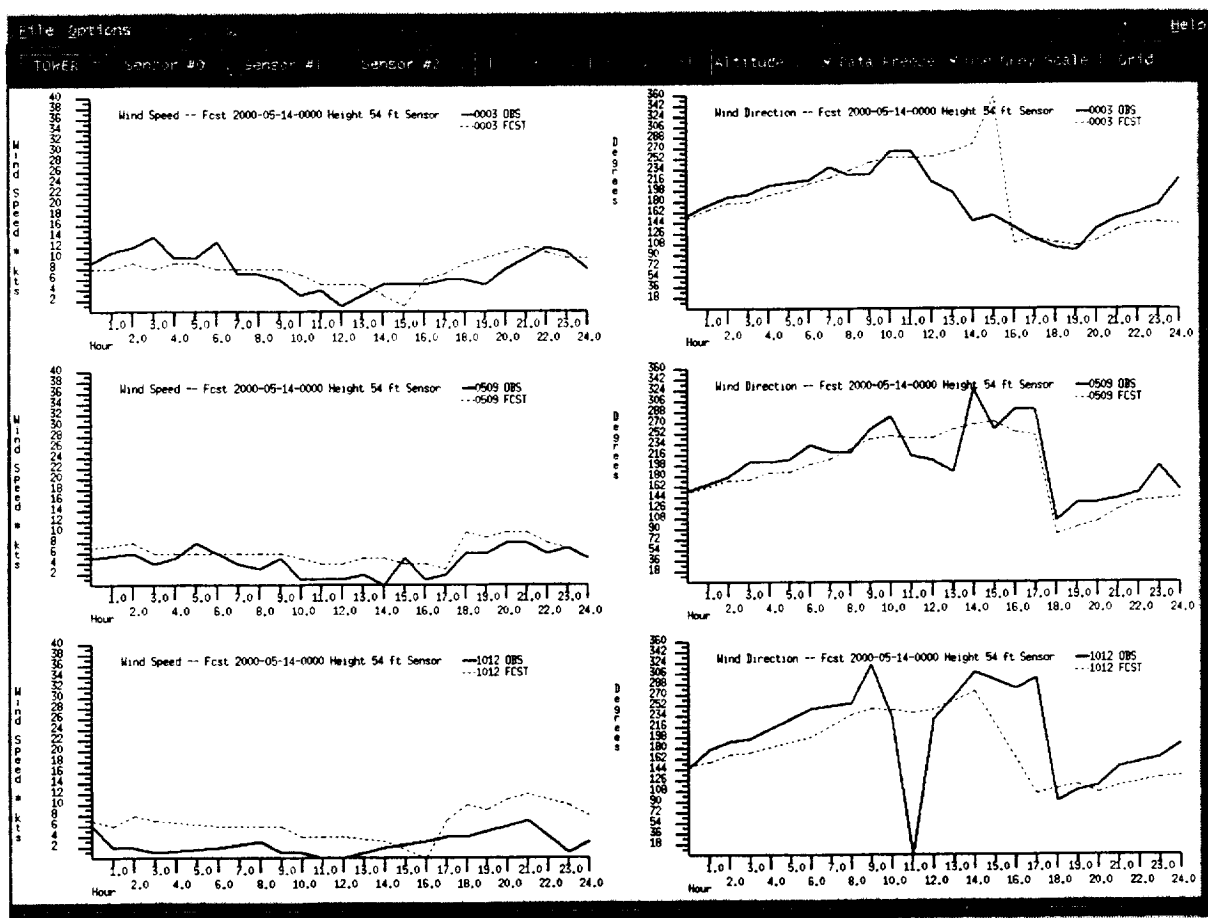| Parameter	RAMS 1200 UTC minus RAMS 0000 UTC	RAMS 4-grid minus RAMS 3-grid (0000 UTC)	RAMS 4-grid minus RAMS 3-grid (1200 UTC)	RAMS minus Eta (0000 UTC)	RAMS minus Eta (1200 UTC)
POD	*100%*	*99.9%*	*99.9%*	*100%*	*99.9%*
FAR	46.2%	14.9%	35.0%	66.5%	*98.1%*
Bias	*100%*	*98.5%*	*99.6%*	*100%*	*100%*
CSI	*100%*	*99.9%*	*99.2%*	*99.9%*	86.1%
HSS	*99.6%*	*99.4%*	96.3%	*99.2%*	58.3%

Figure E1.   A sample KSC/CCAFS wind-tower display from the RAMS verification graphical user interface developed by the AMU used to validate RAMS forecasts versus observations in real-time. This display shows a plot of the RAMS forecast versus observed wind speed and wind direction at towers 3, 519, and 1012 during the 24-h forecast period from the 0000 UTC 14 May 2000 RAMS model prediction.

NOTICE

REPORT DOCUMENTATION PAGE

Form Approved
OMB No. 0704-0188

1. AGENCY USE ONLY (Leave blank)	2. REPORT DATE	3. REPORT TYPE AND DATES COVERED
	May 2001	Contractor Report

4. TITLE AND SUBTIITLE

Final Report on the Evaluation of the Regional Atmospheric Modeling System in the Eastern Range Dispersion Assessment System

5. FUNDING NUMBERS

C-NAS10-96018

6. AUTHOR(S)

Jonathan Case

7. PERFORMING ORGANIZATION NAME(S) AND ADDRESS(ES)

ENSCO, Inc., 1980 North Atlantic Avenue, Suite 230, Cocoa Beach, FL 32931

8. PERFORMING ORGANIZATION REPORT NUMBER

01-001

9. SPONSORING/MONITORING AGENCY NAME(S) AND ADDRESS(ES)

NASA, John F. Kennedy Space Center, Code AA-C-1, Kennedy Space Center, FL 32899

10. SPONSORING/MONITORING AGENCY REPORT NUMBER

NASA/CR-2001-210259

11. SUPPLEMENTARY NOTES

Subject Cat.: #47 (Weather Forecasting)

12A. DISTRIBUTION/AVAILABILITY STATEMENT

Unclassified - Unlimited

12B. DISTRIBUTION CODE

13. ABSTRACT (Maximum 200 Words)

The Applied Meteorology Unit (AMU) evaluated the Regional Atmospheric Modeling System (RAMS) contained within the Eastern Range Dispersion Assessment System (ERDAS). ERDAS provides emergency response guidance for Cape Canaveral Air Force Station and Kennedy Space Center operations in the event of an accidental hazardous material release or aborted vehicle launch. The RAMS prognostic data are available to ERDAS for display and are used to initialize the 45th Space Wing/Range Safety dispersion model. Thus, the accuracy of the dispersion predictions is dependent upon the accuracy of RAMS forecasts.

The RAMS evaluation consisted of an objective and subjective component for the 1999 and 2000 Florida warm seasons, and the 1999-2000 cool season. In the objective evaluation, the AMU generated model error statistics at surface and upper-level observational sites, compared RAMS errors to a coarser RAMS grid configuration, and benchmarked RAMS against the nationally-used Eta model. In the subjective evaluation, the AMU compared forecast cold fronts, low-level temperature inversions, and precipitation to observations during the 1999-2000 cool season, verified the development of the RAMS forecast east coast sea breeze during both warm seasons, and examined the RAMS daily thunderstorm initiation and precipitation patterns during the 2000 warm season. This report summarizes the objective and subjective verification for all three seasons.

14. SUBJECT TERMS	15. NUMBER OF PAGES 147
Numerical Weather Prediction, Model evaluation	16. PRICE CODE

17. SECURITY CLASSIFICATION OF REPORT	18. SECURITY CLASSIFICATION OF THIS PAGE	19. SECURITY CLASSIFICATION OF ABSTRACT	20. LIMITATION OF ABSTRACT
UNCLASSIFIED	UNCLASSIFIED	UNCLASSIFIED	NONE